



<https://theses.gla.ac.uk/>

Theses Digitisation:

<https://www.gla.ac.uk/myglasgow/research/enlighten/theses/digitisation/>

This is a digitised version of the original print thesis.

Copyright and moral rights for this work are retained by the author

A copy can be downloaded for personal non-commercial research or study,
without prior permission or charge

This work cannot be reproduced or quoted extensively from without first
obtaining permission in writing from the author

The content must not be changed in any way or sold commercially in any
format or medium without the formal permission of the author

When referring to this work, full bibliographic details including the author,
title, awarding institution and date of the thesis must be given

Enlighten: Theses

<https://theses.gla.ac.uk/>
research-enlighten@glasgow.ac.uk

Development of Computer Modelling Techniques
for Microwave Thermography

Valerie Jane Brown, BSc,
Department of Physics and Astronomy,
University of Glasgow

Presented for the degree of Doctor of Philosophy
to the University of Glasgow,
May 1989

© Valerie J Brown, 1989

ProQuest Number: 10999350

All rights reserved

INFORMATION TO ALL USERS

The quality of this reproduction is dependent upon the quality of the copy submitted.

In the unlikely event that the author did not send a complete manuscript and there are missing pages, these will be noted. Also, if material had to be removed, a note will indicate the deletion.



ProQuest 10999350

Published by ProQuest LLC (2018). Copyright of the Dissertation is held by the Author.

All rights reserved.

This work is protected against unauthorized copying under Title 17, United States Code
Microform Edition © ProQuest LLC.

ProQuest LLC.
789 East Eisenhower Parkway
P.O. Box 1346
Ann Arbor, MI 48106 – 1346

Acknowledgements

This work was carried out whilst I was a student in the Department of Physics and Astronomy, University of Glasgow and in receipt of a research studentship award from the Scottish Home and Health Department.

I would like to thank all those who have helped me to carry out the work presented in this thesis. In particular I must thank my supervisor, Dr. D V Land; fellow research students Anne Campbell and Malika Mimi, and also R J Jenkins; Dr. A Watt, Department of Physics and Astronomy, University of Glasgow; Dr J Taylor, formerly Department of Physics and Astronomy, University of Glasgow; Dr. M McKirdy, Department of Surgery, University of Glasgow; Dr. S Fraser, Gartnavel General Hospital and all the volunteers and patients who so kindly acted as "guinea-pigs".

Thanks also to my mum and dad for everything, to Mary for all the twigs of friendship and to Michael.

Table of Contents

Summary

Chapter 1 - Introduction to microwave thermography

1.1 Introduction	1
1.2 Principles of microwave thermography	3
1.3 Thermography and thermometry	5
1.4 Review of microwave thermography	8

Chapter 2 - Basic principles of microwave thermography

2.1 Introduction	15
2.2 Equation of radiative transfer	15
2.3 Antenna response function	19
2.4 Antenna temperature	23

Chapter 3 - Microwave radiometry

3.1 Introduction	25
3.2 Choice of measurement frequency	26
3.3 Temperature resolution	27
3.4 Radiometer equipment	30
3.5 Radiometer sensitivity	31
3.6 Antennas	32
3.7 Calculation of expected microwave signal	38

Chapter 4 - Calculation of temperature distribution in human body

4.1 Introduction	40
4.2 Heat transfer in the human body	40

4.3 Heat exchange with the environment	45
4.4 Balance between heat production and heat loss	51
Chapter 5 - Electrical, thermal and physiological properties of tissue	
5.1 Introduction	53
5.2 A brief note on tissue structure	53
5.3 Frequency dependent dielectric behaviour of tissue	54
5.4 Dielectric properties of water and electrolytes	55
5.5 Dielectric properties of tissue at 3 GHz	57
5.6 Thermal conductivity of tissue	60
5.7 Blood flow and metabolic heat generation in tissue	61
5.8 Characteristics of malignant breast tumours	62
Chapter 6 - Microwave thermography in breast disease	
6.1 Introduction	64
6.2 Anatomy of breast	64
6.3 Breast diseases and imaging	65
6.4 Factors influencing microwave and infra-red thermographic measurements	66
6.5 Numerical modelling of normal breast	73
6.6 Experimental determination of normal breast temperatures	74
6.7 Microwave thermography in patients with breast disease	79
6.8 Experimental determination of breast temperatures in patients with breast disease	81
Chapter 7 - Microwave thermography in rheumatology	
7.1 Introduction	84
7.2 Disease assessment in rheumatology	84

7.3 Microwave thermography in rheumatology	88
7.4 Modelling of temperature distributions in the knee joint	89
Chapter 8 - Conclusions	93
References	98

Summary

Microwave thermography obtains information about the temperature of internal body tissues by a spectral measurement of the intensity of the natural thermally generated radiation emitted by the body tissues. At the lower microwave frequencies radiation can penetrate through tissue for distances useful for a range of medical applications. Radiation from inside the body may be detected and measured non-invasively at the skin surface by a microwave thermography system consisting of a suitable antenna to detect the radiation and a radiometer receiver to measure its intensity. In the microwave region the radiative power emitted per unit bandwidth is proportional to the temperature of the emitting tissue and the total radiative power received from the body tissues, P , is a weighted volume average of temperature

$$P = k B \int_V w(\mathbf{r}) T(\mathbf{r}) dV$$

where k is Boltzmann's constant, B is the bandwidth, $T(\mathbf{r})$ is the temperature at the position \mathbf{r} and $w(\mathbf{r})$ is the weighting function. The weighting function depends on the structure and dielectric properties of the tissues being viewed, the measurement frequency and the characteristics of the antenna.*

The Glasgow developed microwave thermography system operates at a central frequency of 3.2 GHz, chosen to give the optimum compromise between the depth from which radiation may be received, which decreases with increasing frequency, and the lateral spatial resolution which increases with increasing frequency. A Dicke configuration radiometer receiver and a cylindrical low-impedance waveguide antenna, which operates in contact with the skin surface, are used. The output from the radiometer is calibrated to degrees Celsius to give a "microwave temperature" of the tissues being viewed.

The tissue temperature distribution, $T(r)$, reflects the vascular and metabolic state of the tissue. Diseases which affect these physiological functions will result in changes in the tissue temperature and hence in the measured microwave temperature. It

* This function will vary, to a certain extent, from individual to individual for the same region of the body, depending on the anatomical structure present, and, in particular, the thickness of any tissue region.

is not possible, however, to solve the indirect problem of retrieval of the temperature distribution in the tissue from a single frequency measurement of microwave temperature. It is therefore necessary to model the temperature distribution in the tissue and, from this, solve the direct problem of calculation of the microwave temperature. Measured microwave temperatures may then be compared with those modelled to indicate the physiological state of the tissue. Pennes (1948)

The temperature distribution in the tissue may be determined by solution of the steady-state heat transfer equation

$$K \nabla^2 T + W_b c_b (T_a - T) + Q = 0$$

where K is the thermal conductivity of the tissue, W_b is the perfusion rate of blood through the tissue, c_b is the specific heat capacity of the blood, T_a is the arterial blood temperature and Q is the rate of metabolic heat generation in the tissue. The boundary condition of heat loss at the skin surface is governed by the equation

$$K \frac{\partial T}{\partial n} = h (T - T_e)$$

where T_e is the ambient temperature and h is the heat transfer coefficient due to the combined effects of heat loss by radiation, convection and evaporation.

The microwave temperature may be calculated from the modelled temperature distribution and use of plane wave theory to determine the weighting function, with an increased power attenuation constant to account for the response of the antenna.

The modelling of the tissue is simplified by the fact that both the tissue thermal conductivity and the microwave dielectric properties of the tissue depend primarily on the water content of the tissue.

This thermal and electromagnetic modelling has been carried out to determine the expected microwave temperature profiles across the female breast. Microwave and infra-red temperature measurements were made on a group of young, normal women and a group of older, post-menopausal women with breast disease. In general the younger women will have higher water content breast tissue than that of the older

women due to the higher proportion of glandular and connective tissue and the smaller proportion of low water content fat tissue. However, by comparison of the modelled microwave and surface temperatures with those measured on the younger women and on the normal breast of the older group, it was found that it was not possible to distinguish between the breast tissue of the particular groups studied. The modelled temperatures indicated that the effective power penetration depth in breast tissue is less than 8.4 mm and that the thermal conductivity is between 0.29 and $0.46 \text{ Wm}^{-1}\text{K}^{-1}$.

The microwave temperature was found to primarily reflect the level of perfusion in the breast tissue. A wide range of normal perfusion values, from 0.2 to greater than $2 \text{ kgm}^{-3}\text{s}^{-1}$, was found. The microwave temperature is most sensitive to perfusion changes at low values of perfusion.

In patients with breast disease the increased microwave temperature above that of the normal contralateral breast reflects increased vascularity due to disease activity. It is thought that this increased vascularity may only be present at the periphery of the tumour where the neoplastic cells are invading the surrounding tissue, forming capillary-like vessels and providing an abundant vascular network. At the centre of the tumour the blood perfusion may be less than that at the advancing edge. In very large tumours the tissue at the centre may be necrotic. The apparent thermographic size of a tumour might therefore be expected to be larger than its radiographic size determined by mammography.

The microwave and thermal modelling has also been applied to the knee joint. Patients suffering from inflammatory arthritis are known to have increased joint temperatures in those joints affected by disease. Modelled microwave temperatures were determined for the knee joint and compared with those obtained from normal joints and joints affected by rheumatoid arthritis. Rheumatoid arthritis is an inflammatory disease which may affect one or more joints and whose symptoms include pain, swelling of the joint, stiffness and lack of articulation. The increased joint

temperature in patients with rheumatoid arthritis was found to be attributable to increased blood supply to the synovial tissue in the joint cavity. The increased blood supply may result from both an increased volume of synovial tissue and an increased perfusion rate through this tissue.

Microwave thermography may therefore be used clinically as a non-invasive method of monitoring changes in tissue perfusion. Quantitative estimates of tissue perfusion may be determined by comparison of modelled microwave temperatures with those measured. This information will be a useful aid to research both in breast disease and in rheumatology.

Chapter 1 - Introduction to Microwave thermography

1.1 Introduction

Microwave thermography is the measurement of internal temperatures in the human body by detection of the natural thermally generated microwave radiation emitted by the body tissues. This technique has a number of potentially important medical applications for the detection, diagnosis and treatment monitoring of diseases which produce regional or localised changes in the body's normal temperature distributions.

The temperature variation over the surface of the human body and the thermal gradients into the body reflect variations in the physiological properties of blood flow and metabolic heat production. Diseases which cause changes in vascularity or metabolism produce thermal changes in the body which may be investigated by microwave thermography. Initial studies of the clinical applications of microwave thermography have included osteo-articular diseases, vascular disorders, diseases of the acute abdomen and cancers of the breast, thyroid and brain (Barrett, Myers and Sadowsky, 1980; Edrich et al, 1980; Land, Fraser and Shaw, 1986; Abdul-Razzak et al, 1987). The advantage of microwave thermography in the study of these diseases over other thermographic techniques is that microwave radiation is able to pass through human tissue and therefore the subcutaneous temperature may be determined passively and non-invasively. This microwave measurement of internal temperature is related more strongly to physiological conditions in the deeper tissues than to the effects of heat transfer to the environment, which occur mainly in the skin and are strongly reflected in measurements of surface temperature such as in infra-red thermography. Infra-red thermography is a similar technique to microwave thermography but the transmission through body tissues of electromagnetic radiation at the higher infra-red frequencies is only of the order of 0.1 mm and this technique therefore provides a measure of skin temperature. [10]

If microwave thermography is to be widely used and fulfil its potential as a

clinical technique then it is important that it has specific objective criteria for its interpretive use. In order to successfully determine the most effective such criteria it is necessary to fully understand the factors which affect the observed microwave temperatures. The aim of this work has been to develop computer assisted modelling techniques which indicate the influence of each of the factors contributing to microwave measurements, give quantitative assessments of the most important among these factors and can be used in the development of diagnostic criteria for microwave thermography.

The application of microwave thermography to the study of breast cancer and joint disease has been considered in particular. Numerical and analytical models of the temperature distributions in these regions of the body have been developed and used to calculate the expected microwave temperatures of these parts. In the case of breast cancer these models were used to assist in the analysis of microwave and infra-red thermographic measurements on two groups of subjects: a group of normal volunteers in the age range 19-26 and a group of breast patients at the Western Infirmary, Glasgow, in the age range 30-72. This small sample was used to demonstrate the potential of microwave thermography to estimate blood flow and tissue water content in breast tissue of women of different ages and to assess the changes which take place in the breast in the presence of cancer.

In the case of the knee joint work was carried out to improve understanding of the normal microwave patterns observed in limbs and so lead to a better interpretation of the thermographic findings in patients with disease. Infra-red and microwave thermographic measurements were made on normal volunteers and patients suffering from rheumatoid arthritis. Using the theoretical model of expected microwave and infra-red temperatures to compare with the measured values the effect of the anatomy of the limb on the observed temperature profiles was studied and the disease activity indicated by the measured microwave temperatures was assessed.

An introduction to microwave thermography is given in the remainder of this

chapter which describes briefly the basic principles of microwave thermography, gives a brief account of clinical thermometry and thermography and reviews present and previous work in the field of microwave thermography. Chapter 2 discusses more fully the principles behind microwave thermography. Chapter 3 describes the microwave thermography system used in this study and Chapter 4 discusses the modelling of temperature distributions in the human body. Chapter 5 considers the tissue properties which affect microwave thermographic measurements. The application of microwave thermography to the study of breast cancer and joint disease is presented in Chapters 6 and 7 respectively and conclusions are given in Chapter 8.

1.2 Principles of Microwave Thermography

A body which is a perfect absorber of radiation is also a perfect emitter and is known as a black body. The radiation at any wavelength from such a body depends only on the temperature and radiation wavelength and is independent of the nature of the material of the black body. Planck's Law describes the intensity of radiation from a black body at a temperature T in the wavelength region λ to $\lambda+d\lambda$:

$$B_{\lambda} d\lambda = \frac{2hc^2}{\lambda^5 \left(\exp\left(\frac{ch}{\lambda kT}\right) - 1 \right)} d\lambda \quad (1.2.1)$$

where $B_{\lambda}d\lambda$ is the power emitted per unit surface area per unit solid angle in the wavelength interval $d\lambda$, h is Planck's constant (Js), c is the velocity of light (ms^{-1}), λ is the wavelength (m), T is the temperature (K) and k is Boltzmann's constant (J K^{-1}).

Figure 1.1 shows this intensity spectrum for a black body at a temperature of 300K, approximately that of the human body. Human skin behaves very close to a black body at wavelengths between 0.2 and 20 μm for both white and black skin (Mitchell et al, 1967). It is in this region, at about 9.5 μm , that maximum emission of radiation occurs. Infra-red thermography systems have been designed to detect radiation around this maximum, in the wavelength range 3-15 μm (Jones, 1987). Planck's Law can be used to relate the measured radiation in this wavelength range to

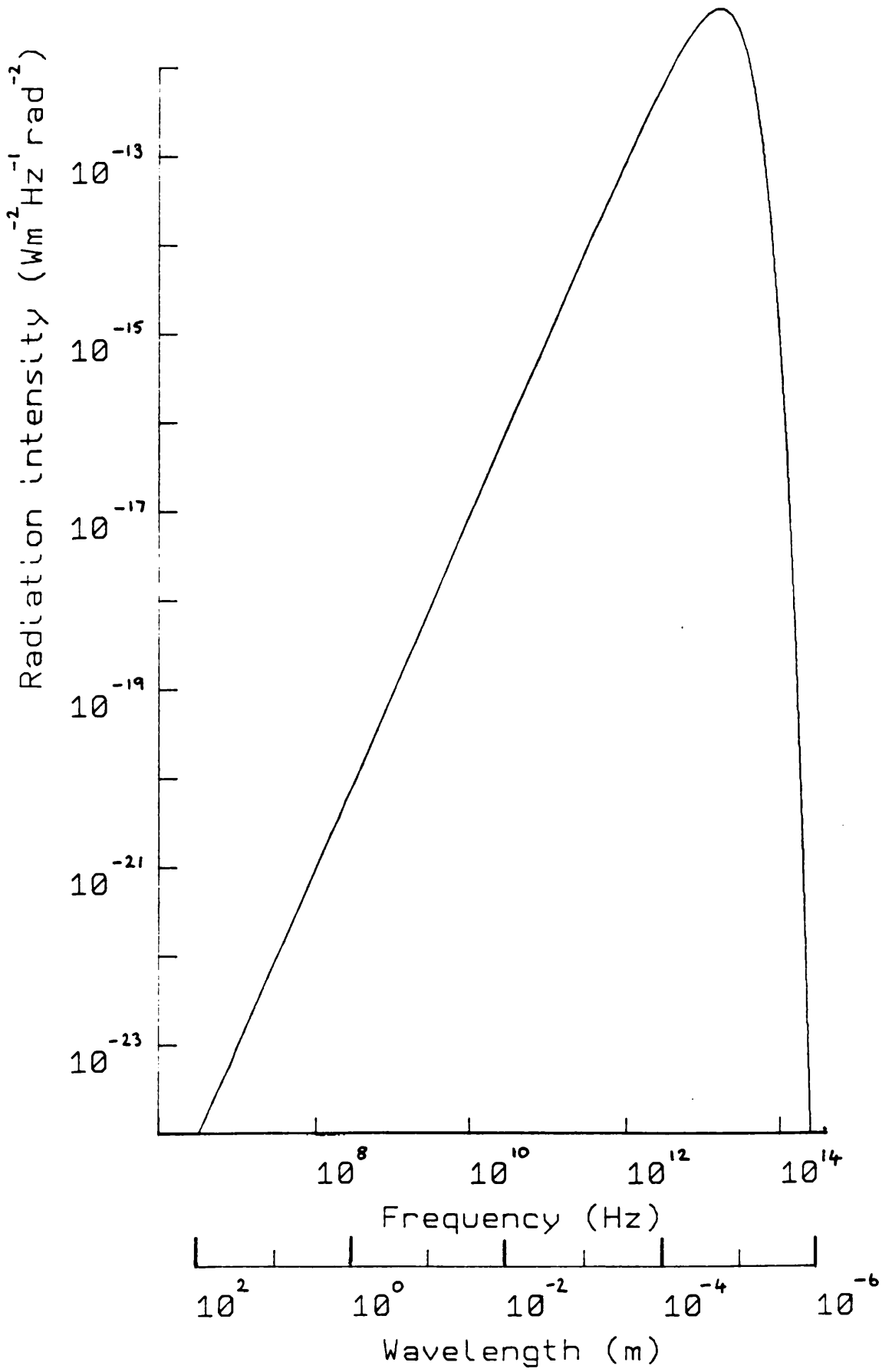


Figure 1.1 Intensity spectrum of a black body at a temperature of 300 K.

the temperature of the skin surface.

The absorption properties of human tissue vary with frequency and it is only in the infra-red region that the emission takes the form of black body radiation. Figure 1.2 illustrates this variation with frequency in the absorption properties of high and low water content tissues in terms of the tissue penetration depth. This depth is the thickness of tissue which will absorb e^{-1} (or 37%) of the power of incident plane-wave radiation. It can be seen that the penetration depth decreases with increasing frequency. The larger the penetration depth the greater the depth in the tissue from which radiation emerging at the surface originates. At a frequency of 3 GHz, for example, the plane-wave penetration depth in high water content tissues, such as muscle and skin, is about 0.8 cm and in low water content tissues, such as fat, it is about 5 cm. Radiation may therefore pass through clinically significant depths in all tissues at this frequency and measurement of the radiation emitted by the body in this spectral region will be related to the internal temperature of the body tissues.

As the wavelength increases, however, although radiation which originates at greater depths in the tissue may be detected the lateral spatial resolution, which is of the order of one half the wavelength in the tissue, decreases.* The choice of frequency for measurement of emitted radiation is, therefore, a compromise between the depth of tissue from which radiation originates and the resolution. The intensity of the radiation is also dependent on the wavelength and, although the emission at microwave wavelengths is approximately 10^8 less than that at infra-red wavelengths, equipment developed originally for radio astronomy can detect radiation of this intensity.

The radiation emitted by the body's tissues is detected by a radiometer system. The radiometer consists of two essential parts: a microwave radiometer receiver which measures the power of the thermal signal and an antenna which receives this power and provides a transition between the radiation emitted by the tissues and the measuring system. The antenna may be designed to operate in contact with or remote from the skin surface. Remote sensing thermography systems are not practical at frequencies below 9

* (Land 1987)

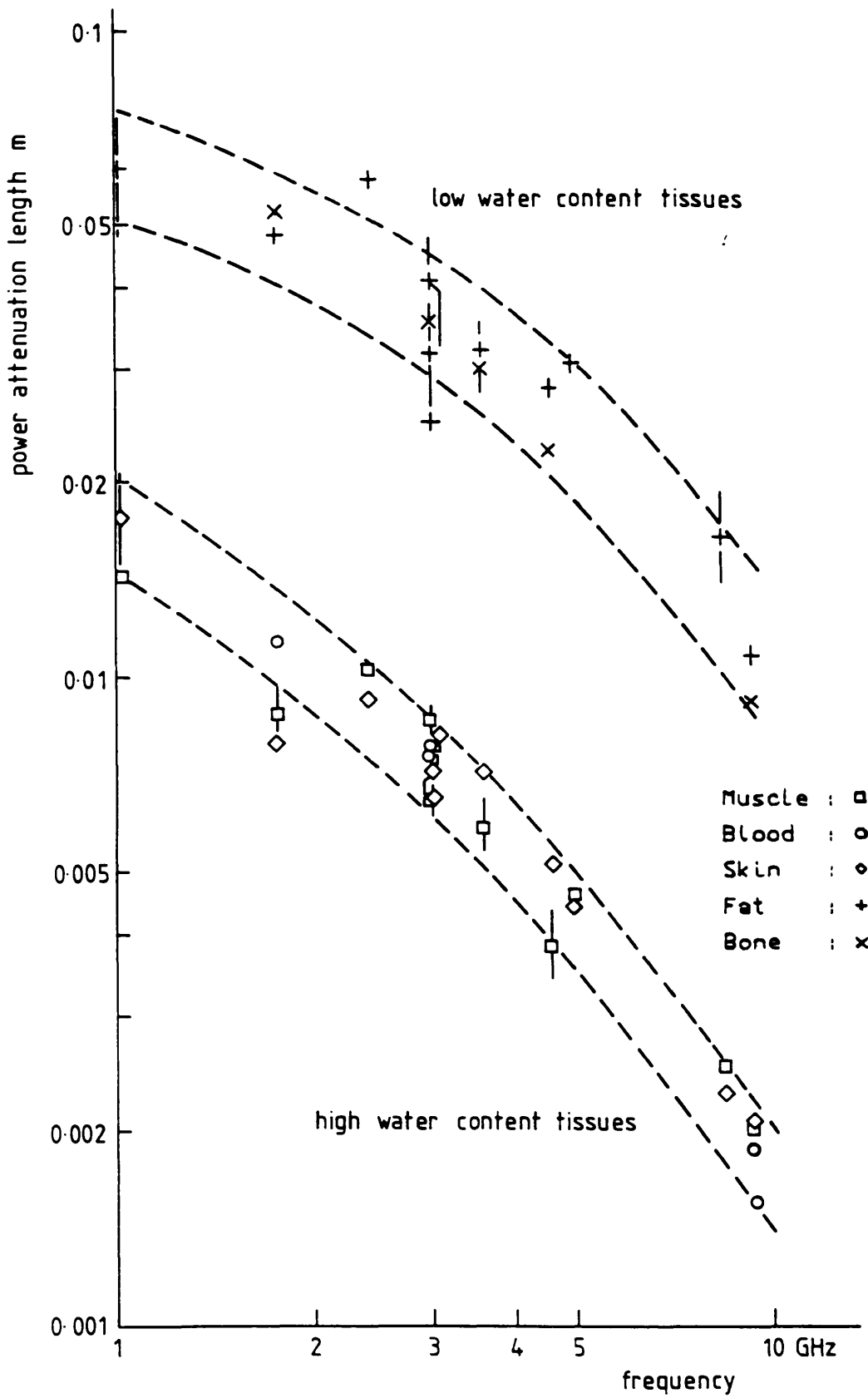


Figure 1.2 Penetration depth of microwave radiation in human tissues.

[Data compiled from Cook (1951,1952), Herrick (1950), England (1950)]

GHz because of the large size of collecting aperture which would be required and because of significant reflections of radiation from the deeper tissues at the skin-air boundary. Contact antennas matched to the impedance of the body tissues and operated flush with the skin surface minimise these reflections and are suitable for lower frequencies.

The total signal received by the radiometer is a weighted volume average of tissue temperature over a volume determined by the absorption properties of the tissues being viewed, the geometry of the tissues and the characteristics of the antenna. This will be discussed more fully in Chapters 2 and 3.

1.3 Thermometry and Thermography

Temperature has been used as a clinical measurement since Hippocrates used his hand to assess a patient's temperature in 400 BC. It was not until 1612 AD, however, that the first thermometer was used to measure body temperature by Sanctorius of Padua, following the development of the air thermometer by Galileo in 1595 AD. By the 1870's temperature measurement was generally adopted as a medical procedure (Solsona, 1978).

Measuring the general temperature of the body remains to this day an important technique for indicating the health of a patient. Normal body "core" temperature is approximately 37 °C but may vary about this throughout the day by as much as 1 °C. It is considered dangerous if the temperature should rise above 41 °C or ^{fall} below 35 °C.

The use of localised temperature measurements as a clinical technique began in about 1956 when Dr. Ray Lawson observed an apparent relationship between locally increased skin temperature and the presence of breast cancer. He initially used thermistors and other means of contact temperature measurement but in an effort to gain more complete information on the superficial thermal characteristics of female breasts he investigated the use of infra-red thermography (Lawson, 1956). Since then thermography has been applied to the investigation of an increasingly wide range of

diseases as may be seen from inspection of a journal such as *Thermology*. *

A measurement of local temperature reflects the vascular and metabolic state of the underlying tissue and the degree of inflammation. Skin temperature can be mapped successfully by infra-red or liquid crystal thermography. The effect of the temperature of the subcutaneous tissues on the skin temperature is extremely difficult to quantify and methods of measuring internal temperature are required to give information about the thermal condition of the deeper tissues and so provide information about their vascular and metabolic state.

1.3.1 Skin temperature measuring techniques

(i) Temperature probes

A variety of thermistor and thermocouple probes are available for point measurements of skin temperature (Cetas, 1985). These must be placed in contact with the skin and so may affect the delicate balance of heat transfer at the skin surface, altering the quantity which is to be determined. They do not provide an overall picture of the temperature distribution on the skin surface unless a large and time-consuming number of measurements are made.

(ii) Liquid crystal plate thermography

This technique makes use of liquid-crystal compounds which exhibit colour-temperature sensitivity in the cholesteric phase and thus reveal the skin temperature pattern as a coloured image. A thin blackened plastic sheet containing liquid crystals dispersed in a translucent polymer is placed firmly and uniformly against the surface being examined and the resulting image is usually photographed to obtain a permanent record of the thermal image. This technique has the disadvantages associated with a contact method of skin temperature measurement but it is cheap and reasonably effective and has been applied to investigate temperature patterns of the female breast, varicose veins patterns and back pain problems. (Jones 1987) [7,8]

* [M Abernathy (ed.); published by American Academy of Thermology]

(iii) Infra-red thermography

This is a non-contact method of measuring skin temperature. The skin surface is imaged by scanning the scene in front of an infra-red detector which transduces the radiant energy incident upon it into an electrical signal. Thermal, photon or pyroelectric type detectors can be used for this purpose, but most commercial systems employ photon detectors. The resultant thermal image is usually displayed quantitatively in the form of a colour picture on a television image tube. Scanning speeds range from one to fifty frames per second depending on the imaging system being used. A thermal resolution of 0.2 °C is provided by most systems designed for routine clinical use, although more complex systems with resolutions of 0.1 °C are available. This technique has a wide range of medical applications and is more accurate than liquid crystal plate thermography. (Jones 1987) [6]

1.3.2 Internal temperature measuring techniques

(i) Invasive techniques

Measurement of the internal temperature may be achieved by insertion of narrow temperature probes, such as thermistors or thermocouples, into the tissue. These are usually mounted in structures similar to hypodermic needles. Non-metallic temperature probes have been developed for use in the electromagnetic fields applied in the hyperthermia treatment of cancer. These fibre-optic thermometers use light propagating through optical fibres as a means of transmitting thermal information. (Christensen, 1981). Invasive measurement of temperature is undesirable due to the danger of physical damage and infection and the discomfort to the patient. It is also only possible to investigate the temperature in a limited volume of tissue with such techniques. [1]

(ii) Non-invasive techniques

A number of possible methods of non-invasive thermometry to determine internal temperatures, other than microwave thermography, are currently being

investigated. The motivation for these studies is often the need for a non-invasive method of monitoring hyperthermia treatment of cancer. This treatment involves heating tumour tissue to a temperature of 42 - 45 °C. Treatment may be either regional, in which case the temperature of normal tissue will be increased and the effectiveness of the therapy depends on the fact that at temperatures between 42 and 43.5 °C cancer cells are destroyed but normal cells are unharmed, → * The techniques considered depend on the measurement of a property of the tissue which has a temperature dependence.

(a) Microwave tomography : This is a method of active imaging involving illumination of the body tissues with microwave radiation. Appropriate tomographical techniques may be used to reconstruct an image of the observed part of the body which depends on the permittivity and conductivity of the tissues. The temperature may be determined from the temperature dependence of these properties with an expected resolution of about 1 °C (Perronet, 1983).

(b) Ultrasonic Tomography : This technique depends on the temperature dependence of the speed of sound in tissue, but may not be used in regions containing bone or gas (Johnson et al, 1977).

(c) NMR Imaging : The temperature dependence of the nuclear magnetic relaxation times of protons, mainly in the tissue water, may be applied with a resulting resolution of 2 °C (Parker, 1984).

(d) X-Ray Computed Tomography : The change in tissue density and hence absorption of X-rays with temperature can provide a technique with an estimated resolution of 1 °C (Fallone et al, 1982). Both this technique and NMR are very expensive.

1.4 Review of microwave thermography

Since 1974, when the first microwave thermography system was proposed for medical use (Enander and Larson, 1974), a number of different groups have been investigating this technique. Research so far has concentrated on the development of

* or local hyperthermia may be applied,

where an attempt is made to raise only the temperature of the tumour using, possibly, radio-frequency heating, microwaves or focussed ultra-sound[11].

suitable radiometric equipment with only limited assessment of the clinical potential of the technique.

One of the first clinical microwave radiometer systems was developed by Barrett and Myers (1979, 1980a,b, 1986) who carried out extensive clinical trials of their equipment in the detection of breast cancer, examining a total of about 6000 female patients. This investigation was chosen because of the need for a simple screening technique for the early detection of breast cancer in view of the risks associated with X-ray mammography^[2] and the uncertainty in the effectiveness of infra-red thermography. [5]

Their original system operated at 3.3 GHz and they later built and clinically tested a 1.3 GHz and a 6 GHz system. All systems consisted of a conventional Dicke-switched radiometer and a rectangular waveguide antenna filled with a low-loss dielectric, which was operated in contact with the skin surface.

Measurements were made at nine points on each breast and a number of different tests were applied to this data to find the best criteria for detection of cancer. This was found to be the maximum temperature difference between symmetrically opposite points on each breast. A threshold value for this difference was chosen above which the scan was designated positive. The performance of their systems indicated true-positive and true-negative detection rates of about 0.7 for microwave thermography. Their sample of patients, however, was not a random selection of the population but consisted of women who attended a breast cancer detection clinic and the results of screening on the general population might have produced different results.

In a subgroup of 1000 patients who underwent infra-red thermography as well as microwave thermography the findings of these two techniques disagreed in 41% of the cancer cases, indicating that different thermal information is extracted from these two methods. They suggested that a combination of both techniques could be used to improve the detection rates and reduce the number of women requiring mammography (Barrett and Myers, 1980).

The equipment used in this study was of a basic design. A compensation for the impedance mismatch at the antenna-tissue interface does not appear to have been used which could result in sensitivity of the results to impedance variations in the tissue. These results should therefore be considered as indicative of the potential of the technique rather than as an absolute measure of the performance to be expected of all microwave thermography systems.

Edrich (1979) developed a remote sensing thermography system which focussed the radiation through a lens or large reflector into a horn and detected the signal with a Dicke radiometer. Measurements were carried out at millimetre wavelengths of 4mm (68 GHz) and 9mm (30 GHz) and at the centimetric wavelength of 3cm (9 GHz). The use of this technique was demonstrated in the monitoring of arthritis, in thermal imaging of the head and neck region and in detection of breast cancer (Edrich, 1980). Millimetre wavelengths are suitable for detection by non-contacting thermography because the emissivity of the skin is close to 1 in this region (i.e. the tissue strongly absorbs radiation of this wavelength) and as a result of this the radiation detected originates within only a few millimetres of the skin surface so that the advantage over infra-red thermography is only slight. At the lower frequency of 9 GHz radiation is less strongly absorbed and a smaller percentage of the total emission originates at the skin surface. This leads to reflection of radiation originating in deeper tissues at the skin-air boundary. To compensate for this measurements were carried out in an environment of 32-33 °C where reflection of radiation from the surroundings at the skin surface would compensate for the internal reflection of radiation. This would appear to be an unsatisfactory arrangement since placing the patient in such a warm environment would cause an increase in blood flow through the skin and so mask the effects of "hot spots" buried deeper in the tissue.

Recently another system using a remote, scanned, focussed-beam antenna operating at a frequency of 9 GHz has been built (Abdul-Razzak et al, 1987). Measurements made on 25 patients with occlusive vascular disease and on 30 normal

controls indicate that a detection rate for this disease may be achieved which is comparable with the present invasive and more costly technique of angiography. The advantage of this method of non-contacting thermography over infra-red thermography is, however, unclear. The spatial resolution achievable is less than that with infra-red and the value of the increased penetration depth is uncertain in view of the reflection of this radiation from deeper in the body at the skin-air boundary.

Thouvenot (1982) has investigated the detection of intracranial lesions by non-contacting radiometers, operating at 9, 30 and 68 GHz, developed by Edrich, and a contacting radiometer developed by Leroy operating at 9 GHz. Nine normal controls showed left-right symmetry and an absence of sharp variations in local temperature, while in a group of 30 patients with tumours, thermal anomalies were seen in all those with superficial lesions. Only 5 deep lesions out of nine were detected. If a lower frequency were to be used to improve the penetration depth it is possible that these results might be improved. A comparison of the results of the contacting and non-contacting systems operating at 9 GHz was, unfortunately not discussed.

The detection of various human cancers by microwave thermography has been studied by Shaeffer (1982) using a 4.7 GHz contacting radiometer. It was found that this system was able to detect breast cancers but had little success detecting deeply seated tumours in other regions of the body such as the lung, esophagus, femur and humerus. This is most probably due to the lack of penetration of the microwave radiation through these tissues, but the physiological changes which take place in the presence of tumours and lead to thermal changes need to be considered as well. In the case of breast cancer it is often possible to detect deeply seated tumours due to vascular changes and Barrett and Myers found no correlation between the temperature rise associated with a tumour and either tumour size or tumour depth. This illustrates the importance of physiological aspects in tumour detection by thermography which must be taken into account as well as the absorbing properties of the tissue.

A method of improvement of detection of tumours by combined local heating

and thermography by microwaves has been proposed by Carr (1982). Preferential heating of the tumour is expected to occur because of its vascular insufficiency, → *

This method may also be applied as a method of simultaneous hyperthermia treatment and monitoring of tissue temperature.

Iskander (1983) has proposed microwave radiometry for measuring changes in the water content of the lung and has constructed a 1 GHz system which has been tested experimentally with "phantom" materials. It is possible to use such a low frequency in this case because the average lung water content is the quantity of interest and spatial resolution is not a restriction. In this application the temperature of the lung is assumed kept constant by the high rate of blood perfusion and changes in the observed microwave radiation are taken to be due to a change in the emission of radiation from the lung with water content. The effect of emission from the cutaneous tissues, however, has to be taken into account and the author proposes combining measurements at 1 GHz with measurements at millimetre wavelengths to determine the surface temperature. Further research is required to clarify the potential of this method.

An improvement in the conventional Dicke-switched radiometers, which are generally used for microwave thermography, has been proposed by Mamouni (1977) and by Ludecke (1978). This modified radiometer is designed to eliminate the effect of reflections at the antenna-tissue interface and more accurately measure the radiation emitted by the body tissues. This type of radiometer has been built at the Universite de Lille with six probes used to receive the signal instead of the usual single antenna (Enel et al, 1984). Each probe consists of a rectangular waveguide filled with a low-loss dielectric and they are placed together to form a 2 x 3 grid. This multi-probe system can be used to provide an improved spatial resolution and reduces the data acquisition time. A micro-computer is used to control switching between the probes, acquisition, storing and processing of the data and the final imaging. Radiometers working at frequencies of 1.5 and 3 GHz have been used to experimentally determine the microwave visibility of a compact thermal structure (Bocquet, 1986) and work has been

* which may occur in malignant tumours other than of the breast, and also at the necrotic core of malignant breast tumours.

carried out to determine the volume of tissue which contributes to the received signal for a defined situation (Robillard, 1982). A clinical investigation of the use of this equipment is currently being carried out (Bocquet, 1988).

The problem of inversion of multi-frequency microwave radiometric data to provide a reconstruction of the temperature distribution in the tissue has been studied by a group at the Universita' Tor Vergata, Rome (Bardati 1986,1987) and initial experimental tests of a proto-type four channel radiometer (with central operating frequencies in the range 1.5 to 5.5 GHz) have been carried out (Bardati, 1987). This is a difficult approach to the problem of interpretation of microwave thermography data but, if successful, will greatly improve the results available from single frequency microwave thermography. It will be particularly useful in the monitoring of hyperthermia treatment where it is necessary to carefully monitor the temperature of the tumour and that of the surrounding tissue.

Correlation microwave radiometry has also been proposed as an improvement of single frequency, single antenna microwave thermography (Mamouni, 1983). This technique uses two identical radiometer channels and antennas. The antennas are arranged to view a common volume of tissue inside the body. Since the signal in each channel is composed of a component from the common region and a component from the rest of the antenna's field of view, the common component may be separated out. The radiometric signal originating at depth inside the tissue may therefore be determined. By adjusting the relative orientation of the two antennas the depth observed inside the tissue may be altered. This technique is still in the early stages of development.

Research in microwave thermography has demonstrated that it is practical to build microwave thermography systems with sufficient sensitivity to detect thermal anomalies and suitable for operation in clinical environments at a very reasonable cost. It is now necessary to clinically evaluate the different applications of this technique. Improvements have been made in radiometers since the relatively simple design of

Barrett and Myers. They carried out the only large scale clinical investigation published so far and further work of this kind should be carried out. It is also important to consider the different factors involved in producing the thermal anomalies associated with disease and observed by microwave thermography. This will lead to improved interpretation of microwave thermographic data and clarification of the areas in which this technique will be useful.

Chapter 2 - Basic Principles of Microwave Thermography

2.1 Introduction

This chapter introduces some fundamental quantities and equations used in radiometric sensing of the human body and examines the formation of the signal received by the radiometer. Many of the concepts involved in this field are also applied in radio astronomy and for consistency, where appropriate, notation and terms used here are similar to those in radio astronomy. The topics discussed here will include emission and absorption of radiation, radiative transfer, the effect of the antenna pattern on the observations and antenna temperature.

2.2 Equation of radiative transfer

Radiation is usually defined in terms of intensity, either spectral intensity which refers to radiation emitted in a small frequency interval about a central frequency or total intensity which refers to the combined radiation at all frequencies. In microwave thermography it is the spectral intensity in a small band of microwave frequencies which is the relevant quantity and this will be referred to in future merely as the intensity.

Intensity, I_ν , is related to the amount of radiative power, dP , in a specific frequency band, $d\nu$, which is transported across an element of area, $d\sigma$, and in directions confined to an element of solid angle $d\omega$,

$$dP = I_\nu \cos\theta d\omega d\sigma d\nu \quad (2.2.1)$$

where θ is the angle between the direction considered and the outward normal to the surface $d\sigma$.

As already described in Chapter 1 the intensity of radiation emitted by a black body, B_ν , is independent of its nature and is a function only of temperature. This function is often referred to as the "Planck function" and is given by the Planck law:

$$B_\nu(T) = \frac{2h\nu^3}{c^2 \left(\exp\left(\frac{h\nu}{kT}\right) - 1 \right)} \quad (2.2.2)$$

At microwave frequencies and body temperatures $h\nu/kT \ll 1$, and the Planck function can be approximated to the Rayleigh-Jeans law,

$$B_{\nu}(T) = \frac{2 k T \nu^2}{c^2} \quad (2.2.3)$$

The intensity, $B_{\nu}(T)$, given in equations (2.2.2) and (2.2.3), is in terms of a frequency bandwidth $d\nu$, whereas in equation (1.2.1) the intensity was given in terms of a wavelength interval, $d\lambda$.

For a non-black body the intensity is dependent on both the temperature and the nature of the material and will be less than that emitted by a black body at the same temperature.

For a small element dm of an isotropic non-black body in an isotropic field of radiation the power emitted in a bandwidth $d\nu$, in directions confined to an element of solid angle $d\omega$, can be expressed as

$$j_{\nu} dm d\omega d\nu \quad (2.2.4)$$

where j_{ν} is the emission coefficient for frequency ν .

A pencil of radiation passing through a thickness dz of this material will be reduced from its original intensity I_{ν} to $I_{\nu} + dI_{\nu}$ where

$$dI_{\nu} = - k_{\nu} \rho I_{\nu} dz \quad (2.2.5)$$

where k_{ν} is the mass absorption coefficient and ρ is the density of the material.

An important relation between these two quantities of emission and absorption is given by Kirchhoff's law (Chandrasekhar, 1939) which states that the ratio of the emission to absorption coefficients of any body in thermodynamical equilibrium is equal to the intensity of the radiation emitted by a black body at the same temperature, T :

$$B_{\nu}(T) = \frac{j_{\nu}}{k_{\nu}} \quad (2.2.6)$$

A small cylinder of material at a temperature above absolute zero, with

cross-sectional area $d\sigma$ and length dz , which has radiation of intensity I_v incident in the z -direction on one face and intensity I_v+dI_v emerging from the second face in the same normal direction will both absorb part of the incident radiation and emit radiation. The power per unit bandwidth through the cross-section of the cylinder in a direction confined to a solid angle $d\omega$ about the z -direction is given by $I_v d\sigma d\omega$, of which an amount $k_v \rho I_v dz d\omega d\sigma$ is absorbed by the cylinder. The power per unit bandwidth emitted by the cylinder is equal to $j_v \rho dz d\omega d\sigma$ and in a steady state condition,

$$dI_v d\sigma d\omega = j_v \rho d\sigma d\omega dz - k_v \rho I_v d\sigma d\omega dz \quad (2.2.7)$$

or

$$\frac{dI_v}{dz} = j_v \rho - k_v \rho I_v \quad (2.2.8)$$

This equation is known as the equation of transfer (Chandrasekhar, 1939).

The ratio of the emission to absorption coefficients is called the source function,

$$S_v = \frac{j_v}{k_v} \quad (2.2.9)$$

and the equation may be expressed in the form

$$-\frac{1}{\rho k_v} \frac{dI_v}{dz} = I_v - S_v \quad (2.2.10)$$

which has a formal solution

$$I(0) = I(d) \exp(-\tau(0,d)) + \int_0^d S_v(z') \exp(-\tau(0,z')) k_v \rho dz' \quad (2.2.11)$$

where $\tau(z,z')$ is known as the optical thickness of the material between the points z and z' and is given by

$$\tau(z,z') = \int_z^{z'} k_v \rho ds \quad (2.2.12)$$

For a material with uniform density, as may be considered the case for human tissue, the optical thickness is

$$\tau(z,z') = k_v \rho (z' - z) \quad (2.2.13)$$

and equation (2.2.11) becomes

$$I(0) = I(d) \exp(-k_v \rho d) + \int_0^d S_v(z') \exp(-k_v \rho z') k_v \rho dz' \quad (2.2.14)$$

Comparison of this equation with the power attenuation of electromagnetic radiation as it passes through a lossy medium indicates that

$$k_v \rho = 2 \alpha \quad (2.2.15)$$

where α is the plane wave field attenuation constant determined by the dielectric properties of the material.

The human body may be considered to be in thermodynamical equilibrium when at rest in an environment of constant temperature and in this case the source function is equal to the Planck function which at microwave frequencies is approximated to Rayleigh-Jeans law, giving the final expression

$$I(0) = I(d) \exp(-2\alpha d) + \frac{2v^2 k}{c^2} \int_0^d 2\alpha T(z') \exp(-2\alpha z') dz' \quad (2.2.16)$$

The physical meaning of this equation is that the intensity of radiation emitted at the body surface in a given direction is the sum of the emission at all the interior points at position z' reduced by an amount $\exp(-2\alpha z')$ to account for absorption by the intervening matter. The emission at each interior point depends on the temperature at that point and the dielectric properties of the material which determine α . If more than one type of material is present then integration should be performed over each region. For a layered material with three regions, corresponding to a skin layer of thickness t_1 , a fat layer of thickness t_2 , and an infinite muscle layer, the intensity emitted at the surface, neglecting the effect of reflections at the boundaries, will be

$$I(0) = \frac{2v^2 k}{c_1^2} \int_0^{t_1} 2\alpha_1 T(z) \exp(-2\alpha_1 z) dz + \frac{2v^2 k}{c_2^2} \exp(-2\alpha_1 t_1) \int_{t_1}^{t_1+t_2} 2\alpha_2 T(z) \exp(-2\alpha_2 z) dz + \frac{2v^2 k}{c_3^2} \exp(-2\alpha_1 t_1) \exp(-2\alpha_2 t_2) \int_{t_1+t_2}^{\infty} 2\alpha_3 T(z) \exp(-2\alpha_3 z) dz \quad (2.2.17)$$

where the subscripts 1, 2 and 3 refer to the skin, fat and muscle layers respectively.

Radiative transfer models for layered dielectric materials, which include the wave effects of reflection and interference have been developed (Wilheit, 1978, Bardati and Solimini, 1984). These models were developed originally for applications in remote sensing of the earth's surface but are applicable also to imaging of the human body.

If the temperature T is uniform throughout the material the intensity emitted by a homogeneous slab of thickness d is given by

$$\frac{2 v^2 k T}{c^2} (1 - \exp(-2\alpha d)) \quad (2.2.18)$$

It can be seen that if αd is very large, in other words the material is "optically thick" then the intensity emitted is approximately equal to that emitted by a black body at the same temperature. If the material is optically thin (i.e. $\alpha d \ll 1$) then the intensity emitted is approximately

$$\frac{2 v^2 k T}{c^2} 2 \alpha d \quad (2.2.19)$$

and is much less than that emitted by a black body at the same temperature.

2.3 Antenna response function

The noise power available per unit bandwidth, w , at the terminals of a resistor with resistance R and temperature T is given by (Nyquist 1928)

$$w = kT \quad (2.3.1)$$

Consider an antenna in contact with a lossy material of the same impedance and connected to a terminating resistor by a lossless transmission line which is also impedance matched to the antenna. If the system is in thermodynamic equilibrium and is at a uniform temperature T , then the terminating load, being a resistor at temperature T , radiates an average power of kT watts per unit bandwidth through the transmission line and into the lossy material. The condition of thermodynamic equilibrium requires that the antenna must also receive kT watts per unit bandwidth from the lossy material. If the antenna, transmission line and load are at a temperature different from the lossy

medium the antenna must still receive the same power per unit bandwidth.

The power per unit bandwidth, P , received by the antenna may also be expressed as

$$P = \frac{1}{2} \int_V I_v(\mathbf{r}) P_n(\mathbf{r}) dV \quad (2.3.2)$$

where $I_v(\mathbf{r})$ is the intensity of radiation emitted by the volume element dV at position \mathbf{r} , with origin at the position of the antenna. $P_n(\mathbf{r})$ is the normalised power response pattern of the antenna given by

$$P_n(\mathbf{r}) = \frac{P(\mathbf{r})}{\max (P(\mathbf{r}))} \quad (2.3.3)$$

and is referred to as the antenna pattern. The factor of 1/2 in equation (2.3.2) arises because the radiation is of an incoherent, unpolarized nature and, because any antenna is responsive to only one polarisation component, only half of the incident power is received.

By the reciprocity theorem (Slater 1942) the transmitting and receiving power patterns of an antenna are identical. This means that the power dissipated in a volume element when the antenna is radiating into the lossy medium is proportional to the power received from that volume element when the antenna is receiving. The power, P , dissipated in a subvolume dV is given by

$$P = \frac{1}{2} \sigma | \underline{E}_0 |^2 dV \quad (2.3.4)$$

where σ is the conductivity ($\Omega^{-1}m^{-1}$), and $\underline{E} = \underline{E}_0 e^{i\omega t}$ is the electric field.

The receiving power response pattern must be proportional to this and so

$$P_n(\mathbf{r}) = A | \underline{E}(\mathbf{r}) |^2 \quad (2.3.5)$$

where A is a constant of proportionality.

From equation (2.2.19) the intensity of radiation emitted in the region of the Rayleigh-Jeans law by a small thickness, dz , of homogeneous material is given by

$$I_v(\mathbf{r}) = \frac{2 v^2 k T(\mathbf{r})}{c^2} 2\alpha dz \quad (2.3.6)$$

Using (2.3.5) and (2.3.6) in (2.3.2) we have

$$P = \frac{v^2 k}{c^2} A \int_V 2\alpha T(\mathbf{r}) | \underline{E}(\mathbf{r}) |^2 dV \quad (2.3.7)$$

For a uniform temperature T it has already been shown from thermodynamical considerations that the power received per unit bandwidth is equal to kT and so we must have

$$\frac{v^2 A 2\alpha}{c^2} \int_V |E(\underline{r})|^2 dV = 1 \quad \text{or} \quad \frac{2\alpha}{\lambda^2} \int_V P_n(\underline{r}) dV = 1 \quad (2.3.8)$$

In general, for a lossy material, it is a difficult problem to determine theoretically the distribution $E(\underline{r})$. The antenna pattern, however, may be described approximately by an exponential variation in the direction of the central axis of the antenna in a single region of tissue, while the lateral response is considered to be uniform over an area of effective aperture size, A_e , and zero outside this area.

i.e.

$$\begin{aligned} P_n(\underline{r}) &= \exp\left(-\frac{z}{\delta'}\right) && \text{if } (x,y) \in A_e \\ &= 0 && \text{if } (x,y) \notin A_e \end{aligned} \quad (2.3.9)$$

where δ' is the effective power penetration depth which is related to the effective field attenuation constant, α' , by the equation

$$\delta' = \frac{1}{2\alpha'} \quad (2.3.10)$$

This is the normalised power pattern having a maximum value of 1 at $z=0$ and for this form of power pattern equation (2.3.8) requires that

$$A_e = \frac{\delta}{\delta'} \lambda^2 \quad (2.3.11)$$

where δ is the plane wave power penetration depth.

The effective power penetration depth must always be less than the plane wave power penetration depth, and it should be noted that the plane wave penetration depths in tissue indicate the maximum possible performance of a radiometer system. These plane wave depths will not in practice be achievable because the tissue being viewed is in the near-field of the antenna. If we assume, however, that we may have a far-field antenna response then we have a minimum effective aperture size given by

$$A_e = \lambda^2 \quad (2.3.12)$$

and equation (2.3.2) is given by,

$$P = k \int_0^{\infty} 2\alpha T(z) \exp(-2\alpha z) dz \quad (2.3.13)$$

for a temperature variation in the z-direction only.

It can be seen by comparison with equation (2.2.16) and applying equation (2.2.1) that this corresponds to observing the radiation emitted at the surface with an antenna which has a product of effective area and solid angle equal to λ^2 . This is in agreement with antenna theory for an antenna viewing sources in its far-field which gives (Kraus 1966)

$$A_e = \frac{\lambda^2}{\Omega_A} \quad (2.3.14)$$

where Ω_A is the beam solid angle,

$$\Omega_A = \int_{4\pi} P_n(\theta, \phi) d\Omega \quad (2.3.15)$$

In the case where the effective power penetration depth is less than that of the plane wave penetration due to near field effects the effective aperture size A_e is larger than λ^2 , indicating a widening of the response pattern of the antenna.

Since the effective aperture size must vary, according to (2.3.11), as λ^2 this cancels out the λ^{-2} dependence of the intensity of the emitted radiation and substituting equations (2.3.6), (2.3.9) and (2.3.11) into (2.3.2) gives

$$P = k \int_0^{\infty} T(z) 2\alpha' \exp(-2\alpha'z) dz \quad (2.3.16)$$

for a temperature variation in the z-direction only and for a single region of tissue. The quantity $2\alpha'\exp(-2\alpha'z)dz$ is proportional to the power deposited in a thickness of tissue dz at position z . The power deposited in any region of tissue may be calculated from the time averaged Poynting vector, S_{av} , where

$$S_{av} = \frac{1}{2} \text{Re} (\underline{E}^* \times \underline{H}) \quad (2.3.17)$$

The electric and magnetic fields, \underline{E} and \underline{H} , may be calculated by solution of Maxwell's equations and the power deposited in a small thickness of tissue dz , for power propagation in the z-direction, is given by

$$\frac{dS_{av}}{dz} dz$$

Equation (2.3.16) may therefore be expressed

$$P = k A \int_0^{\infty} T(z) \frac{dS_{av}}{dz} dz \quad (2.3.18)$$

where A is a constant of proportionality such that $AS_{av}(0)=1$.

This equation may be used to determine the power received per unit bandwidth from a planar layered volume of tissue, with known dielectric properties in each layer and temperature distribution $T(z)$, assuming that there is no impedance mismatch between the antenna and the volume of tissue. The effect of the antenna is assumed to increase the field attenuation constant from α to α' and with this assumption the derivative of the Poynting vector in the layered material may be calculated using plane wave theory (Johnk, 1975).

2.4 Antenna temperature

The antenna temperature, for a lossless antenna, is not the physical temperature of the antenna itself but is related to the temperature of the radiation sources viewed by the antenna. If the power received by the antenna per unit bandwidth is equal to w then the antenna temperature is defined to be

$$T_A = \frac{w}{k} \quad (2.4.1)$$

If a volume of homogeneous lossy material at a uniform temperature T is being viewed by the antenna and this material completely fills the entire volume V of the antenna's pattern then the antenna temperature is equal to the physical temperature of the material. If the material does not entirely fill the volume V then the antenna temperature will be less than the physical temperature of the material. The antenna temperature in this case will be the equivalent temperature required for a material filling the entire volume to emit the same power. This is an analogous situation to that of the intensity emitted at the surface of a planar layer of lossy material discussed in section

2.2. If the material completely fills the volume seen by the antenna then it is effectively a semi-infinite layer and the power received by the antenna is equal to that emitted by a black body at the same temperature, if the antenna is matched to the material. Otherwise the power received is less than that emitted by a black body at the same temperature and it is necessary to know the antenna pattern $P_n(\underline{r})$, the geometry of the emitting volume and the coefficient 2α to determine the physical temperature. If the temperature is not uniform then it is not possible to determine the temperature distribution in the material from a measurement of microwave power at a single frequency even if the antenna pattern and geometry of material are known.

Chapter 3 - Microwave Radiometry

3.1 Introduction

Microwave techniques developed to detect and measure the emission from astronomical sources can be applied, with some modifications, to the detection of radiation from the human body. The requirements which must be considered in the design of a medical microwave radiometer are

- (1) spatial resolution
 - (2) penetration depth of microwave radiation through tissue
 - (3) temperature resolution
- and (4) system response time

The spatial resolution and the penetration depth are both dependent on the frequency at which the radiometric measurement is made, and also on the design of the receiving antenna. The temperature resolution is determined by the sensitivity of the radiometer, which is affected by statistical fluctuations in the thermal noise emitted by the source and by the receiver, and by spurious variations in the gain of the receiver. The temperature resolution required for clinical applications of a single frequency microwave thermography system is about 0.1°C , which may be achieved by appropriate receiver design. The system response time should be as short as possible, but is limited by the requirements of temperature resolution; a shorter response time reduces the sensitivity of the radiometer. A response time of longer than 10 seconds would most likely be considered unsuitable for clinical applications because of the length of time required for data collection.

The following sections of this chapter discuss the measurement frequency which provides the best compromise between the requirements of spatial resolution and penetration depth, and the factors which affect the temperature resolution. The microwave radiometric system used in this study is described and the factors affecting the antenna response pattern are considered. Experimental and theoretical determinations of response patterns of antennas suitable for microwave thermography

are reviewed.

3.2 Choice of measurement frequency

In microwave radiometry it is important to carefully consider the central frequency at which a spectral measurement of the radiation emitted by the human body is to be made, since this choice of frequency strongly influences the lateral spatial resolution available and the possible depth of penetration of the microwave radiation.

The lateral resolution, determined from geometrical optics, is of the order of one half the wavelength in the tissue, λ_t ,

$$\frac{\lambda_t}{2} \equiv \frac{\lambda_o}{2\sqrt{\epsilon_r}} \quad (3.2.1)$$

where λ_o is the wavelength in free space and ϵ_r ' is the relative dielectric constant.

As the frequency increases the wavelength in the tissue decreases and the achievable resolution improves.

The depth of penetration of microwave radiation through tissue, however, decreases as the frequency increases (see figure 1.2). The choice of measurement frequency is therefore a compromise between lateral spatial resolution and the depth in tissue from which temperature information is received. In order to obtain a clinically useful penetration depth in all tissues figure 1.2 indicates that the measurement frequency should be below 10 GHz. As noted in section 2.3 this plane wave penetration depth indicates the maximum depth from which a signal may be received. In practice this depth will be reduced by the effects of the antenna pattern. This distance, however, is a very useful measure to determine the optimum performance of microwave radiometry.

The inverse of power penetration depth, the power attenuation constant, which is twice the field attenuation constant, is given by the expression (Lorrain and Corson, 1970),

$$2\alpha = \frac{4\pi}{\lambda_0} \sqrt{\frac{\epsilon_r'}{2}} \left\{ \left(1 + \left(\frac{\epsilon_r''}{\epsilon_r'} \right)^2 - 1 \right)^{\frac{1}{2}} \right\}^{\frac{1}{2}} \quad (3.2.2)$$

where ϵ_r'' is the loss factor. When $\epsilon_r'' / \epsilon_r'$, which is the loss tangent, $\tan\delta$, is small (i.e. less than one) this expression is given approximately by

$$2\alpha = \frac{2\pi\sqrt{\epsilon_r'}}{\lambda_0} \tan \delta \quad (3.2.3)$$

This is a valid approximation for body tissues.

Maximum spatial resolution occurs at a minimum of equation (3.2.1) and maximum penetration depth occurs at minimum of equation (3.2.3). The product of these two functions is proportional to the loss tangent, $\tan \delta$, and a minimum value of this, in the microwave region, will provide the best compromise between the requirements of lateral spatial resolution and penetration depth. The loss tangent of physiological saline solution has a minimum value at around 3 GHz. This arises because between 1 and 10 GHz the dielectric constant is relatively constant, being at the beginning of the dielectric dispersion due to the polar water molecules. The contribution to the loss factor from the dielectric dispersion is increasing in this frequency range, while the contribution from the ionic conductivity is decreasing. These factors combine to produce a loss tangent minimum at 3 GHz (see figure 5.2). The loss tangent of body tissues can be expected to follow this behaviour since the dielectric properties of tissue at microwave frequencies are strongly dependent on the water content of the tissue. This indicates that 3 GHz represents the optimum measurement frequency for microwave thermography (Land, 1987).

3.3 Temperature resolution

3.3.1 Noise signals

Thermal radiation is characterised by a very wide spectrum. The amplitudes and phases of different frequency components are completely independent and the intensity of this thermal noise signal is very low. The radiometer which detects and measures this signal must be a very sensitive, low noise broad-band receiver. The minimum

temperature change which may be detected is limited by fluctuations in the receiver output caused by the statistical nature of the noise waveform. This noise is proportional to the system temperature, which may be divided into two principal parts, that contributed by the antenna temperature, due to the source of thermal radiation, T_A , and that contributed by the receiver, T_R . The sensitivity is equal to the rms noise temperature of the system which is given by (Kraus, 1966),

$$\Delta T_{\min} = \frac{K_s T_{\text{sys}}}{\sqrt{\Delta v_{\text{HF}} \tau_{\text{LF}}}} \quad (3.3.1)$$

where K_s is the sensitivity constant (dimensionless),

T_{sys} is the system noise temperature at the antenna terminals, $T_{\text{sys}} = T_A + T_R$, (K),

Δv_{HF} is the pre-detection bandwidth (Hz),

and τ_{LF} is the post-detection equivalent integration time (s).

The constant K_s depends on the type of receiver and its mode of operation, but is of the order of unity. The system noise temperature at the antenna terminals depends on the antenna noise temperature, the receiver noise temperature, the physical temperature of transmission line between the antenna and receiver and the efficiency of the transmission line. The sensitivity of the radiometer may be improved by increasing the pre-detection bandwidth but this is limited practically by the frequency over which the antenna may be matched to the body tissues. Increasing the post-detection integration time will also improve the sensitivity but this is limited by the required response time of the system. The effect of reducing the noise temperature, T_R , while improving the sensitivity, becomes progressively less worthwhile because the antenna noise temperature, T_A , due to the source, is always present.

3.3.2 Gain fluctuations

The gain of the receiver may vary due to supply voltage changes to active devices and changes in the ambient temperature. Stabilised voltages are easily provided, but inherent gain variations of a few percent per degree Celsius in active devices

require precise temperature sensitive compensation. Practical measures can reduce gain variations to 1 - 10 % over the typical environmental temperature ranges encountered in clinical use.

In a receiver which measures the total noise power from the antenna and receiver the output reading, R , is proportional to the total input noise temperature and to the receiver gain, G ,

$$R = G (T_A + T_R) \quad (3.3.2)$$

A small fractional variation in the gain, dG , will cause a change in the output dR ,

$$dR = dG (T_A + T_R) \quad (3.3.3)$$

For a typical situation where T_A is 310 K, T_R is 400 K and a change in gain of only 1% occurs, the output reading will change by 7 K causing a serious reduction in the temperature resolution. Another problem with this type of radiometer is that any variation in the noise temperature, T_R , will be indistinguishable from a variation in the antenna temperature caused by a source temperature change.

The effect of gain variations can be reduced by the use of a Dicke radiometer configuration in which the receiver input is continually switched between the antenna and a comparison noise source at a frequency high enough to ensure that the gain is stable over a switching period (Dicke, 1946). The output from the radiometer is now a square wave rather than a steady dc voltage. The size of the square wave represents the difference in magnitude between the signal from the antenna and the signal from the reference source. A synchronous detector is used to measure this signal and give an output which is directly proportional to this difference,

$$R = G (T_A + T_R) - G (T_{ref} + T_R) = G (T_A - T_{ref}) \quad (3.3.4)$$

and the change in output due to a change in gain is now given by

$$dR = dG (T_A - T_{ref}) \quad (3.3.5)$$

It can be seen that this change can be made negligibly small by adjusting the reference temperature to be equal to the antenna temperature, and that the measured signal is not dependent on the noise temperature T_R .

3.4 Radiometer equipment

The radiometer used in this study was a 3 GHz system designed and built by Dr. D V Land, University of Glasgow. This equipment was designed to be suitable for routine clinical use. A diagram of the radiometer design is shown in figure 3.1 and figure 3.2 shows a photograph of this equipment.

The radiometer is Dicke-switched between the antenna and a reference source. After low noise pre-amplification over the bandwidth 3.0 to 3.5 GHz the signal is converted by a mixer and local oscillator at 3 GHz down to an intermediate frequency (IF) band of 0 to 500 MHz for further amplification. The signal is then measured by a square law detector. The amplified and detected input difference signal, $G (T_A - T_{ref})$, at the 1 kHz switching frequency is further amplified, synchronously detected and passed through a low-pass filter (~ 1 Hz). Compensation is applied for the gain variation with temperature of the microwave pre-amplifier. The microwave difference signal and the reference source temperature signal are added, and scaled to provide a calibrated antenna temperature in degrees Celsius.

The reference noise source is a standard microwave 50Ω coaxial load, heated to approximately 40°C . This temperature is measured with a semiconductor temperature sensor. When the Dicke switch is on the antenna the noise from the reference source is directed to the antenna by a circulator where some of it is reflected at the antenna-skin boundary back into the receiver. This compensates for the radiation reflected internally back into the tissue. The accuracy of this method depends on how close the reference temperature is to that of the source. Self-balancing radiometers have been proposed (Ludecke, 1978) which adjust the reference temperature to be equal to that of the source and so eliminate the effect of reflections at the boundary. This method is more complex than that used here and is accompanied by a reduced receiver sensitivity and a longer response time for a given temperature resolution.

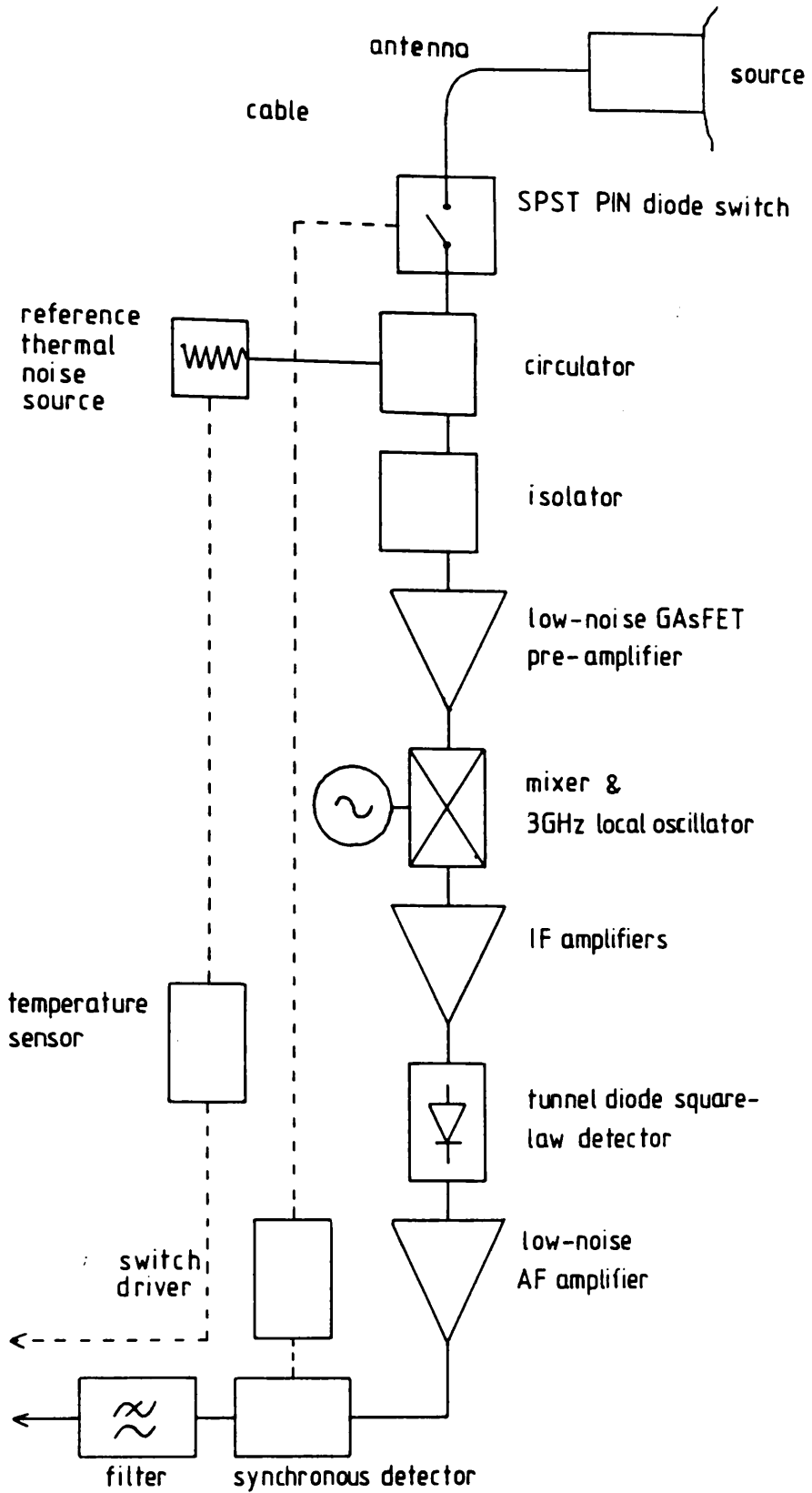


Figure 3.1 3 GHz microwave radiometer design

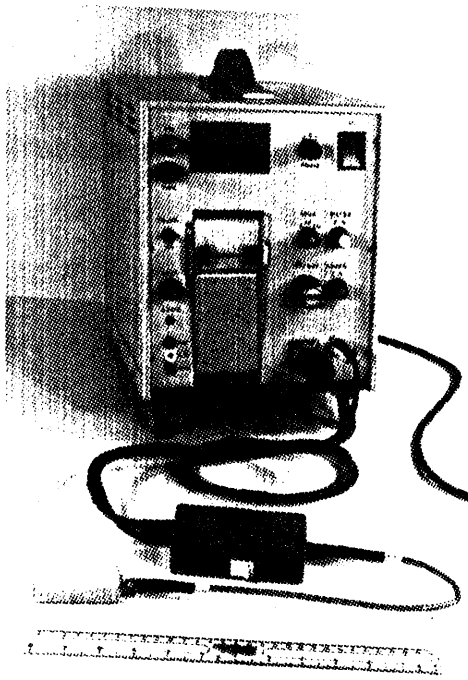


Figure 3.2 Glasgow microwave thermography system

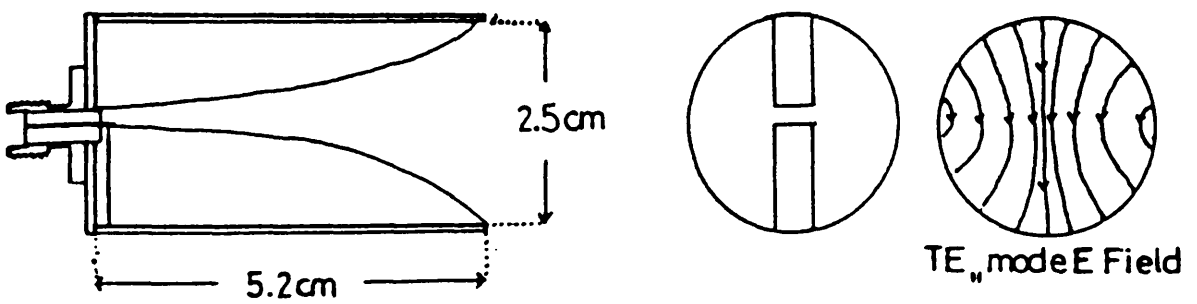


Figure 3.3 Cylindrical waveguide antenna used in Glasgow microwave thermography system

3.5 Radiometer sensitivity

The radiometer sensitivity is given by equation 3.3.1. For the 3 GHz radiometer the equivalent noise temperature of the receiver, T_R , can be measured to be approximately 400 K, primarily due to the losses in the input components (antenna, switch, circulator, cables) and the noise of the GASFET pre-amplifier (Land, 1983). The pre-detection bandwidth is 500 MHz and the equivalent integration time, τ_{LF} , is approximately 2 seconds critically damped. The source temperature will be close to 310 K. For a Dicke radiometer with square-wave modulation and square wave multiplication in the synchronous detector the sensitivity constant K_S is 2. This is twice the value for a total power receiver because the receiver is only switched to the source for half the time. Using equation 3.3.1 this gives an rms ac noise in the radiometer output of 0.04 K.

The peak to peak magnitude of the noise is approximately eight times the rms value (Meredith, 1964), while 95% of the signal will be within 3.92 times the rms value, for a Gaussian distribution. This 95% value is 0.16 K and is a convenient measure of the temperature resolution of the system. The peak to peak variation was measured to be 0.16-0.18 K.

The resolution will also be affected by fluctuations in the gain of the receiver caused mainly by the relatively slow ambient temperature changes. The largest effect is from the GASFET pre-amplifier which, after compensation, has a <1% change in gain for a temperature change of 1 K. Since the difference between the antenna temperature and the source temperature will always be less than about 5 K, a change of 1 K will cause a maximum change in output of 0.05 K. A variation of more than 1 K in the operating temperature is unlikely to take place in the time to scan one patient, which is usually less than 20 minutes. The variation in gain does not therefore in practice reduce the temperature resolution, but affects the absolute temperature calibration of the system.

The temperature resolution of the radiometer may be improved by reducing the receiver noise. In this way it would be possible to reduce the temperature resolution from 0.16 K to 0.025 K at the cost of convenience of use (Newton, 1986). As the sensitivity is increased, however, variations in gain will become relatively more important.

3.6 Antennas

3.6.1 Antenna design

The antenna used in the Glasgow microwave thermography system is a cylindrical waveguide antenna, with an internal diameter of 2.5 cm and 5.2 cm in length with a tapered fin-line type waveguide to coaxial line transition (see figure 3.3). The signal is transmitted from the antenna to the radiometer by flexible coaxial cable. The antenna waveguide is loaded with a low-loss dielectric (Emerson and Cummings Eccoflo HiK dielectric powder, $\epsilon_r^* = 12 - j 0.0084$).

The waveguide modes which may propagate in the operating bandwidth of 3.0 to 3.5 GHz are the TE_{11} - mode and the TM_{01} - mode. The dielectric filling allows the dimensions of the guide to be smaller than those required for a hollow guide since it reduces the wavelength by a factor of $\sqrt{\epsilon_r}$ in an unbounded volume of dielectric. For the cylindrical waveguide antenna used in the Glasgow microwave thermography system the cut-off frequency for the TE_{11} - mode is 2.03 GHz and the cut-off frequency for the TM_{01} - mode is 2.65 GHz. The fin-line transition, however, will couple only to the TE_{11} - mode field.

The most commonly used contact antenna for clinical microwave thermography is a dielectric filled rectangular waveguide antenna operating in the TE_{10} -mode. Guy (1971) in a study of multi-mode rectangular waveguide antennas showed that this mode gave optimum heating in the muscle layer of a planar tissue model consisting of a layer of fat 2cm thick above a semi-infinite layer of muscle. By the reciprocity theorem this antenna will receive maximum signal from the muscle tissue and so will have the

best response with depth for a rectangular waveguide antenna. From diffraction considerations rectangular and cylindrical waveguide antennas of the same dimensions should have very similar behaviour.

Table 3.1 lists contact antennas which have been used clinically for microwave thermography.

3.6.2 Antenna pattern

The antenna pattern, introduced in Chapter 2, determines the contribution of a small volume element of the tissue to the total signal. It is a difficult problem to calculate theoretically the antenna pattern, which depends on a large number of parameters as follows:

- (i) frequency
- (ii) dimensions and geometry of guide
- (iii) dielectric loading of guide
- (iv) dielectric properties of observed tissue

and (v) geometry of tissue

The antenna pattern may be determined either theoretically by numerical methods, in which case the tissue geometry is usually assumed to be in planar layers, or experimentally using "phantom" materials which simulate the dielectric properties of the tissue. The antenna pattern reduces the effective penetration depth of the microwave radiation from that of the plane wave and this may be used to characterise the response of the antenna.

Cheever et al (1987) have calculated theoretically the effective penetration depth in a homogeneous volume of tissue from a hollow TE_{10} - mode rectangular waveguide antenna for a range of antenna sizes and tissue dielectric properties. The TE_{10} - mode is the dominant mode for a rectangular waveguide. The operating frequency was mid-way between cut-off for the TE_{10} - mode and the TE_{20} - mode. The calculations were carried out using the mode-matching technique (Harrington, 1961), which involves a number

Frequency (GHz)	Antenna	Dimensions (cm)	Dielectric constant of antenna loading	Reference
3.3	Rectangular waveguide	2.3 x 1.0	11	Barrett and Myers (1977)
1.3	"	"	30	Myers, Sadowsky and Barrett (1979)
6.0	"	"	2	"
4.7	Rectangular waveguide	1.83 x 0.92	9.8	Carr, El-Mahdi and Shaeffer (1982)
3.0 and 1.5	Rectangular waveguide (6 antennas arranged in a 2 x 3 grid to form a multi-probe)	2.2 x 1.1	25	Enel, Leroy, Van de Velde and Mamouni (1984)
1.1, 2.6, 4.0 and 5.5	Truncated rectangular waveguide (multi-frequency radiometry system)	~ 4.8 x 2.2 at lower frequencies ~ 2.3 x 1.0 at higher frequencies	6?*	Bardati et al (1987)
3.2	Cylindrical waveguide	2.5 diameter	12	Land (1987)

[* Emerson and Cummings STYCAST]

Table 3.1 Contact antennas used in clinical microwave thermography

of approximations, and experimental measurements in liquids verified that these approximations gave adequate results. The calculations showed that there were two limiting cases for the effective penetration depth in tissue; the plane wave penetration depth and a penetration depth determined by the size of the aperture. The plane wave penetration depth, the upper limit, is approached when the observed dielectric is lossy or the aperture is large and the lower limit, in which the aperture determines the penetration depth, is approached when the aperture is electrically small.

The Microwave Thermography Group at the Université de Lille, France have also studied theoretically the radiation patterns of TE_{10} -mode rectangular waveguides (Robillard, 1980,1982, Nguyen, 1980 and Audet, 1982). Numerical calculations have been carried out to determine the effective penetration depth from a variety of waveguide aperture sizes operating at frequencies of 1, 3 and 9 GHz and filled with dielectrics of relative permittivity 1 to 25. The effective penetration depth in two types of homogeneous tissue was calculated; one representing the dielectric properties of muscle and the other the dielectric properties of fat. In both tissues the effective penetration depth was reduced by reducing the width of the guide. This is in agreement with the results of Cheever for a hollow waveguide and is to be expected as diffraction effects increase as the ratio of aperture size to wavelength in tissue decreases. The diffraction effects are important because at the frequencies considered the wavelength in the tissue is of the order of the dimensions of the dielectrically loaded waveguide. Larger diffraction effects widen the lateral response of the antenna and so reduce the on-axial response causing a decrease in the effective penetration depth.

An increase in the dielectric constant of the waveguide filling requires a reduction in the dimensions of the guide in order to restrict propagation to the TE_{10} -mode. This means that the guide dimensions are determined within certain limits by the type of dielectric loading if multi-mode propagation is to be avoided. The dielectric loading of the guide and the waveguide dimensions also determine the transverse-wave impedance of the guide. The impedance mismatch at the antenna-tissue

interface causes a reflection of the radiation signal from the tissue and it is desirable that this reflection should be minimised. Nguyen et al (1980) verified that, although closer values of the permittivities of the guide and the tissue improve the matching, the reflection coefficient will be less than 0.2 if the ratio of permittivity of guide dielectric to permittivity of tissue is between 0.5 and 5.

In the muscle "phantom" Robillard et al (1980) found effective penetration depths very close to those of the plane wave penetration depth, in agreement with Cheever's results for lossy dielectrics. At 3 GHz, with dielectric constants of the guide loading between 4 and 9 and guide widths between 3 and 5 cm the effective penetration depth was calculated to be between 89% and 100% that of the plane wave value and the reflection coefficient was between 0.17 and 0.40. Increasing the dielectric constant of the guide loading to 25 reduced the reflection coefficient to 0.04 but also reduced the penetration depth to 61% of its plane wave value. This illustrates the compromise necessary when choosing the dielectric loading between the reflection coefficient and the effective penetration depth. In the fat "phantom" the permittivity is much lower and, for similar sizes of waveguides to those used with the muscle "phantom", dielectric loadings with permittivities in the range 4 to 9 gave reflection coefficients between 0 and 0.26 and effective penetration depths between 16% and 37% those of the plane wave value. These values are greatly reduced from those in the muscle "phantom" because of the longer wavelength in the fat "phantom" and the resulting larger diffraction effects.

These computational results indicate the effective penetration depth from the antenna in homogeneous tissues and illustrate the correlations which exist between this quantity and the size of aperture and the dielectric loading. The antenna pattern also depends on the structure of the tissues being observed and Edenhofer (1980) has computed the near-field characteristics of a rectangular waveguide antenna in contact with planar layers of tissue. The tissue model used is a surface layer of skin 2mm thick over a 5mm layer of fat and followed by an infinite muscle region. The time-averaged

Poynting power flux density was calculated in three dimensions for frequencies of 1 and 3 GHz. The guide was filled with dielectric of relative permittivity 10 and the guide dimensions were 6.2 by 3.1 cm at 1 GHz and 2.3 by 1.1 cm at 3 GHz. It was found that at 3 GHz the power was attenuated by e^{-2} by 0.67 cm of tissue and as a result only about 13% of the total signal would originate in the muscle layer. At 1 GHz the same attenuation required 1.9 cm of tissue, but the electrically effective lateral area of tissue which contributed to the signal was 11 cm^2 , compared with 1.25 cm^2 at 3 GHz. This illustrates the degradation in spatial resolution which accompanies an improved penetration depth at lower frequencies. At 3 GHz the effective penetration in fat was approximately 12% of its plane wave value and that of skin was 38% of its plane wave value. This small effective penetration in skin is probably due to strong near-field effects close to the antenna aperture in the thin skin layer. At 1 GHz the effective penetration depth in the muscle layer was approximately 60% of the plane wave value and this, because of the larger aperture size, indicates an upper limit for effective penetration in muscle tissue of the smaller guide at 3 GHz.

Newton (1986) has determined experimentally the antenna pattern at 3 GHz for the cylindrical waveguide used in the Glasgow microwave thermography system and two rectangular waveguide antennas loaded with the same dielectric material. The radiation patterns were measured in homogeneous tissue "phantoms", simulating fat and muscle tissue, using a small probe to radiate broad-band noise. The radiometer reading was recorded for different positions of the probe in the liquid "phantom". At positions very close to the antenna interaction between the probe and antenna causes a distortion of the true radiation pattern as currents are set up in the coaxial cable which supports the diode noise source of the probe. To reduce this effect in the calculation of the effective penetration depth the distance at which the power was reduced to 0.1 of its initial value was measured and used to calculate the e^{-1} penetration depth. The rectangular waveguide with dimensions 2.7 by 6.2 cm gave, within errors, the same effective penetration depth as the cylindrical waveguide with diameter 2.5 cm, because

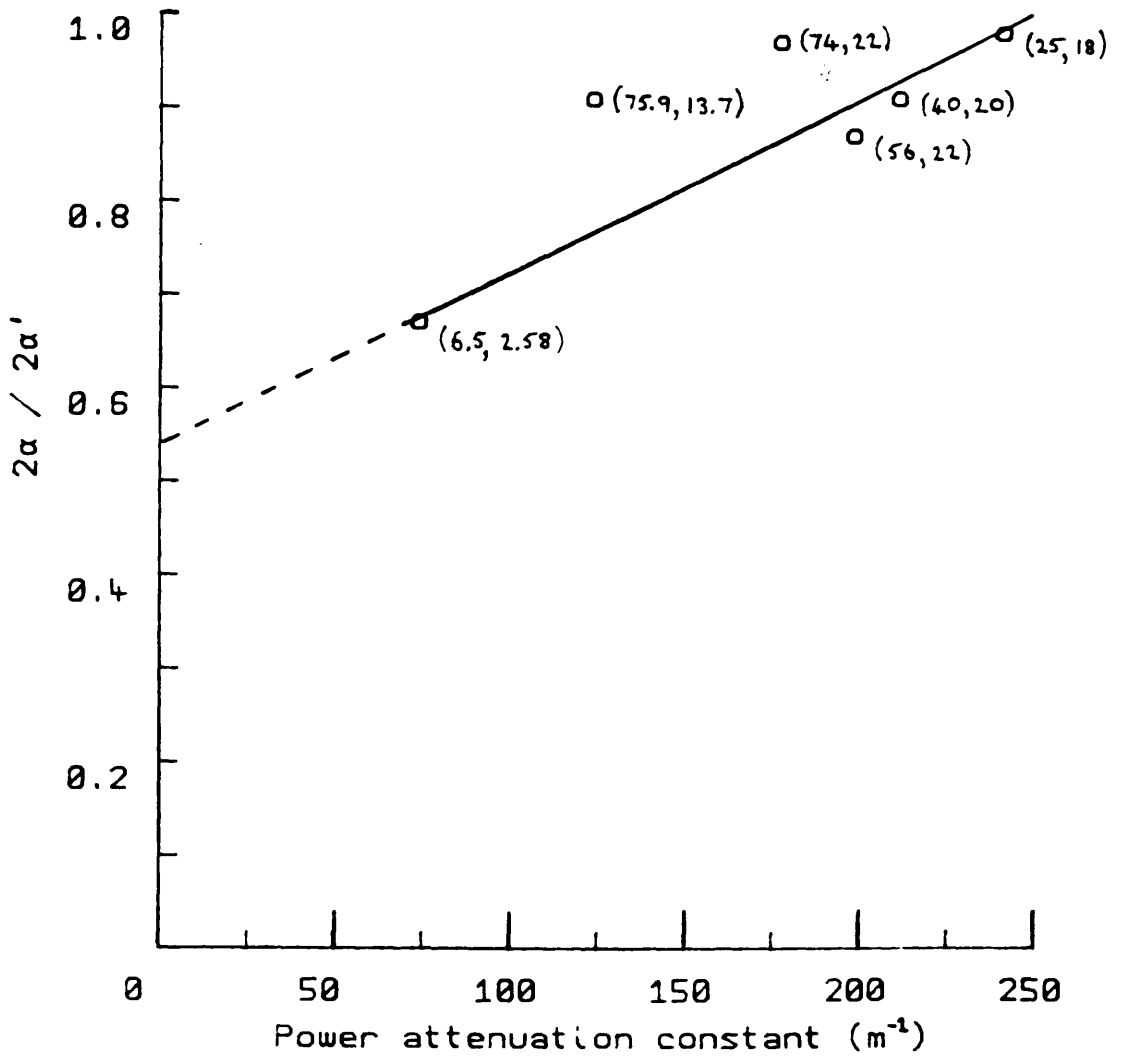
of the similar x dimension. In fat phantom (5-j3) the effective penetration depth was 40% of the plane wave value. An estimated value for the effective penetration in fat tissue (5-j1) was given to be 20% of the plane wave value. The smaller rectangular waveguide (2.3 by 0.5 cm) which propagates only the TE₁₀- mode at 3GHz, as opposed to the 10 modes propagated at this frequency by the larger guide, has an estimated effective penetration depth in fat of only 7% of the plane wave value. In muscle phantom the effective penetration depth for this smaller guide was 50% of the plane wave value while the other two guides gave approximately 75% of the plane wave value. This result for the smaller guide is less than the 61% value obtained theoretically by Robillard for a guide (2 by 1 cm; e=25) in a similar muscle phantom. For a similar size of guide (2.3 by 1 cm; e=9) at a lower frequency of 2.45 GHz Cheung (1981) found a value of 67% of the plane wave value.

The response pattern of the cylindrical antenna used in the Glasgow thermography system has also been measured using a non-resonant perturbation technique (Land 1988). This technique avoids interaction effects with a probe close to the antenna. Different homogeneous liquid "phantom" materials have been used to determine effective penetration depths (Mimi, to be published) and the results are shown in figure 3.4.

The linear relationship shown on the graph has been used to relate empirically the plane wave power attenuation constant, 2α , which may be calculated from the dielectric properties of the tissue using equation (3.2.2), to the ratio of plane wave power attenuation constant to effective power attenuation constant, $2\alpha'$. This approximate relationship is necessary to account for the effects of the antenna in any tissue with a given power attenuation constant and is given by the equation

$$\frac{2\alpha}{2\alpha'} = 1.83 \times 10^{-3} 2\alpha + 0.544 \quad (3.6.1)$$

For the two liquids with dielectric constants greater than 70, saline and de-ionised water, the effective penetration depth is closer to the plane wave penetration depth than



Figures in brackets : (ϵ_T' , ϵ_T'')

Data from Mimi (to be published)

Figure 3.4 Comparison of experimental measurements of effective attenuation constant, $2\alpha'$, with plane wave attenuation constant, 2α , for the cylindrical waveguide antenna used in the Glasgow microwave thermography system

will be expected in tissue of the same power attenuation constant, because of the smaller wavelength in these liquids, due to the higher dielectric constant than will be found in tissue, resulting in reduced diffraction effects.

3.7 Calculation of expected microwave signal

The impedance mismatch at the boundary between the antenna and the body will cause a reflection of radiation which will affect the signal measured. If there is an impedance mismatch at the antenna-tissue interface which results in a field reflection coefficient of $\rho e^{-j\theta}$, then $|\rho|^2 kT_A$ of the power emitted per unit bandwidth by the tissue is reflected. By thermodynamical considerations the tissue must emit $(1 - |\rho|^2)kT_A$. In a Dicke radiometer the signal received is not proportional to the temperature T_A , but to the difference between the temperature of the reference source, T_{ref} , and the antenna temperature, T_A . The power received by the radiometer per unit bandwidth is therefore

$$(1 - |\rho|^2) k (T_A - T_{ref}) \quad (3.7.1)$$

If a self-balancing radiometer, as proposed by Mamouni and Ludecke, is used in which the reference temperature is adjusted to be equal to the antenna temperature then there is no effect on the received signal due by this reflection.

In the Glasgow microwave thermography system, since the reflected signal from the reference source is also received, the total signal after calibration to $^{\circ}\text{C}$, is (Land, 1983)

$$|\rho|^2 (1 - a^2) T_e + |\rho|^2 a^2 T_{ref} + (1 - |\rho|^2) T_A \quad (3.7.2)$$

where T_e is the ambient temperature and a is the power transmission factor for both the signal path from aerial to switch and the signal path from reference source to switch.

An effective reference temperature, T_{ref}^* , may be defined to be

$$T_{ref}^* = (1 - a^2) T_e + a^2 T_{ref} \quad (3.7.3)$$

and (3.7.2) may be written

$$|\rho|^2 T_{ref}^* + (1 - |\rho|^2) T_A \quad (3.7.4)$$

The reflection coefficient, $|\rho|^2$, may be calculated approximately by assuming

plane wave reflection at the antenna-tissue boundary. The transverse wave impedance of the waveguide is given by

$$Z = \frac{Z_0}{\left(\epsilon_r' - \left(\frac{\lambda_0}{\lambda_{oc}}\right)^2\right)^{\frac{1}{2}}} \quad (3.7.5)$$

where Z_0 is the impedance of air (377Ω), ϵ_r' is the relative dielectric constant of the waveguide filling, λ_0 is the free space wavelength and λ_{oc} is the cut-off wavelength.

For the antenna used in the Glasgow microwave thermography system this impedance is 141Ω at a frequency of 3.2 GHz.

Figure 3.5 shows the variation in the plane wave reflection coefficient at the antenna-tissue boundary with the relative dielectric constant of the tissue. In this case the loss of the tissue has been neglected since it has a negligible effect on the impedance of the tissue. The range of dielectric constants found in tissue is between 2 and 55 (see Chapter 5) and it can be seen that in this range the average reflection coefficient is about 0.1. The Glasgow microwave thermography system is therefore calibrated assuming a 0.1 reflection coefficient at the antenna-tissue boundary and the expected microwave signal is calculated as follows:

$$\frac{(|\rho|^2 - 0.1) T_{ref}^* + (1 - |\rho|^2) T_A}{(1 - 0.1)} \quad (3.7.6)$$

The antenna temperature, T_A , may be determined as described in sections 2.6 and 2.7 and this equation (3.7.6) may be used to calculate the expected microwave signal. This signal, calibrated to $^{\circ}\text{C}$, will be referred to henceforth as the "microwave temperature". In Chapters 6 and 7 the expected microwave temperature will be calculated for modelled temperature distributions in tissue.

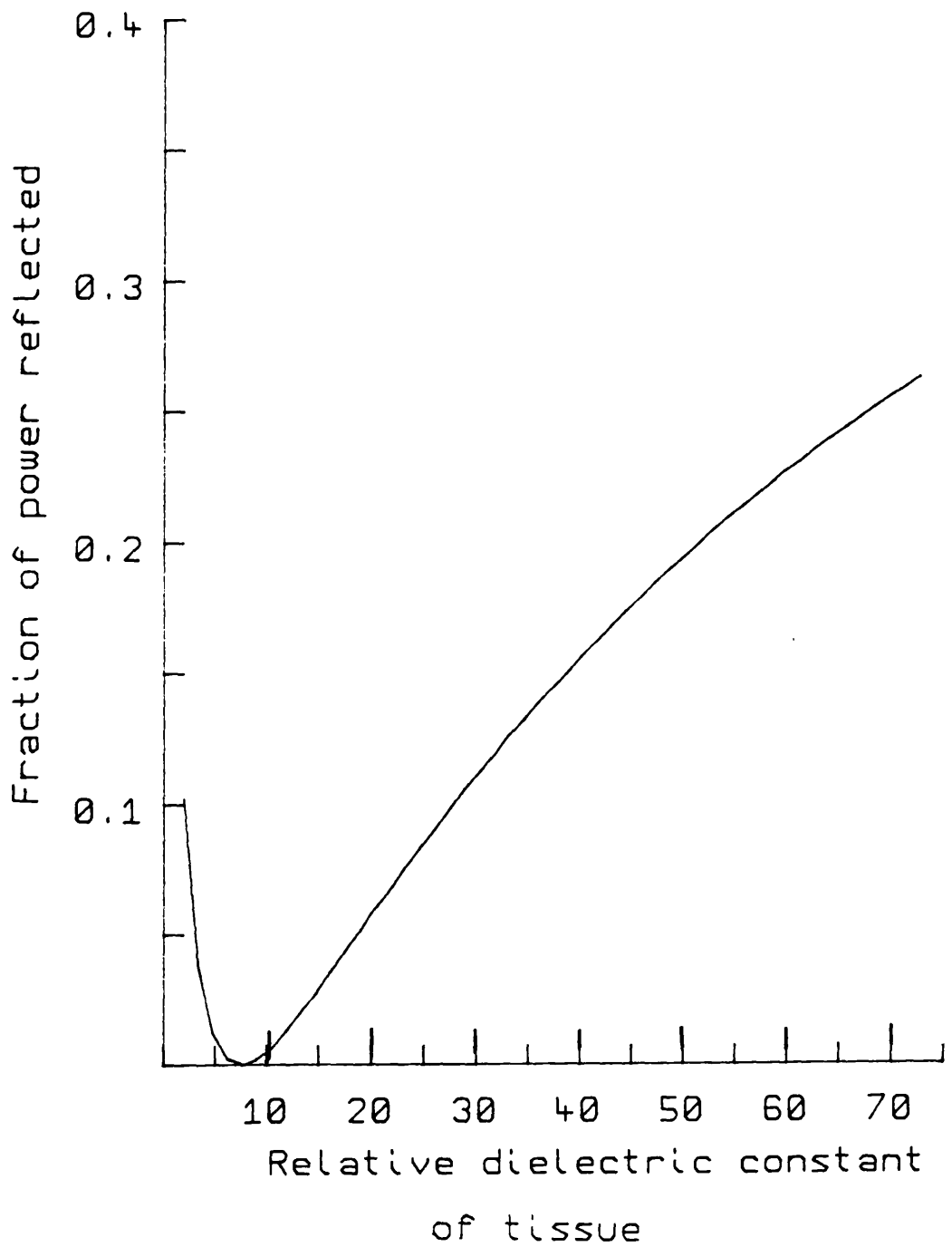


Figure 3.5 Power reflection coefficient at antenna-tissue boundary at 3 GHz

Chapter 4 - Calculation of temperature distributions in the human body

4.1 Introduction

This chapter introduces the most commonly used equation governing heat transfer in the human body. The limitations of this equation are discussed and alternative descriptions of heat transfer are reviewed. The transfer of heat to the environment is discussed and a quantitative estimate of the heat lost at the skin surface in a normal clinical environment is made.

4.2 Heat transfer in the human body

Heat is generated in the human body as a result of chemical reactions which take place at a cellular level. This heat is then distributed throughout the body by means of the vascular system which acts as a method of heat transport from large sources of heat production, such as the organs, to other areas of the body such as the limbs. Heat is lost to the environment at the skin surface and through the respiratory tract at a level which is controlled by the body's thermoregulation system to ensure a constant body temperature.

The vascular system in the body has a highly complex structure (Figure 4.1). The circulation of the blood through the body may be divided into two separate systems; the pulmonary division and the systemic division. The heart pumps the blood through both these systems by means of two ventricles. The right ventricle propels blood through the pulmonary artery to the lungs, while the left ventricle pumps blood through the aorta and systemic arteries to the rest of the body. The main arteries form a distribution system which, through the small arteries and arterioles, delivers blood to the capillary system. The capillary system consists of numerous, tiny microscopic tubes with many branches in all directions. The combined volume of this system is small but the total surface area is immense and it is through the capillary walls that exchange of nutrients and heat takes place. Since the surface area is large it is reasonable to assume that the surrounding tissue comes to equilibrium temperature with the blood flowing in

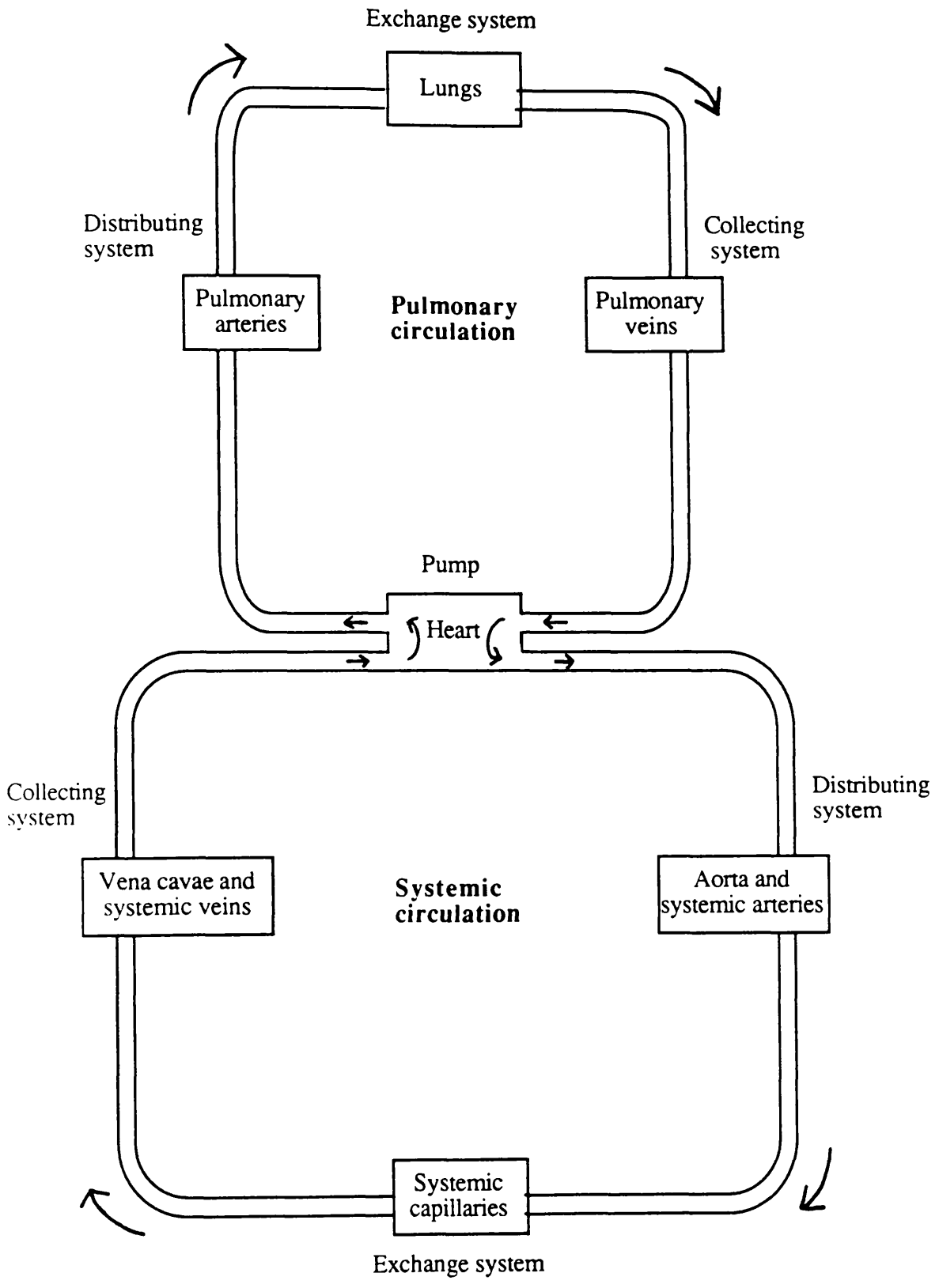


Figure 4.1 The circulatory system of the human body

the capillaries. The blood is then collected in small venules and fed to veins which drain the blood back to the heart atria where it is pumped through another cycle. Heat is also transferred through the body by conduction due to the thermal gradients in the tissue.

In order to formulate an equation of energy balance in the tissue it is necessary to assume that the properties of each tissue type are uniform and isotropic over the volume being considered. Since this is not necessarily the case, the tissue properties are taken to be equal to the average value over the volume considered.

The earliest equation of heat transfer in tissue was given by Pennes (1948) who stated that

$$\rho c \frac{\partial T}{\partial t} = K \nabla^2 T + W_b c_b (T_a - T) + Q \quad (4.2.1)$$

where ρ is the density of the tissue (kgm^{-3}),

c is the specific heat capacity of the tissue ($\text{Jkg}^{-1} \text{K}^{-1}$),

T is the temperature distribution in the tissue (K),

K is the tissue thermal conductivity ($\text{Wm}^{-1} \text{K}^{-1}$),

W_b is the rate of blood perfusion ($\text{kgm}^{-3}\text{s}^{-1}$),

T_a is the arterial blood temperature (K),

c_b is the specific heat capacity of blood ($\text{Jkg}^{-1} \text{K}^{-1}$),

and Q is the rate of metabolic heat production (Wm^{-3}).

In this equation the left-hand term represents the the rate of change of stored energy in an infinitesimal control volume. The first term on the right-hand side represents the rate of transfer of energy due to conduction while the second term represents the heat transferred to the tissue by arterial blood flowing in the capillaries. The third term represents the heat generated by metabolic processes. It is in the second term, used to describe the effects of perfusion, that a number of assumptions are inherent. Firstly it is assumed that the exchange of heat between the blood and tissue takes place entirely in the capillary bed and that this exchange is complete resulting in the tissue and blood reaching the same temperature. It is also assumed that there is no directionality involved in the capillary blood flow. Furthermore heat exchanges between

artery-vein pairs and between large blood vessels and the surrounding tissue are neglected.

The validity of this second term has been critically questioned by a number of authors (Wulff 1974, Klinger 1974, Chen and Holmes 1980, and Weinbaum and Jiji 1985). The mathematical difficulty involved in the derivation of this term has been highlighted by Wulff. He pointed out that this perfusion term has resulted from an application of global energy balance which has then been applied to local tissue energy balance to provide consistency with the other terms in the equation. This is a contradiction of the requirement that each application of the First Law of Thermodynamics is restricted to a unique control system. The equation also implies that two temperatures exist simultaneously at the same point in space, namely the tissue temperature T and the blood temperature T_a . Wulff suggests that this term is replaced by

$$- \rho_b c_b \underline{V} \cdot \nabla T \quad (4.2.2)$$

where \underline{V} is the local mean apparent blood velocity vector (ms^{-1}) and ρ_b is the density of blood. This convective term accounts for the directionality associated with the blood flow.

A solution to the equation of heat transfer with this term (4.2.2) representing the effects of blood flow would describe the temperature at each point in the tissue, but due to the lack of detailed knowledge of the convection field in the tissue this is not generally possible (Klinger 1980).

Weinbaum and Jiji (1984a, b, 1985) have proposed that heat transfer between blood and tissue is primarily due to incomplete countercurrent exchange between thermally significant artery and vein pairs, rather than due to heat exchange between capillaries and surrounding tissue. They have produced an equation to describe this mechanism, but this equation has been challenged by Wissler (1987a, b) who points out that their alternative formulation cannot be used to describe rewarming of cool tissue by increased blood flow. This is an effect which is well-known physiologically

and is described by the blood flow term in Pennes original equation. The original term represents blood flow as a set of spatially distributed heat sinks whose effectiveness is proportional to the difference between the blood and tissue temperatures and the rate of blood flow. The Weinbaum and Jiji equation results in the effect of perfusion being described as principally causing an increased effective conductivity. This equation may be an appropriate alternative to Pennes original equation in certain applications but careful consideration should be given to the assumptions involved.

Chen and Holmes (1980) have approached this problem of the effects of perfusion by considering the nature of biological tissue and describing the macroscopic effects of the microscopic vascular structure. They have considered the exchange of heat between the different sizes of blood vessels and the surrounding tissue. The characteristic length over which the blood in the vessel comes to equilibrium temperature with the surrounding tissue was estimated and compared to the typical vessel length. It was found that blood travelling in the main arteries remains at essentially a constant temperature, and that most of the equilibration takes place in vessels whose diameter is between that of the main arteries and the arterioles. Blood flowing in the arterioles, capillaries and venules is essentially at a temperature equal to that of the tissue. The effect of heat exchange between vessel pairs, as considered by Weinbaum and Jiji, was not treated.

Chen and Holmes propose that the equation of heat transfer in living tissue should be

$$\rho c \frac{\partial T}{\partial t} = \nabla \cdot K \nabla T + \nabla \cdot K_e \nabla T + W_b^* c_b (T_a^* - T) - \rho_b c_b \underline{V} \cdot \nabla T + Q \quad (4.2.3)$$

The second term on the right hand side represents a conductivity term, where K_e is an effective conductivity, due to the fact that the component of blood flow parallel to the thermal gradient enhances the thermal conductivity. This term assumes that the conductivity enhancement is isotropic because of the random arrangement of the microvasculature. The next term is similar to that of Pennes, representing a distributed heat source due to blood flow. The temperature T_a^* is the temperature reached by the

blood after it has passed through the larger vessels (arteries and veins) whose contribution to tissue heating should be treated individually. W_b^* is the total perfusion rate through the smaller vessels and does not include blood delivered through the larger vessels. As a result of this treatment of the problem only the macroscopic temperature may be determined. The smallest volume of interest, whose average temperature is to be determined, must be large enough to contain all bifurcations from terminal arteries to arterioles, because it is in these vessels that equilibration with tissue temperature occurs. The fourth term is a convection term of the type proposed by Klinger and Wulff and accounts for the contribution of the mean blood flow vector, \underline{V} .

This equation includes a description of all the expected effects of the microcirculation with the effects of large vessels to be calculated individually. The currently available information on vascular structure, however, is not detailed enough to allow determination of K_e , W_b^* and \underline{V} , and Chen suggests that in the absence of this information the standard equation proposed by Pennes should be employed.

For microwave thermography, where the experimental measurement of temperature is a volume average over a scale much larger than the largest vessels the use of Pennes equation to estimate macroscopic temperatures is entirely appropriate. The calculated temperature distribution must be combined with the antenna response function (see section 2.3) and efforts in increasing the accuracy of the estimated temperature distribution must be carefully considered in view of the inaccuracy which will arise in the estimated microwave temperature due to uncertainty in the antenna pattern.

Further study of heat transfer in the body is required in order to clarify the effects of the microvasculature and determine the limitations of Pennes equation. This work will be on a measurement scale much smaller than that employed in microwave thermography.

4.3 Heat exchange with the environment

The differential equation governing heat transfer in the body cannot be solved without knowledge of the appropriate boundary conditions. The most important condition to consider is that of the heat exchange which takes place between the skin surface and the environment.

The constancy of man's body temperature implies that a balance must be maintained between the metabolic heat generated in the body and the heat lost to the environment and, in fact, this is achieved mainly by controlling heat loss from the skin surface. The principle method of physiological control of heat loss in comfortable environmental temperatures is the regulation of the blood flow to the skin which may be increased (vasodilation) or reduced (vasoconstriction) in order to raise or lower the skin temperature and so increase or reduce heat loss. In more extreme conditions heat loss can be increased by sweating or panting and decreased by erection of the surface hairs on the skin. At very low temperatures shivering can be used to increase heat production.

Microwave thermography measurements are carried out on patients in a comfortable clinical environment. The area to be scanned is unclothed, while the rest of the body is normally lightly clothed. In this situation heat loss from the skin occurs by means of radiation, convection and evaporation of insensible perspiration. The heat loss by conduction is negligible. The total heat loss must be equal to the heat generated by metabolic activity in order to maintain a constant body temperature.

4.3.1 Heat loss by radiation

The net rate of heat loss per unit surface area of a body with a surface temperature T_s surrounded by walls at a temperature T_e is given by the Stefan-Boltzmann Law to be

$$H_r = \sigma_s e (T_s - T_e)^4 \quad (4.3.1)$$

where σ_s is Stefan's constant ($5.67 \times 10^{-8} \text{ Wm}^{-2} \text{ K}^{-4}$) and e is the emissivity of the

skin surface which can be assumed equal to 1 (Mitchell, 1967) since the main loss of radiation occurs in the infra-red region in which the skin behaves as a black body.

In a comfortable environment the temperature difference $T_s - T_e$ will be small compared to the mean temperature $T_m = 0.5 (T_s + T_e)$ and equation (4.3.1) may be written (Draper and Boag 1971)

$$H_r = 4 \sigma_s e T_m^3 (T_s - T_e) \quad (4.3.2)$$

$$H_r = 4 \sigma_s e T_m^3 (T_s - T_e) \quad ;$$

and a radiative heat transfer coefficient may be defined to be (4.3.3)

$$h_r = 4 \sigma_s e T_m^3 \quad \text{range } 20\text{-}26 \text{ } ^\circ\text{C while the skin}$$

temperature will be approximately in the range 28-35 $^\circ\text{C}$. This gives an estimated radiative heat transfer coefficient of $6.2 \pm 0.2 \text{ Wm}^{-2} \text{ } ^\circ\text{C}^{-1}$.

4.3.2 Heat loss by convection

Heat loss by convection is due to the transport of heat away from the skin surface by the movement of air surrounding the body. Convection may be either due to changes in the temperature or the density of the air caused by the warming of a layer of air next to the skin surface (free convection) or due to an external force, such as air-conditioning, impelling the air past the surface (forced convection). The rate of convection is governed by a large number of factors including the temperature difference between the air next to the skin and the bulk air, the air density, its viscosity, specific heat capacity, thermal conductivity, temperature coefficient of expansion, the shape and orientation of the surface and the air velocity in the case of forced convection. These variables may be grouped into dimensionless quantities which each describe a particular aspect of the air behaviour important in convection.

The rate of convective heat flux per unit surface area is usually expressed for convenience in the form

$$H_c = h_c (T_s - T_e) \quad (4.3.4)$$

where values of h_c , the coefficient of convective heat transfer, have been found

empirically, generally for engineering applications, for different surface geometries in terms of the dimensionless parameters. These values can be applied to man to provide an estimate of the convective heat loss. Table 4.1 gives experimental measurements from a number of investigators of the coefficient of convective heat transfer for humans. These values are chiefly in the range 2.1 - 5.6 Wm⁻²°C⁻¹ and consider the airspeed in a normally ventilated room to be between 0.1 and 0.2 ms⁻¹.

The dimensionless quantities involved in estimation of convective heat loss include:

(i) Reynolds number, Re (ratio of inertial force to viscous drag force)

$$Re = \frac{u_a \rho_a L}{\eta_a} \quad (4.3.5)$$

where u_a is the average air speed, L is the characteristic length of the object (diameter or length), ρ_a is the density of the air and η_a is its viscosity

(ii) Nusselt number, Nu (ratio of convective heat flux to conductive heat flux)

$$Nu = \frac{h_c L}{K_a} \quad (4.3.6)$$

where K_a is the thermal conductivity of air

(iii) Prandtl number, Pr (ratio of kinematic viscosity to thermal diffusivity)

$$Pr = \frac{\eta_a c_a}{K_a} \quad (4.3.7)$$

where c_a is the specific heat capacity of air

(iv) Grashof number, Gr (ratio of buoyancy forces to viscous drag forces)

$$Gr = \frac{g \beta_a L^3 \Delta T \rho_a^2}{\eta_a^2} \quad (4.3.8)$$

where g is the acceleration due to gravity, β_a is the coefficient of thermal expansion of air and ΔT is the temperature difference between the surface of the object and the surrounding air.

The ratio $Gr/(Re)^2$, representing the ratio of buoyancy forces to (inertial forces)², indicates the ratio of free to forced convection. If this value is greater than about 16 then free convection will dominate and if it is less than about 0.1 forced convection will dominate while between these limits a mixture of free and forced

Coefficient of convective heat transfer h_c ($Wm^{-2} \text{ } ^\circ C^{-1}$)	condition	remarks	reference
2.3	seated	free convection	Seagrave (1971)
2.1	seated	$0.05 \leq U \leq 0.2 \text{ ms}^{-1}$	Gagge et al (1965)
3.1	seated		Nishi and Gagge (1970)
2.4 - 4.6	seated	$0.15 \leq U \leq 0.20 \text{ ms}^{-1}$	Nishi (1973)
2.5 - 4.5	standing	$0.11 \leq U \leq 0.22 \text{ ms}^{-1}$	Nishi (1973)
2.7	standing	free convection	Seagrave (1971)
$2.7 + 8.7 U^{0.67}$ (5.6 at $U = 0.2$)	reclining	$0.2 \leq U \leq 1.2 \text{ ms}^{-1}$	Colin and Houdas (1967)
$3.05 + 10.6 U$ (4.1 at $U = 0.2$)	reclining	$U \leq 0.25$	Missenard (1973)
3.9	semi-reclining		Winslow et al (1937)
2.5		free convection	Buettner (1934)'
$3.5 + 18.6 \sqrt{U}$		low air flow speed	Winslow and Herrington (1949)
0.9 - 1.6		no air flow	Hardy and Dubois (1938)
3.8	chest wall	$0.1 \leq U \leq 0.2 \text{ ms}^{-1}$	Draper and Boag (1971)
4.6	upper surface of female breast	"	"
5.0	lower surface of female breast	"	"

Table 4.1 Experimental measurements of convective heat transfer coefficients for humans

convection will exist (Leyton, 1975).

The body may be considered as composed of cylinders of different sizes (Wissler, 1961) and appropriate empirical engineering formulae may be used to determine the coefficient of convective heat loss, h_c . Table 4.2 lists the formulae used to estimate the coefficient of convective heat transfer, assuming free convection, for cylinders representing the head, trunk, arms and legs. The air-speed required for free convection to dominate is also estimated and is found to be less than 0.07 ms^{-1} . In a normally ventilated room, with an air-speed between 0.1 and 0.2 ms^{-1} , convective heat loss from the body will fall in the region of mixed convection. The McAdams rule for mixed convection states that in this region both the free convection and the forced convection transfer coefficients should be calculated and the larger value taken. Measured values obtained for flow through vertical tubes did not deviate by more than 25% from values calculated by this rule (Eckert 1959). The transfer coefficients for forced convection with an air-speed of 0.2 ms^{-1} were also calculated and are also shown in table 4.2. Following the McAdams rule, the larger values will be considered as estimates of the convective heat transfer coefficient. Considering these values and the experimental values from Table 4.1 it was decided to use as an estimate of the convective heat transfer coefficient the value $4 \pm 1 \text{ Wm}^{-2}\text{C}^{-1}$ and to apply this value to all areas of the body, since within the limits of error involved, it is not possible to determine the difference in convective heat loss caused by the varying body geometry.

4.3.3 Heat loss by evaporation

In a normal clinical environment sweating will not be present and heat loss by evaporation will be due to insensible perspiration. This is the passage of water through the skin surface and is thought to be a diffusion process (McLean, 1975).

The diffusion process through the skin is governed by the equation

$$\frac{dm_D}{dt} = (\chi_w(T_s) - \chi_s) h_D \quad (4.3.9)$$

where dm_D/dt is the rate of diffusion through the skin,

Physical properties of dry air at 20°C

Density : 1.2 kgm^{-3} specific heat : $1.007 \times 10^3 \text{ Jkg}^{-1} \text{ }^\circ\text{C}^{-1}$

dynamic viscosity : $1.81 \times 10^{-5} \text{ kgm s}^{-1}$

thermal conductivity : $2.57 \times 10^{-2} \text{ Wm}^{-1} \text{ }^\circ\text{C}^{-1}$

Prandtl number : 0.71

Free convection (for $T_s - T_e = 10^\circ\text{C}$, $\text{Gr.Pr} = 1.04 \times 10^9 \text{ L}^3$)

	radius (m)	length (m)	length (m)	Characteristic length (m)	Gr.Pr	Nu	h_c ($\text{Wm}^{-2} \text{ }^\circ\text{C}^{-1}$)	Wind speed for free convection to dominate (ms^{-1})
Arms	0.045	0.65	0.09	0.09	7.6×10^5	$0.47 (\text{Gr.Pr})^{0.25}$ = 13.9	4.0	$U \leq 0.04$
Legs	0.070	0.83	0.14	0.14	2.8×10^5	$0.47 (\text{Gr.Pr})^{0.25}$ = 19.2	3.5	$U \leq 0.05$
Head	0.089	0.25	0.25	0.25	1.6×10^5	$0.56 (\text{Gr.Pr})^{0.25}$ = 35.4	3.6	$U \leq 0.07$
Trunk	0.130	0.80	0.26	0.26	1.8×10^5	$0.47 (\text{Gr.Pr})^{0.25}$ = 30.6	3.0	$U \leq 0.07$

Forced convection ($U = 0.2 \text{ ms}^{-1}$ $\text{Re} = 1.32 \times 10^4 \text{ L}$ $\text{Nu} = 0.615 \text{ Re}^{0.466}$)

	radius (m)	length (m)	length (m)	Characteristic length (m)	Gr.Pr	Nu	h_c ($\text{Wm}^{-2} \text{ }^\circ\text{C}^{-1}$)	Wind speed for forced convection to dominate (ms^{-1})
Arms	0.045	0.65	0.09	0.09	7.6×10^5	$0.615 \text{ Re}^{0.466}$ = 16.7	4.8	$U \geq 0.55$
Legs	0.070	0.83	0.14	0.14	2.8×10^5	$0.615 \text{ Re}^{0.466}$ = 20.5	3.8	$U \geq 0.67$
Head	0.089	0.25	0.25	0.178	1.6×10^5	$0.615 \text{ Re}^{0.466}$ = 22.9	3.3	$U \geq 0.90$
Trunk	0.130	0.80	0.26	0.26	1.8×10^5	$0.615 \text{ Re}^{0.466}$ = 27.3	2.7	$U \geq 0.92$

Table 4.2 Estimation of coefficient of convective heat transfer
[data and formulae from Leyton (1975)]

$\chi_w(T_s)$ is the concentration of air saturated with water vapour at the skin temperature, χ_s is the concentration of water vapour at the skin surface and h_D is the diffusion coefficient, a property of the skin.

In the absence of sweating this is equal to the rate of evaporation of water from the skin surface

$$\frac{dm_M}{dt} = (\chi_s - \chi_a) h_M \quad (4.3.10)$$

where χ_a is concentration of water vapour in the air and h_M is a transfer coefficient.

These two equations may be combined to give

$$\frac{dm}{dt} = (\chi_w(T_s) - \chi_a) h \quad (4.3.11)$$

where

$$\frac{1}{h} = \frac{1}{h_D} + \frac{1}{h_M}$$

The evaporative heat loss due to the evaporation of this water is given by

$$H_e = \frac{dm}{dt} L = h L (\chi_w(T_s) - \chi_a) \quad (4.3.12)$$

where L is the latent heat of evaporation of water. The concentration of water vapour χ is identical to the density, ρ_v , of the water vapour in air. The density may be related to the vapour pressure (the partial pressure of water vapour in air) by the gas laws, assuming water vapour to be a perfect gas, as follows (Leyton, 1975):

$$\chi = \rho_v = \frac{M_w e \rho_a}{M_a p} \cong \frac{0.622 \rho_a e}{p} \quad (4.3.13)$$

where M_w and M_a are the molecular weights of water (18×10^{-3} kg) and moist air (29×10^{-3} kg) respectively,

p is the total air pressure,

and e is the vapour pressure, the partial pressure of water vapour in air.

Substituting (4.3.13) into equation (4.3.12) we have

$$H_e = \frac{h L 0.622 \rho_a}{p} (e_w(T_s) - e_a) \quad (4.3.14)$$

The relationship between saturation vapour pressure and temperature is approximately linear in the region of skin and environmental temperatures ($20 \leq T \leq 35$) and $e_w(T_s)$ may be expressed

$$e_w(T_s) \cong m T + c \quad (4.3.15)$$

where $m = 1.635 \text{ mmHg } ^\circ\text{C}^{-1}$ and $c = -16.5 \text{ mmHg}$

If ϕ_a is the relative humidity of the air; the ratio of vapour pressure of air to the saturation vapour pressure at the same temperature, then

$$H_e = h_e (T_s - T_e^*) \quad (4.3.16)$$

where
$$T_e^* = \phi_a T_e + (1 - \phi_a) c / m \quad (4.3.17)$$

The heat loss due to evaporation is therefore proportional to the difference between the skin temperature and the equivalent environmental temperature which is dependent on the humidity. Measurements of insensible perspiration have been made by several workers. Buettner (1953), Webb, Garlington and Schwartz (1957), Zollner, Thauer and Kauffman (1955) and Brebner, Kerslake and Waddell (1956) all found a linear relationship between insensible perspiration and air vapour pressure, in agreement with the theory and suggesting that this loss is in fact a diffusion process. Goodman and Wolf (1969), however, claimed a non-linear relationship and postulated that this process was not entirely due to diffusion.

For the purposes of estimating heat loss by evaporation the important fact is that this process depends, at least approximately, on the difference in vapour pressures (equation 4.3.14) and not the difference in temperatures as is the case for radiation and convection. For convenience, however, it is desirable to express the evaporative loss in terms of the temperature difference.

If we assume that the relative humidity indoors is 0.5, that the room temperature is 24°C and that the skin temperature is 34°C , then the partial pressure difference is approximately 28 mmHg. Using equation 4.3.14, with the rate of mass transfer determined from the combined results of the workers listed above [$0.622h_{p_a}/p = 0.133 \times 10^{-6} \text{ kgm}^{-2}\text{s}^{-1}\text{mmHg}^{-1}$], and the latent heat of evaporation of sweat measured by Snellen, Mitchell and Wyndham (1970) [$2.59 \times 10^6 \text{ Jkg}^{-1}$], gives an estimate of the rate of heat loss from the skin surface due to evaporation as 9.5 Wm^{-2} . This is in reasonable agreement with the value of evaporative heat loss per unit surface area of 8.3 Wm^{-2}

(assuming a body surface area of 1.8m^2) given by Richards (1973). The value of the evaporative heat transfer coefficient, in terms of the temperature difference between the skin surface and the environmental temperature, may be estimated by assuming an average temperature difference of $10\text{ }^\circ\text{C}$. The approximate value of the heat transfer coefficient due to evaporation may then be taken to be $0.9 \pm 0.2\text{ Wm}^{-2}\text{ }^\circ\text{C}^{-1}$.

4.3.4 Total heat loss

The heat transfer coefficients for radiation, convection and evaporation may be combined to give the total heat transfer coefficient

$$h = h_r + h_c + h_e = 11 \pm 1\text{ Wm}^{-2}\text{ }^\circ\text{C}^{-1}$$

The heat loss from the body may therefore be expressed as

$$H = h (T_s - T_e) \quad (4.3.18)$$

In the steady state condition this heat loss must be equal to the heat transferred inside the tissue to the skin surface

$$K \frac{\partial T}{\partial n} = h (T_s - T_e) \quad (4.3.19)$$

This equation expresses the continuity of heat flux across the skin boundary and may be used as a boundary condition in solving equation (4.2.1).

4.4 Balance between heat production and heat loss

The average metabolic rate for males is approximately 45 Wm^{-2} (Brown 1973) which implies that the average temperature difference between the skin and the environment required to maintain a balance between the heat produced and that lost is approximately $4\text{ }^\circ\text{C}$ for an unclothed body and for a heat transfer coefficient of $11\text{ Wm}^{-2}\text{ }^\circ\text{C}^{-1}$ (neglecting the loss of heat through the respiratory tract). This is much lower than the $10\text{ }^\circ\text{C}$ difference assumed earlier in estimating the loss by evaporation. It can be seen that both the evaporative and convective coefficients as determined previously are dependent on the difference between the skin temperature and the environmental temperature, while only the radiative coefficient h_c is essentially

independent of this difference. It was found that the temperature difference required to balance the heat lost and the heat generated is 3.8 °C. This temperature difference gives a new coefficient of evaporative heat transfer of 2.4 Wm⁻² °C⁻¹ and alters the convective transfer coefficient to 78% of its value with a 10 °C temperature difference. This gives a new combined heat transfer coefficient of 11.7 Wm⁻² °C⁻¹. This is still within the error limits of the original estimate and indicates that the combined coefficient is not strongly dependent on the temperature difference between skin and environment.

Chapter 5 - Electrical, thermal and physiological properties of tissue

5.1 Introduction

This chapter considers the properties which affect the thermal state of human tissue and the detected microwave signal. The temperature distribution, as discussed in Chapter 4, is determined principally by the physiological properties of blood flow and metabolic heat production and the thermal conductivity, while the microwave emission is dependent on the temperature distribution in the tissue and the microwave power penetration depth. This penetration depth depends on the dielectric properties of the tissue.

The importance of tissue water content on the both the dielectric properties and the thermal conductivity will be discussed in this chapter and a review of measured values of these properties given. The blood flow expected in different organs and tissues will be given and its relationship to metabolic heat will be discussed. Finally the characteristics of malignant human breast tumours will be considered.

5.2 A brief note on tissue structure

Water is a very important part of the composition of the human body forming, on average, 50-70% of the body weight of adult males and 45-65% of adult females; the actual amount present depending on age and obesity. This fluid provides the essential constant internal environment necessary for the vital life processes of the body's cells.

The vital building block of all tissue types is the cell. Cells can vary widely in shape, size, structure and function. Each tissue is made up of different types of cells and is specialised to perform a particular task. In a simplified and ideal form the cell may be considered to be a spherical mass of protoplasm, bound by a delicate membrane, which contains various microscopic and sub-microscopic substances. Polysaccharides, proteins, nucleic acids and lipids form the principal large organic molecules in the protoplasm, with the proteins far exceeding the other macromolecules

in number and variety. Water forms the solvent of the intracellular fluid in which these molecules of the protoplasm are suspended. It is also present in the intercellular fluid, and in the plasma of the vascular and lymphatic systems.

The fluids of the body are essentially solutions of electrolytes occupying three hypothetical "compartments"; the intracellular fluid which contains 67% of the body's total water content, the intercellular fluid which contains 25% and the plasma which contains 8%. The fluids in each of these compartments vary in their ionic composition. The major difference between the intercellular fluid and the plasma is the protein content, while the intracellular fluid has a vastly different ionic profile from these two (Windle 1976). Plasma and intercellular fluid may be treated as 0.9% NaCl solution.

5.3 Frequency dependent dielectric behaviour of tissue

The behaviour of electromagnetic radiation in non-magnetic materials depends on the dielectric properties of the tissue, namely the electrical conductivity, σ , and the permittivity, ϵ . These two quantities are often conveniently expressed in terms of a complex relative permittivity, ϵ_r^* , given by

$$\epsilon_r^* = \epsilon_r' - j \epsilon_r'' = \frac{\epsilon}{\epsilon_0} - j \frac{\sigma}{\omega \epsilon_0} \quad (5.3.1)$$

where ϵ_0 is the permittivity of free space ($8.85 \times 10^{-12} \text{ Fm}^{-1}$), ω is the angular frequency and ϵ_r'' is known as the loss factor.

For propagation of time-harmonic plane waves, in the positive direction of the z-axis, in an infinite, homogeneous, isotropic, linear medium the wave number will be complex with a real part, γ , given by

$$\gamma = \frac{2\pi}{\lambda_0} \sqrt{\frac{\epsilon_r'}{2} \left\{ \left(1 + \left(\frac{\epsilon_r''}{\epsilon_r'} \right)^2 \right)^{\frac{1}{2}} + 1 \right\}^{\frac{1}{2}}} \quad (5.3.2)$$

where λ_0 is the wavelength in free space, and an imaginary part, α , given by

$$\alpha = \frac{2\pi}{\lambda_0} \sqrt{\frac{\epsilon_r'}{2}} \left\{ \left(1 + \left(\frac{\epsilon_r''}{\epsilon_r'} \right)^2 \right)^{\frac{1}{2}} - 1 \right\}^{\frac{1}{2}} \quad (5.3.3)$$

The imaginary part is the field attenuation constant introduced earlier in equation (2.2.15) and related to the power penetration depth by equation (2.3.10). It can be seen that in a non-conducting material with $\sigma=0$, α is zero and there is no attenuation of the wave. The real part is equal to $2\pi / \lambda$ where λ is the wavelength in the material.

In order to determine the plane wave power penetration depth at a given frequency it is necessary to know the dielectric properties of the tissue at that frequency. The frequency dependent nature of the dielectric properties of tissue has been studied (Schwan 1957, Pethig 1984) and it has been found that the dielectric constant of tissue decreases with frequency in three major steps which have been labelled the α , β and γ dispersions.

The low frequency α dispersion takes place at around 100 Hz and is associated with interfacial electrical polarizations occurring at the cell membrane. In the radio-frequency range the β -dispersion is due to the capacitive, charge storing properties of the cell membrane. A minor dispersion has been observed to take place at 100-900 MHz and is thought to be caused by the relaxation of the protein molecule or the water molecules bound to the protein or both. At high frequencies, above about 1 GHz, the capacitance of the cell membrane provides a low impedance in series with other impedance elements provided by the proteins and the intercellular fluid, and has little effect. In this region the dielectric behaviour is essentially that of a macromolecular suspension, and the dielectric dispersion is due to the relaxation of the polar water molecule. The dielectric tissue properties, at the microwave thermography frequency of 3 GHz, are therefore dominated by the behaviour of the tissue water.

5.4 Dielectric properties of water and electrolytes

The two main theories which may be applied to describe the frequency dependent behaviour of the dielectric properties of polar fluids are the Debye equations

and the Cole-Cole equations (Franks, 1972). The Deybe equations assume only one relaxation time for the polar molecules while the Cole-Cole equations allow a spread of relaxation times. In the case of water the spread of relaxation times is small and here the Deybe equations will provide a sufficiently accurate description of the dielectric properties of water.

The Deybe equations are as follows:

$$\epsilon_r' = \epsilon_\infty + \frac{\epsilon_s - \epsilon_\infty}{1 + \left(\frac{f}{f_c}\right)^2} \quad ; \quad \epsilon_r'' = \frac{(\epsilon_s - \epsilon_\infty) \left(\frac{f}{f_c}\right)}{1 + \left(\frac{f}{f_c}\right)^2} \quad (5.4.1)$$

where f is frequency, f_c is the characteristic frequency of rotation of the polar molecules, ϵ_s is the static dielectric constant and ϵ_∞ is the high frequency limit of the dielectric constant.

The static dielectric constant, as a function of temperature, is given by the equation provided by the best fit to the data of Malmberg and Maryott (1956)

$$\epsilon_s = 87.740 - 0.40008 T + 9.398 \times 10^{-4} T^2 - 1.140 \times 10^{-6} T^3 \quad (5.4.2)$$

where T is the temperature in $^{\circ}\text{C}$.

The high frequency dielectric constant at 37°C is about 4.2 and the characteristic frequency of rotation at this temperature is 25 GHz (Franks 1972). Figure 5.1 shows the Deybe dispersion of water.

The addition of salts, present in the biological fluid does not significantly affect the above values but an additional loss due to the ionic conductivity of the ions must be added to the pure water loss factor. The ionic conductivity of the intercellular fluid can be expected to be the same as that of a 0.9% saline solution due to the sodium and chlorine ions in this fluid. At 37°C this ionic conductivity is about $2 \Omega\text{m}^{-1}$ (Stogryn, 1971). The complex permittivity of this solution at 3 GHz and 37°C , calculated from the Deybe equations describing the dielectric behaviour of water and with the additional ionic conductivity is

$$\epsilon_r' - j \epsilon_r'' = 73.2 - j 20.3 \quad (5.4.3)$$

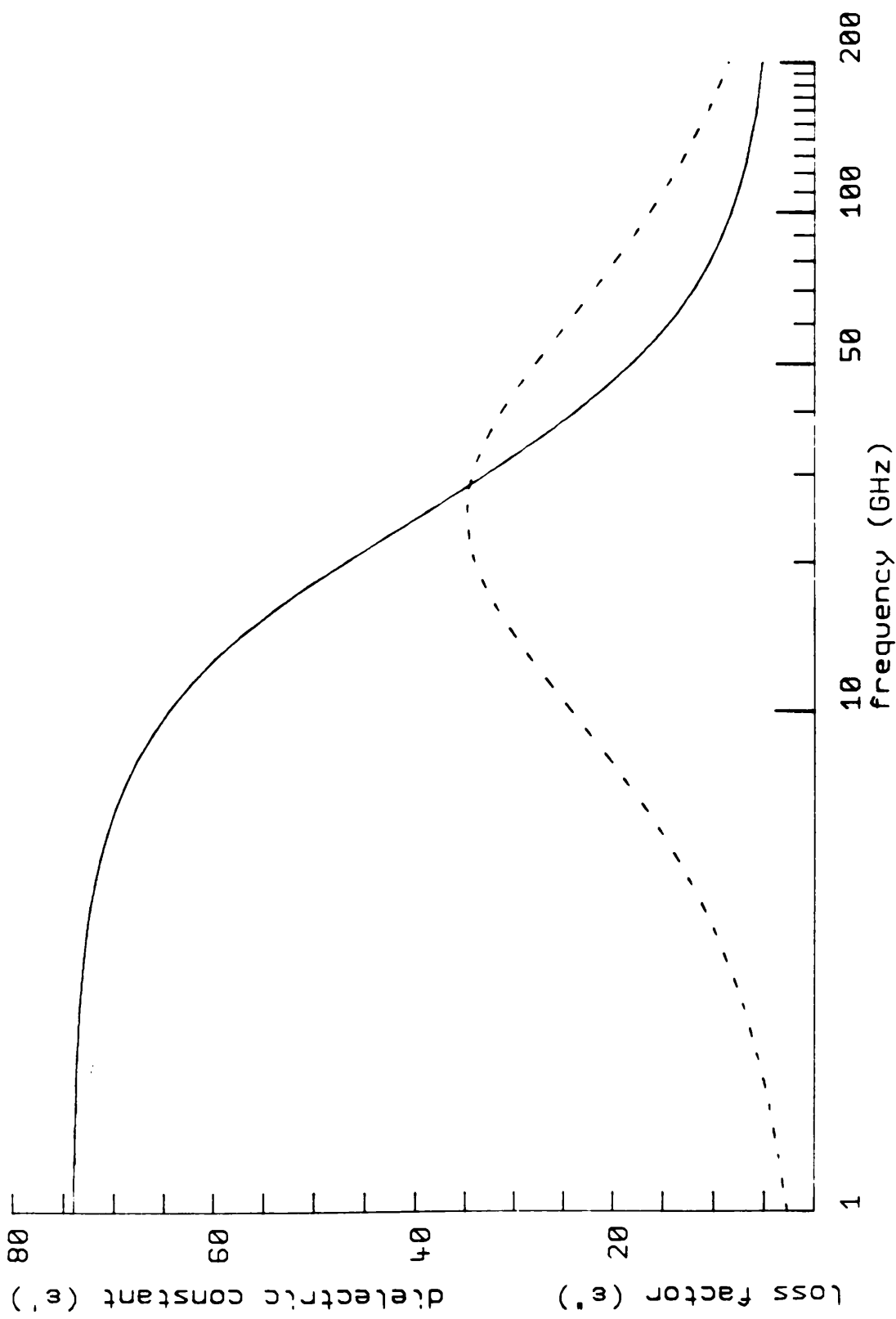


Figure 5.1 Deybe dielectric dispersion of water at 37 °C

These values most probably represent the upper limits for the dielectric properties of tissue. The calculated plane wave penetration depth at 3 GHz from these values is 6.8 mm, but it is possible that some tissue penetration depths may be smaller than this, depending on the ratio of the loss factor to relative dielectric constant. This ratio is the loss tangent (see section 3.2) and is shown as a function of frequency for physiological saline in figure 5.2 as determined from the Debye theory. This figure also shows the measured loss tangents of different tissue types [Cook, 1951,1952; Herrick, 1950, England, 1950]

5.5 Dielectric properties of tissue at 3 GHz

A number of investigators have considered the dielectric behaviour of tissue and attempted to relate the water content to the dielectric properties (Schwan and Foster, 1977; Schepps and Foster, 1980; Foster et al, 1980). This is a very difficult problem. Some of the water present in the tissue is bound to proteins and is therefore unable to rotate freely in an alternating electric field, but it is difficult to define exactly this amount (Cooke and Kuntz, 1974). It is also necessary to determine whether bulk water molecules in tissue have the same characteristic frequency of rotation and high and low frequency limits of dielectric constant as free water molecules. A number of equations (Maxwell, 1881; Fricke, 1924; Bruggeman, 1935) have been developed which describe the dielectric properties of suspensions of particles in terms of the dielectric properties of the suspended and the suspending mediums, and the relative volumes of the two mediums present. These mixture equations may be applied successfully to describe the dielectric behaviour of blood (Cook, 1951) or suspensions of protein (Grant, 1968) but in the more complicated case of tissue it seems that a mixture equation of this form may only account approximately for the dielectric properties of different tissues in terms of water content. This is most probably due to the factors mentioned above together with the complicated structure of tissue and the variation in structure between tissue types.

The dielectric properties of tissue have been tabulated by Stuchly and Stuchly

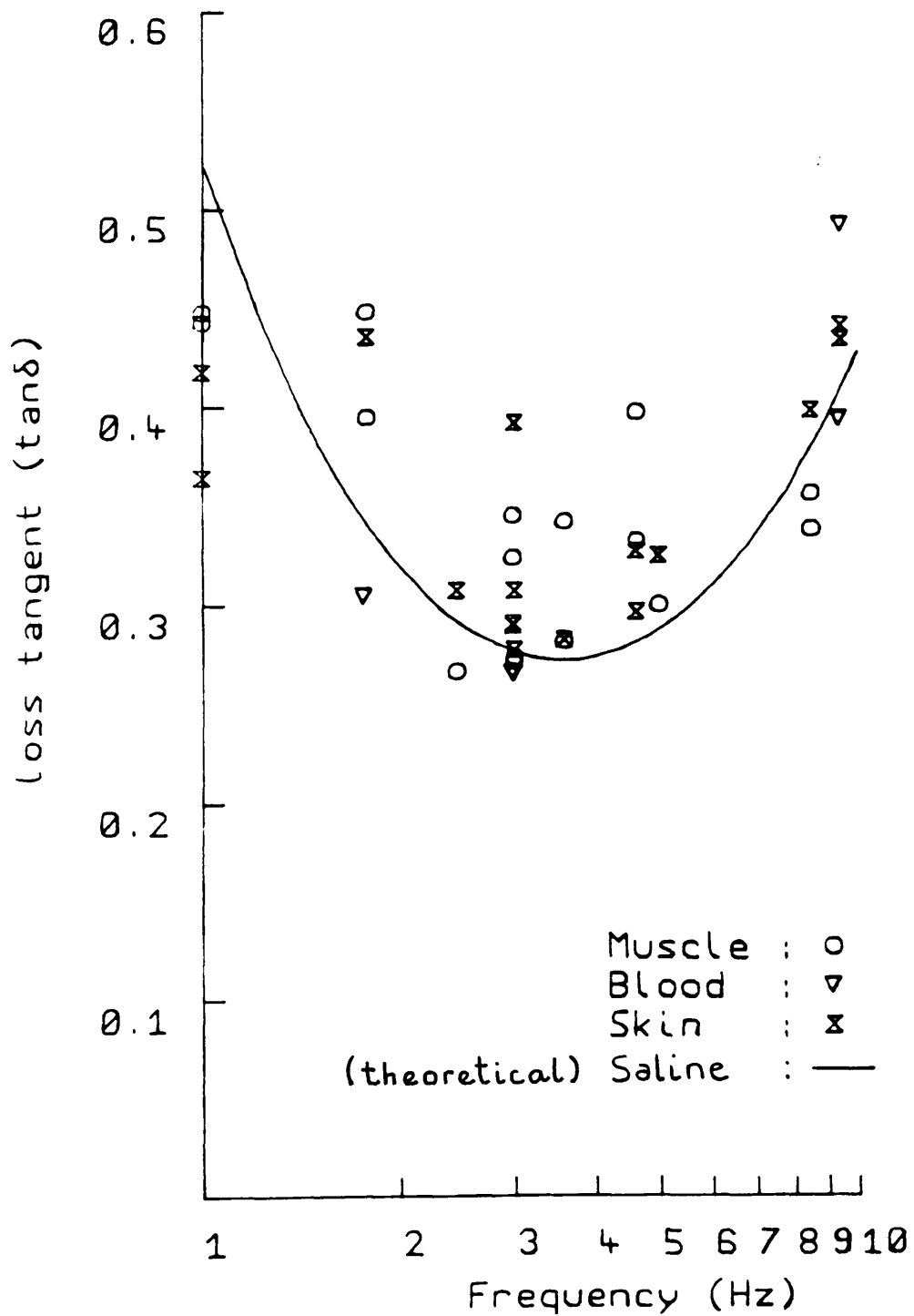


Figure 5.2 Variation of loss tangent of human tissues at microwave frequencies and 37 °C
 [Data compiled from Cook (1951,1952), Herrick (1950) and England (1950)]

(1980) and, more recently, by Foster and Schwan (1986). The difference in measured complex permittivities between the same tissues from various non-aquatic mammals is small in the frequency range 0.1-10 GHz (Stuchly and Stuchly 1984), except perhaps in the case of fat tissue. The difference between measurements using excised (in vitro) or living (in vivo) tissues (Foster and Schwan 1986) is also small. Any consistent difference due to either of these factors is indistinguishable among the variations due to tissue heterogeneity.

The values of measured dielectric properties of tissue at 3 GHz and 37 °C, both in vivo and in vitro, and human and animal, as compiled from the literature are given in Table 5.2, together with the calculated plane wave power penetration depths from these values. The tissue water contents are given in Table 5.1. It can be seen that tissue divides clearly into two categories; high water content tissues with water contents above 60% by weight, which includes the majority of tissues and organs, and the lower water content tissues of fat and bone.

Figure 5.3 shows the measured values of dielectric constant, as listed in Table 5.2, as a function of tissue water content. The calculated dielectric constants from mixture theory, assuming tissue to be composed of physiological saline solution and protein or fat, are also shown. The upper and lower limits for the dielectric constant are set by the cases where the tissue is composed of fibres which are, respectively, parallel and perpendicular to the applied electric field. It can be seen that the experimental values fall between these two limiting cases. The mixture equations of Maxwell and Bruggeman are also shown. Maxwell's equation considers tissue to be a suspension of spherical particles in physiological saline solution. In deriving this equation Maxwell assumed that the suspended particles had no effect on each other, therefore requiring a very dilute solution (high water content tissue) for application of this equation. However, experiments suggest that this equation is a reasonable approximation for much larger concentrations (Lewin, 1947). Fricke (1924) extended this theory to account for suspensions of ellipsoids. Bruggeman (1935), using the same tissue model

<u>Tissue</u>	<u>Water content (% weight)</u>	<u>Water content (% volume)</u>
Whole blood	78.5	83
Blood plasma	91	93
Blood corpuscles	68 - 72	73 - 77
Muscle	70 - 80	75 - 84
Skin	62 - 76	68 - 80
Fat	5 - 20	4 - 18
Liver	71 - 77	76 - 81
Lung	79 - 84	83 - 87
Spleen	75 - 80	80 - 84
Kidney	78 - 84	82 - 87
Whole brain	73 - 78	78 - 82
Grey matter of brain	80 - 85	84 - 88
White matter of brain	68 - 73	73 - 78

(i) Percentage weight water contents compiled from Altman and Dittmer (1964), Best and Taylor (1950), Spells (1960), Mitchell (1945) and Pethig (1984)

(ii) Water content by percentage volume calculated by assuming a density of 1.3 g cm^{-3} for the non-water content of the tissue, except in the case of fat where a density of 0.86 g cm^{-3} was used.

Table 5.1 Water contents of human organs and tissues

	Dielectric constant ϵ'	Loss factor ϵ''	Power penetration depth (cm)	Source	Reference
<u>Fat</u>					
	3.9 - 7.2	0.67 - 1.36	2.3 - 6.2	Human	Herrick (1950)
	4.92	1.46	2.4	Human	Cook (1951)
	3.94	0.87	3.7	Human	Cook (1951)
	7.0	1.75	2.4	Human	Cook (1951)
	11.6	2.25	2.4	Human	Cook (1951)
	5.2	1.5	2.4	Human	England (1950)
	7.2	1.7	2.5	Human	England (1950)
<u>Bone</u>					
	7.5	1.0	4.3	Human	Herrick (1950)
	8.35	1.32	3.4	Human	Cook (1951)
<u>Bone marrow</u>					
	4.2-5.8	0.7-1.35	2.4 - 5.6	Human	Herrick (1950)
<u>Muscle</u>					
**	52.5	16.2	0.72	Cat	Kraszewski (1982)
**	55.5	17.2	0.70	Rat	Kraszewski (1982)
	53	16.8	0.70	Cat	Kraszewski (1982)
	46	16.8	0.65	Canine	Schepps (1980)
	45 - 48	13 - 14	0.77 - 0.85	Human	Herrick (1950)
	50	17.1	0.67	Human	Cook (1951)
	51	18	0.64	Human	Cook (1951)
	52	18.9	0.62	Human	Cook (1951)
**	56	17.3	0.69	Rat	Burdette (1980)
	47	15	0.74	Bovine	Brady (1981)
<u>Whole blood</u>					
	55 - 56	15 - 18.6	0.65 - 0.08	Human	Herrick (1950)
	56	15.9	0.76	Human	Cook (1952)
	53	15	0.78	Human	England (1950)

Table 5.2 Dielectric properties of tissues and organs at a frequency of 3 GHz and at 37 °C

[** indicates measurement *in-vivo*, otherwise measurement *in-vitro*]

	Dielectric constant ϵ'	Loss factor ϵ''	Power penetration depth (cm)	Source	Reference
<u>Liver</u>					
	43	13	0.87	Bovine	Brady (1981)
	53	14.4	0.81	Canine	Schepps (1980)
	42 - 43	12 - 12.2	0.85 - 0.88	Human	Herrick (1950)
	49	13.8	0.81	Cat	Kraszewski (1982)
**	47	12.6	0.88	Cat	Kraszewski (1982)
**	46	12.7	0.85	Rat	Kraszewski (1982)
<u>Spleen</u>					
**	52	15	0.78	Cat	Kraszewski (1982)
**	52.3	15.1	0.77	Rat	Kraszewski (1982)
	52	15.3	0.76	Cat	Kraszewski (1982)
	46	16.2	0.68	Canine	Schepps (1980)
<u>Kidney</u>					
**	47.5	13.8	0.80	Cat	Kraszewski(1982)
**	50.6	13.5	0.85	Rat	Kraszewski (1982)
	47	13.2	0.83	Cat	Kraszewski (1982)
**	47	12	0.92	Canine	Burdette (1980)
**	49	18	0.63	Canine	Burdette (1980)
	48	15	0.75	Bovine	Brady (1981)
<u>Skin</u>					
	40	13.1	0.80	Human	Cook (1951)
	42.4	13.1	0.80	Human	Cook (1951)
	51.1	15.2	0.76	Human	Cook (1951)
	40.9	16.8	0.62	Human	England (1950)
	52.2	17	0.68	Human	England (1950)
	50.2	14.8	0.77	Human	England (1950)

Table 5.2 (continued) Dielectric properties of tissues and organs at a frequency of 3 GHz and at 37⁰ C

[** indicates measurement *in-vivo*, otherwise measurement *in-vitro*]

	Dielectric constant ϵ'	Loss factor ϵ''	Power penetration depth (cm)	Source	Reference
Brain					
(cerebellum - 76 % water content by weight)					
	40	12.2	0.83	Mouse	Nightingale (1983)
(cerebrum - 74 % water content by weight)					
	39	12.5	0.81	Mouse	Nightingale (1983)
(brain stem - 72 % water content by weight)					
	36	10.7	0.90	Mouse	Nightingale (1983)
(white matter - 72% water content by weight)					
	33	9	1.02	Canine	Foster (1979)
(grey matter - 82% water content by weight)					
	44	12	0.88	Canine	Foster (1979)
(whole)					
	33	18	0.53	Human	Lin (1975)
**	52.5	13.7	0.85	Rat	Burdette (1980)
Eye parts					
(retina - 89% water content by weight)					
	56.2	16.4	0.74	Rabbit	Gabriel (1983)
(choroid - 78% water content by weight)					
	51.9	13.3	0.87	Rabbit	Gabriel (1983)
(iris - 77% water content by weight)					
	51.7	15.6	0.74	Rabbit	Gabriel (1983)
(cornea - 75% water content by weight)					
	49.9	17.9	0.63	Rabbit	Gabriel (1983)
(cortex - 71% water content by weight)					
	48	13.4	0.83	Rabbit	Gabriel (1983)
(nucleus - 71% water content by weight)					
	22.7	9.9	0.78	Rabbit	Gabriel (1983)

Table 5.2 (continued) Dielectric properties of tissues and organs at a frequency of 3 GHz and at 37 °C

[** indicates measurement *in-vivo*, otherwise measurement *in-vitro*]

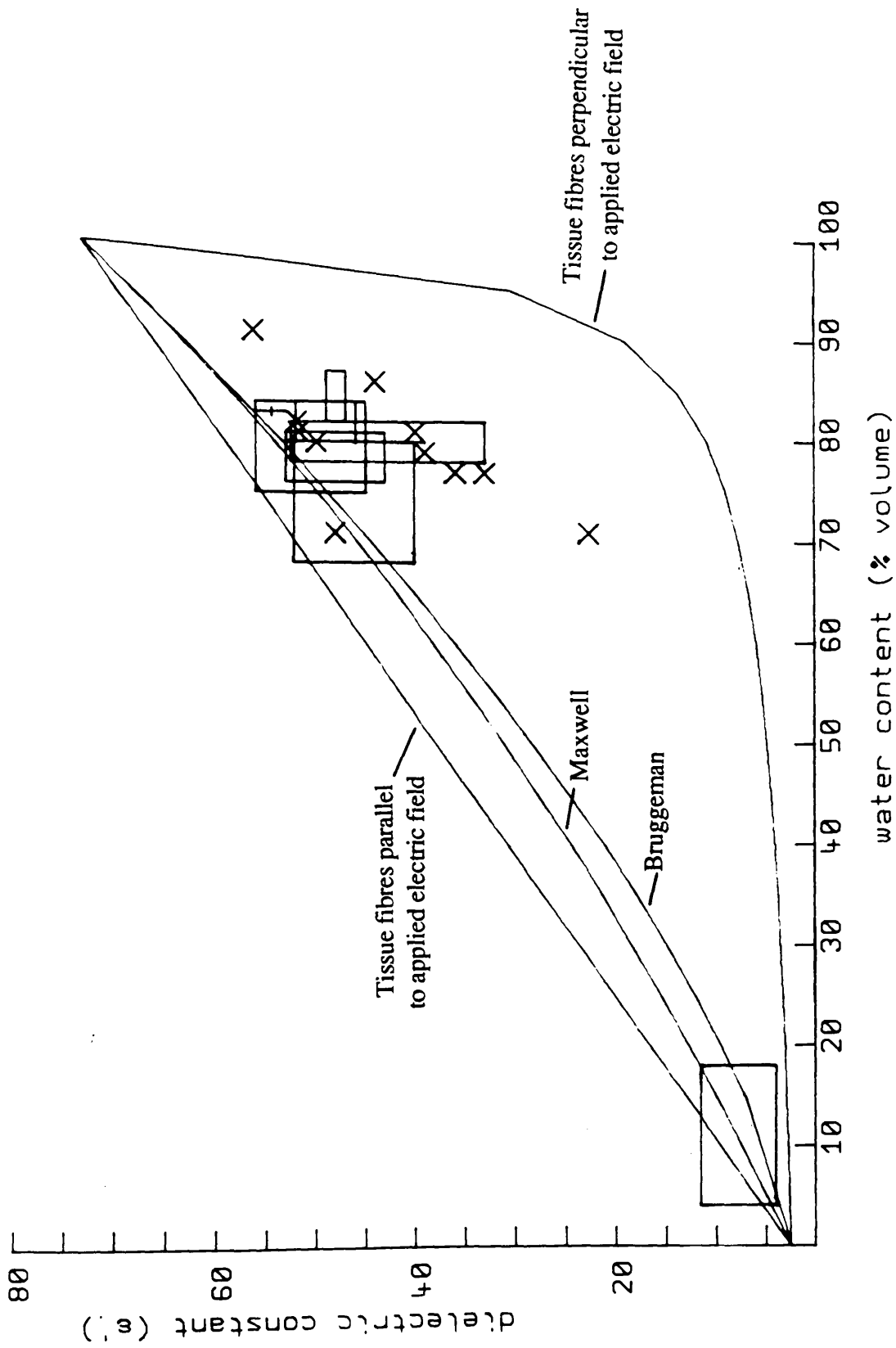


Figure 5.3 Variation of dielectric constant with water content of tissues at 3 GHz and at

37 °C [Data from Tables 5.1 and 5.2]

as that of Maxwell, took interparticle interaction into account in the derivation of his mixture equation.

Bone, because of its very different structure from the soft tissues, cannot be considered in terms of these mixture equations, and is consequently not included in figure 5.3 or the subsequent figures which consider tissues in terms of their water content.

Figure 5.4 illustrates the variation in loss factor with tissue water content. The experimental values from Table 5.2 are shown together with Maxwell's mixture equation. In figure 5.5 the power penetration depth is shown. The theoretical curve is determined from the calculated variation of dielectric constant and loss factor with tissue water content using Maxwell's mixture equation. For tissues with water contents greater than 66% by volume (60% by weight) the decrease in penetration depth with water content can be seen to be very gradual. These high water content tissues have measured penetration depths between 6 mm and 9 mm, while the low water content tissues have a much larger range, with penetration depths between 23 mm and 63 mm.

Using the measured values and the theoretical curve to estimate the penetration depth for the water content range for which experimental data is not available the penetration depth of tissue may be related to the tissue water content by means of the following three categories:

<u>WATER CONTENT (% weight)</u>	<u>PENETRATION DEPTH (mm)</u>
low water content (0-30)	14 - 63
medium water content (30-60)	9 - 14
high water content (60-100)	6 - 9

These divisions are represented by the dotted line in figure 5.5.

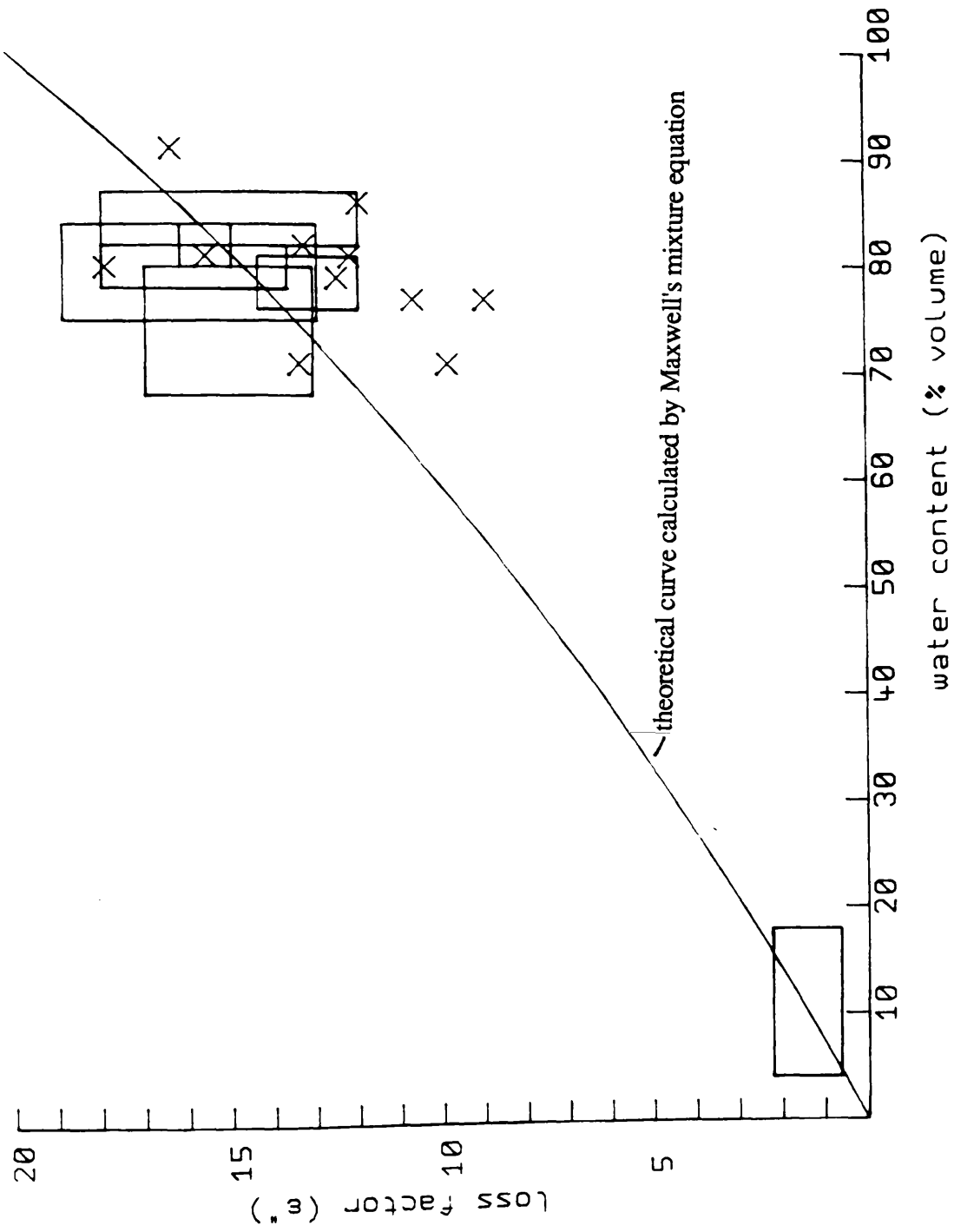


Figure 5.4 Variation of loss factor with water content for tissues at 3 GHz and at

37 °C [Data from Tables 5.1 and 5.2]

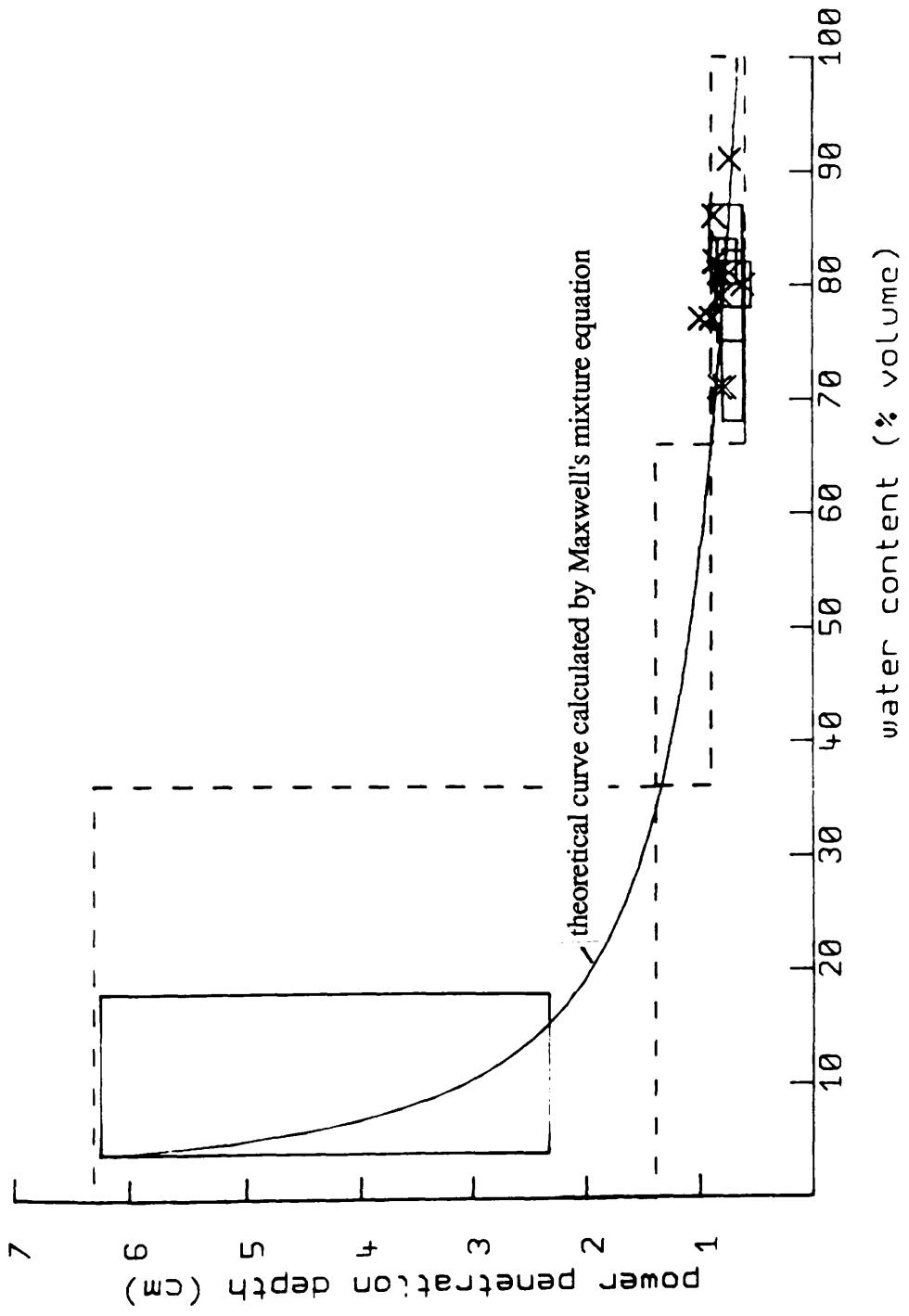


Figure 5.5 Variation of power penetration depth with water content for tissues at 3 GHz and at 37 °C

[Data from Tables 5.1 and 5.2]

5.6 Thermal conductivity of tissues

As in the case of the dielectric properties of tissue, it is expected that the water content of tissue will determine to a certain extent the tissue thermal conductivity. Water has a thermal conductivity of $0.623 \text{ Wm}^{-1} \text{ K}^{-1}$ at 37°C , which is the highest thermal conductivity of any of the components of soft biological tissue. The other major constituents of body tissue, protein and fat, have thermal conductivities of 0.18 and $0.19 \text{ Wm}^{-1} \text{ K}^{-1}$ respectively (Poppendiek, 1966). The thermal conductivity of various tissues have been measured by a number of investigators and a comprehensive tabulation of results is given by Chato (1969). Table 5.3 lists the values of thermal conductivity for some human tissues at 37°C and figure 5.6 illustrates these measured values as a function of tissue water content together with the theoretical curve from Maxwell's mixture equation, which may also be applied to thermal conductivity. Representative values of the thermal conductivity of tissues in each of the water content categories above, with an extra division to account for very high water content tissues, may taken to be as follows:

<u>WATER CONTENT (% weight)</u>	<u>THERMAL CONDUCTIVITY ($\text{Wm}^{-1} \text{ K}^{-1}$)</u>
low water content (0-30)	0.18 - 0.31
medium water content (30-60)	0.31 - 0.44
high water content (60-80)	0.44 - 0.52
very high water content (>80)	0.52 - 0.62

High values for the thermal conductivity of bone, compared with those expected from its water content, have been reported (Kirkland 1967) and bone will be considered to have a thermal conductivity of $0.8 \text{ Wm}^{-1} \text{ K}^{-1}$. This exceeds the thermal conductivity of water and is possibly due to the large amount of minerals present in bone.

It is important to note that only in vitro measurements of thermal conductivity have been considered. In vivo measurements include an additional conductivity effect

<u>Tissue</u>	<u>Thermal conductivity (Wm⁻¹ °C⁻¹)</u>	<u>Reference</u>
Whole blood	0.51	Spells (1960)
Blood plasma	0.58	Spells (1960)
Blood corpuscles	0.48	Spells (1960)
Muscle	0.41	Lipkin (1954)
	0.44	Hatfield (1953)
Skin	0.39 (living, blood flow occluded)	Lipkin (1954)
	0.32 (excised, moist)	Lipkin (1954)
Fat	0.22	Lipkin (1954)
	0.20	Hatfield (1953)
Liver	0.51	Valvano (1985)
Lung	0.45	Valvano (1985)
Spleen	0.54	Valvano (1985)
Water	0.62	CRC Handbook (1977)
100 % protein	0.18	Poppendiek (1966)
100 % fat	0.19	Poppendiek (1966)

Table 5.3 Thermal conductivities of human organs and tissues at 37 °C

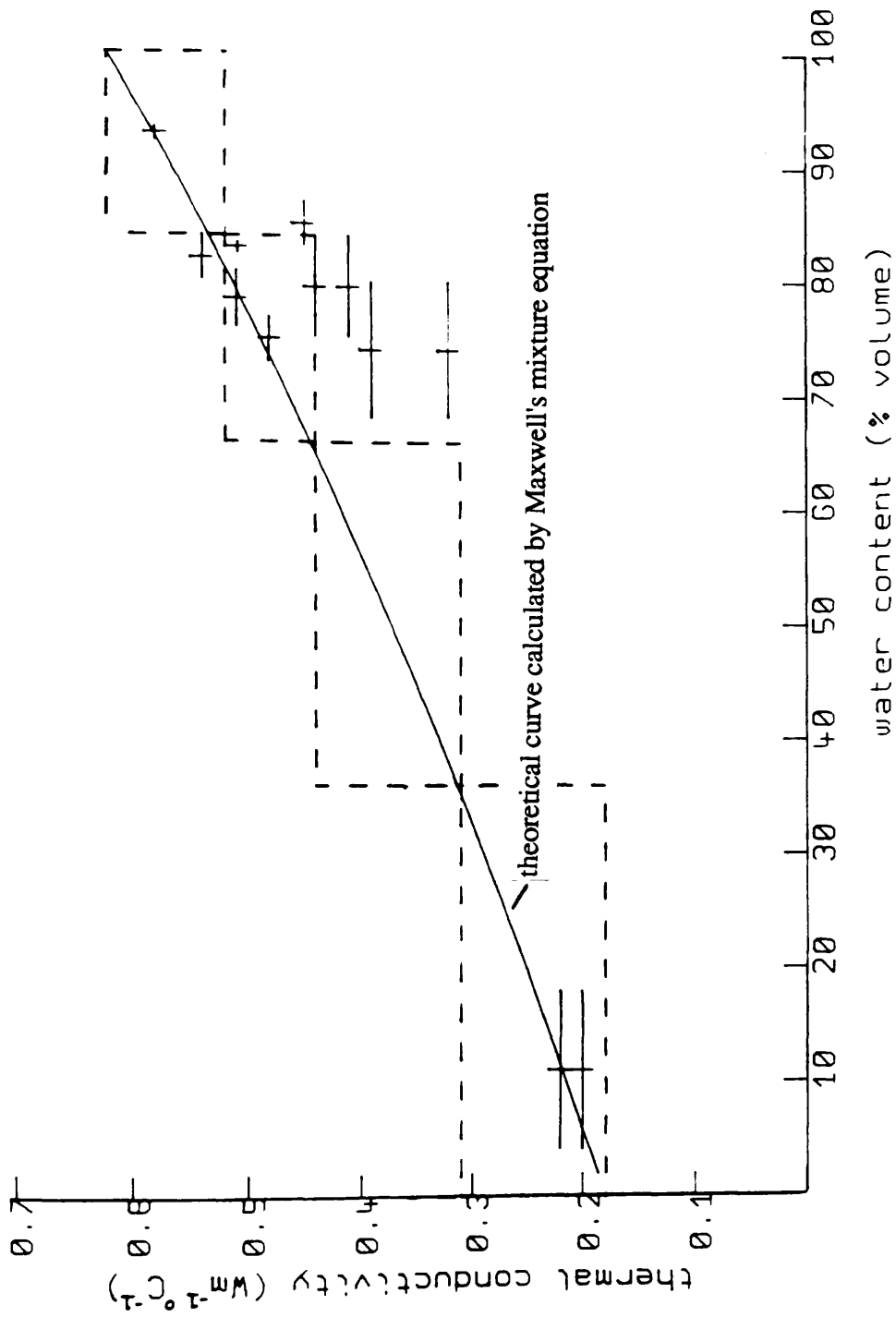


Figure 5.6 Variation of thermal conductivity with water content for human tissues at

37 °C

[Data from Tables 5.1 and 5.3]

due to the flow of blood. In applying equation (4.2.1) to determine temperature distributions in tissue it is the actual thermal conductivity which is required. Measurements of in vivo thermal conductivity would be required if equation (4.2.3) were to be applied.

Gautherie (1980) has reported measured values of thermal conductivity in healthy breast tissue, from post-operative samples, of $0.12 \text{ Wm}^{-1} \text{ }^{\circ}\text{C}^{-1}$ for fat tissue, $0.25 \text{ Wm}^{-1} \text{ }^{\circ}\text{C}^{-1}$ for fibrous tissue and $0.32 \text{ Wm}^{-1} \text{ }^{\circ}\text{C}^{-1}$ for glandular tissue. These values for fat are significantly lower than those reported by other investigators.

5.7 Blood flow and metabolic heat generation in tissue

The physiological properties which determine the internal temperature distribution are the rates of blood perfusion and metabolic heat generation. These two quantities may be related by considering a volume of tissue perfused by blood at a rate of $W_b \text{ kgm}^{-3}\text{s}^{-1}$. The tissue extracts oxygen from the blood supply and this amount is determined by the difference in oxygen content between the arterial and the venous blood, $d \text{ ml O}_2$ per 100 ml blood. Due to the breaking of the oxygen-oxygen bond $2 \times 10^4 \text{ J}$ of heat are liberated for each litre of oxygen used. The density of blood is $1.06 \times 10^3 \text{ kgm}^{-3}$ and the rate of metabolic heat production $Q \text{ Wm}^{-3}$ is therefore

$$Q = 189 d W_b \quad (5.7.1)$$

Table 5.4 gives the blood flow of various organs and tissues, the arterial-venous O_2 difference and the rate of metabolic heat generation calculated from these values using equation 5.7.1. It can be seen that the kidney, liver, heart and brain have a high blood flow per unit volume and are large sources of metabolic heat, while resting skeletal muscle, skin and the tissues grouped under other, which include bone, cartilage, fat and connective tissue, have a low blood flow per unit volume and are relatively avascular tissues. The rate of heat production in these tissues is much less than that in the organs.

The blood flow distribution in the body may be significantly altered under stress

Tissue	Arterial-venous oxygen difference (ml O ₂ / 100 ml)	Blood perfusion rate (kgm ⁻³ s ⁻¹)	Metabolic heat production rate (Wm ⁻³)
Brain	6	10.5	11.7 x 10 ³
Heart	11	13.6	27.7 x 10 ³
Liver	5	18.6	17.3 x 10 ³
Kidney	1.5	59.9	16.7 x 10 ³
Muscle	5	0.8	0.7 x 10 ³
Skin	2	1.6	0.6 x 10 ³
Other	5	0.2	0.2 x 10 ³

[Data from Smith and Kampine (1984)]

Table 5.4 Typical blood perfusion rates, arterial-venous oxygen extractions and aerobic metabolic heat production rates in the main organs and tissues of a normal adult at rest.

conditions, such as severe exercise, but the values for a subject at rest, as given in Table 5.4, are appropriate for a patient in a normal clinical environment. The skin blood flow, since this is a method of control of heat loss, may vary depending on the environmental conditions.

There is very little data for blood perfusion in normal breast tissues, but it is likely that, in normal conditions, the perfusion of the breast will have values in the range between resting muscle and fat tissue (Wells 1977). The range of perfusion in the normal breast is therefore likely to be between 0.2 and $0.8 \text{ kgm}^{-3}\text{s}^{-1}$.

5.8 Characteristics of malignant breast tumours

The very high water content of malignant tumours is a well known characteristic (Homburger and Fishman 1953). As a result of this it is expected that tumour tissue will have power penetration depth and thermal conductivity in the very high water content category (i.e. $6 \leq \delta \leq 9 \text{ mm}$ and $0.52 \leq K \leq 0.62 \text{ Wm}^{-1} \text{ }^\circ\text{C}^{-1}$).

The blood flow in patients with breast carcinoma has been studied in vivo by Beaney et al (1984) using positron emission tomography. Nine post-menopausal patients with breast cancers varying in size from a largest diameter of 3cm to 14 cm were successfully studied. For the smaller tumours the whole neoplasm was analysed, while for the two largest tumours, which exhibited necrotic centres, this area of mostly dead tissue was excluded. The blood flow in the contra-lateral normal breast, including as much of the breast as possible, was also studied. The blood flow in normal breasts was found to be in a range between 0.5 and $1.0 \text{ kgm}^{-3}\text{s}^{-1}$ with an average value of $0.7 \text{ kgm}^{-3}\text{s}^{-1}$. The perfusion in tumours was found to be between 1.4 and $5.6 \text{ kgm}^{-3}\text{s}^{-1}$ with an average of $3.3 \text{ kgm}^{-3}\text{s}^{-1}$. The metabolic heat production from consumption of oxygen (assuming a value of energy release of $2 \times 10^4 \text{ J l}^{-1}$) was between 1.1×10^3 and $3.5 \times 10^3 \text{ Wm}^{-3}$ in tumours with an average value of $2.2 \times 10^3 \text{ Wm}^{-3}$, while in normal tissue the values ranged from 1.1×10^3 to $2 \times 10^3 \text{ Wm}^{-3}$ with an average of $1.5 \times 10^3 \text{ Wm}^{-3}$.

These results indicate that perfusion is significantly greater in viable tumour tissue than in normal breast tissue, but that there is only a small difference in the oxygen metabolic rate. Beaney suggests that glucose metabolism may be disproportionately larger than oxygen metabolism in breast tumours compared with normal breast tissue. The total heat produced by both the oxygen and the glucose metabolism may therefore reach a significantly higher value in tumours than in the surrounding normal tissues.

Mantyla (1979) has investigated the blood flow in a variety of human tumours using the xenon clearance method. For three different types of tumours from a variety of locations in the body, and with approximately 30 tumours in each group, the average blood flow was found to be $6.7 \text{ kgm}^{-3}\text{s}^{-1}$ for lymphomas, $3.0 \text{ kgm}^{-3}\text{s}^{-1}$ for anaplastic carcinoma and $4.4 \text{ kgm}^{-3}\text{s}^{-1}$ for differentiated tumours. These values are in reasonable agreement with those of Beaney for unclassified tumours occurring in the breast. Mantyla concludes that "most human tumours have a considerably lower blood flow than what one would expect to find in the surrounding normal tissue". In the case of breast tumours, however, the results of Beaney strongly indicate that this is not the case. In tumours occurring in the organs and glands the blood flow in tumours may be lower than that in the surrounding tissue but in the case of breast tissue, with normal perfusion rates lower than those of organs and glands, the blood flow is most probably greater than that of the surrounding normal tissue.

Chapter 6 - Microwave Thermography in Breast Disease

6.1 Introduction

This chapter examines the use of microwave thermography in the study of breast disease. A brief description of the structure of the breast will be given followed by a short discussion of breast imaging. The relationship between microwave temperature and the electrical, thermal and physiological properties considered in Chapter 5 will be discussed. The results of numerical modelling of the breast to determine the expected microwave and infra-red temperatures from both cancerous and normal breasts will be presented and compared with measurements on patients with breast disease and normal volunteers.

6.2 Anatomy of the breast

The female breast consists of glandular tissue and fat arranged within a supporting connective tissue. This connective tissue contains fibrous bands which attach the breast firmly to the skin and to the muscles on the deep surface of the breast (see figure 6.1). The glandular structure consists of alveoli (small sac-like dilations which are inconspicuous in the non-lactating breast) which lead into lactiferous ducts. The ducts are larger than the alveoli and are embedded in the fibrous connective tissue and fat. Each duct dilates into a sinus and opens onto the nipple. (Rehman 1978)

In the normal mature breast the relative amounts of fat and glandular tissue present vary among individuals. As the menopause approaches the breast as a whole shrinks and the glandular portion involutes. In fatty breasts there is an increase in the amount of fat and with advancing years the glandular tissue is replaced by fat. If little fat is present or involution is incomplete there may be a relative increase in the amount of fibrous tissue (Evans and Gravelle 1973).

As a result of the varying relative amounts of fat, glandular tissue and fibrous connective tissue which may form the breast, the microwave penetration depth may be expected to vary from individual to individual, with a difference between pre- and

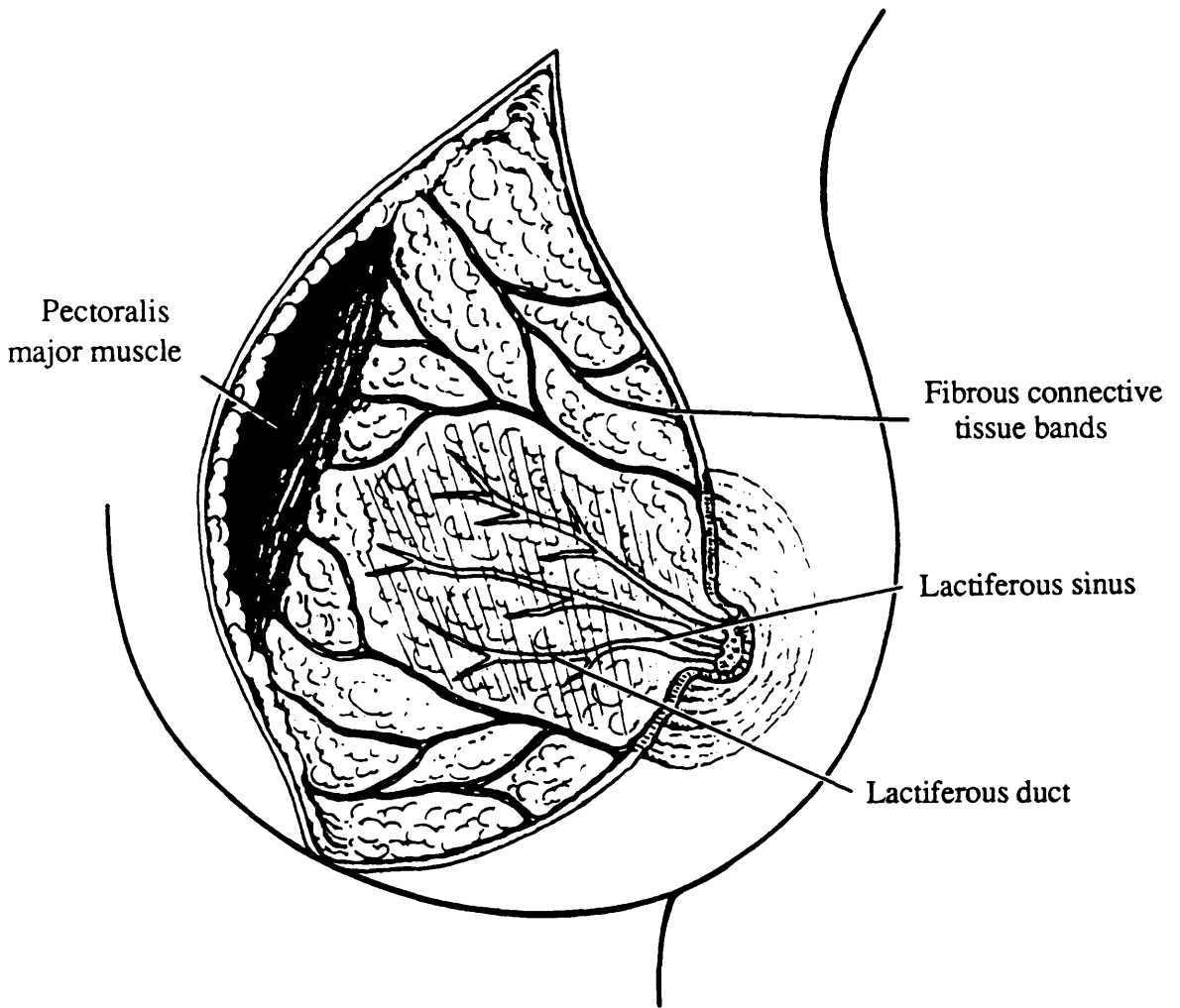


Figure 6.1 Structure of the female breast

post-menopausal breasts, due to the difference in the average breast tissue water content. Those with fatty breasts, most probably post-menopausal women, might be expected to have greater microwave penetration depths through the breast tissue, since this tissue will have a lower water content than that containing greater relative amounts of glandular tissue.

6.3 Breast diseases and imaging

There are many diseases which affect the female breast but the most common are cystic disease, fibroadenomas and cancer, which together account for more than 90% of breast lesions (Haagensen 1971). Cysts, the most common lesions, are hollow, benign tumours containing fluid or soft material. In the breast they are, in most cases, the result of blockage in milk ducts due to inflammation. They are well delineated and slightly mobile. Fibroadenomas, which occur generally in young women, are also benign tumours and are composed of gland-like tissue. They are very mobile, solid, and well-delineated. These benign tumours, cysts and fibroadenomas, grow slowly at one spot, pressing neighbouring parts aside but not invading them, unlike malignant tumours, cancers, which spread rapidly from point to point and invade and destroy surrounding tissues. Cancers are solid, poorly delineated and immobile. A wide range of growth rates of malignant tumours have been reported, with doubling rates varying from 30 days to 300 days. Early detection and treatment of cancer has been shown to reduce mortality (Roebuck 1986) and it is important that imaging techniques are able to detect breast cancer at the early stages and to distinguish between benign and malignant lesions. The ability to detect small early cancers is important if an imaging technique is to be used as a screening method. At present mammography, examination of the breast by means of low energy radiography, is the principal imaging technique and studies have shown that this method is much superior to clinical examination in detecting cancers less than 2 cm in diameter (Roebuck 1986). Other more recent techniques, such as microwave and infra-red thermography, and ultrasonic imaging, have not been

evaluated as fully as mammography, but may provide useful additional methods of imaging to be used

(i) in women with dense glandular tissue in which detection of lesions by mammography is difficult,

(ii) to give additional information to aid in diagnosis,

or (iii) as preliminary screening methods to identify high risk women who may then be given mammography. This would reduce the number of women exposed to x-rays and the risk associated with this.

An excellent, comprehensive review of methods of breast imaging has been given by Jones (1982).

6.4 Factors influencing microwave and infra-red thermographic measurements

The effects of the tissue properties, principally blood flow and tissue water content, on the measured microwave and surface temperatures may be studied theoretically by considering plane layers of tissue. In this section a single planar region of tissue is used to grossly illustrate these effects, and a two-region planar model is used to indicate the effects of the skin layer on these temperatures. The effects of reflections occurring at the boundary between the skin and the underlying tissue and at the interface between the antenna and tissue are included, as is the effect of enhanced attenuation in the tissue due to the antenna response pattern.

6.4.1 Single region model

In the case of a semi-infinite planar layer of homogeneous tissue the solution to the steady state heat transfer equation in one-dimension,

$$K \frac{d^2 T}{dz^2} + w_b c_b (T_a - T) + Q = 0 \quad (6.4.1)$$

with the boundary equation at the surface given by

$$K \frac{dT}{dz} = h (T - T_e) \quad \text{at } z = 0 \quad (6.4.2)$$

and the condition that the temperature remains finite as the depth in the tissue increases is

$$T(z) = \frac{T_e - T_a'}{1 + \frac{K\beta}{h}} \exp(-\beta z) + T_a' \quad (6.4.3)$$

$$\text{where } T_a' = T_a + \frac{Q}{w_b c_b} \quad \text{and} \quad \beta = \sqrt{\frac{w_b c_b}{K}}$$

This equation describes the temperature distribution in the tissue and from this the measured microwave temperature may be determined, using (2.3.16) to calculate the antenna temperature due to the radiation emitted by the tissue, and (3.7.6) to include the reflection of power which takes place at the antenna-tissue boundary and the calibration of the Glasgow microwave thermography system to an assumed power reflection coefficient, $|\rho|^2$, of 0.1.

The antenna temperature, T_A , for this temperature distribution is

$$T_A = \frac{T_e - T_a'}{\left(1 + \frac{K\beta}{h}\right) \left(1 + \frac{\beta}{2\alpha'}\right)} + T_a' \quad (6.4.4)$$

For the Glasgow microwave thermography system the power transmission factor, a , is approximately 0.84, the reference temperature is 40°C and the environmental temperature at which measurements are made is usually 25°C. This gives an effective reference temperature, T_{ref}^* of 35.5°C and the measured microwave temperature, T_M , in this case is, from equation (3.7.6),

$$T_M = \frac{(1 - |\rho|^2) T_A + (|\rho|^2 - 0.1) 35.5}{0.9} \quad (6.4.5)$$

The difference between the measured microwave temperature, T_M , and the antenna temperature, the actual microwave temperature of the tissue, T_A , is clearly zero when T_A is equal to 35.5°C or the power reflection coefficient is 0.1. The antenna temperature is unlikely to differ from 35.5°C by more than 3.5°C, while the power

reflection coefficient will not vary from 0.1 by more than about 0.1, giving a maximum difference between the actual source temperature, T_A , and the measured temperature, T_M , of 0.4 °C.

Figure 6.2 illustrates the effect of tissue water content and blood perfusion rate on the microwave temperature, T_M , calculated from equations (6.4.4) and (6.4.5), and the surface temperature, T_S , given by

$$T_S = \frac{(T_e - T_a')}{\left(1 + \frac{K\beta}{h}\right)} + T_a' \quad (6.4.6)$$

for a single region of tissue.

The surface temperature depends on the temperature difference $T_e - T_a'$, the effective thermal resistance of the perfused tissue, Z_t , given by

$$Z_t = \frac{1}{K\beta} = \frac{1}{\sqrt{W_b c_b K}} \quad (6.4.7)$$

and, in series with this, the thermal resistance between the skin and the environment given by the inverse of the heat transfer coefficient, h . The skin temperature increases as the effective resistance of the tissue is decreased, which occurs with increasing thermal conductivity (i.e. water content) or perfusion. The effective tissue resistance decreases rapidly at first with increasing perfusion which leads to a large surface temperature increase for a small increase in perfusion at low values of perfusion, as can be seen clearly in figure 6.2.

The antenna temperature, T_A , given by equation (6.4.4) may also be expressed as

$$T_A = \frac{(T_S - T_a')}{\left(1 + \frac{\beta}{2\alpha'}\right)} + T_a' \quad (6.4.8)$$

and so can be seen to depend on the surface temperature T_S and the dimensionless parameter $\beta/2\alpha'$. This parameter may also be expressed as δ'/d and represents the ratio of the effective power penetration depth, δ' , to the characteristic depth of the temperature variation, d , which is equal to β^{-1} . The depth, d , is the thickness of tissue

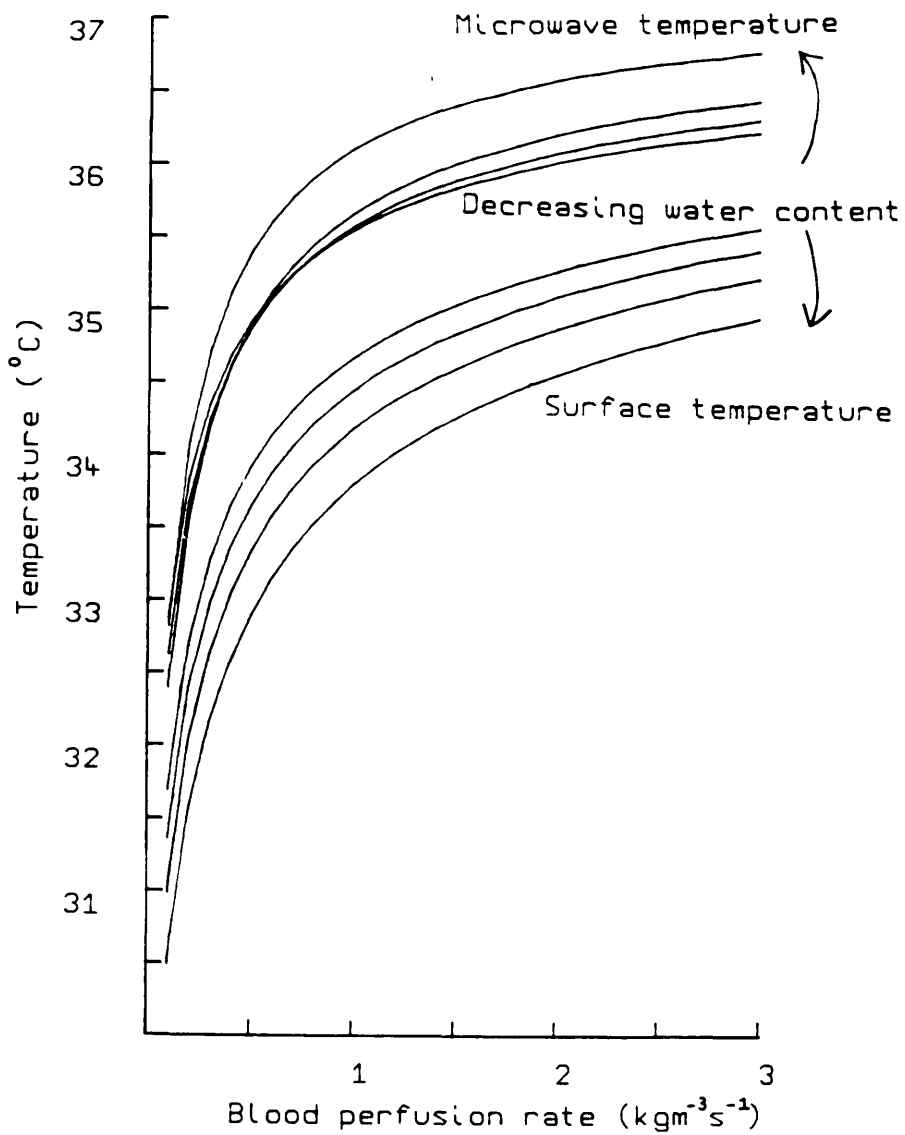


Figure 6.2 Variation of microwave and surface temperatures with blood perfusion rate for tissues of 10, 30, 50 and 70 % water content [with properties as shown in table below]

Approximate water content (% volume)	Thermal conductivity ($\text{Wm}^{-1}\text{°C}^{-1}$)	ϵ_r'	ϵ_r''	δ (cm)	δ' (cm)
10	0.21	7	1.7	2.33	1.45
30	0.29	23	6	1.20	0.84
50	0.37	37	10	0.92	0.67
70	0.46	51	14	0.77	0.60
Skin	0.44	45	15	0.68	0.55

Table 6.1 Typical properties of different water content tissues

required to reduce the difference between the tissue temperature and the core temperature, T_a' , by e^{-1} of this difference at the skin surface. The ratio δ'/d indicates the fraction of the temperature variation in the tissue which is "seen" by the microwave radiometer. The total depth of temperature variation, the depth of tissue over which the temperature rises from skin temperature to close to core temperature will occur typically over about three characteristic lengths and so if δ'/d is equal to about three the entire temperature variation is seen, while for values less than this only a fraction will be "seen". As the ratio δ'/d becomes larger the microwave temperature approaches the core temperature and becomes less sensitive to changes in blood perfusion rate.

At a given value of blood perfusion an increase in tissue water content will increase the thermal conductivity and decrease the penetration depth. The increased thermal conductivity causes an increase in the microwave temperature while the decreased penetration depth decreases this temperature. These effects mean that in a high water content tissue, although the radiometer does not "see" to such a large depth as in low water content tissues, a larger amount of heat is carried to the surface of the tissue. These are compensating effects in the detection of "hot spots" in the tissue. The overall effect of increased water content, however, is to decrease the microwave temperature (see figure 6.2). The difference in microwave temperature between different water content tissues is smaller than the difference seen in the surface temperatures.

For a single region of tissue the reflection of power at the antenna-tissue boundary has been shown in figure 3.5. Figure 6.3 shows the variation of microwave temperature with surface temperature for different water content tissues, for the Glasgow microwave thermography system with a mismatch at the antenna-tissue boundary and for an antenna which is matched to the tissue. The variation in surface temperature is due to different values of blood perfusion between 0.1 and $3 \text{ kgm}^{-3}\text{s}^{-1}$. The 50% water content tissue has not been shown in this figure because there is very little difference between this tissue and the 70% water content tissue. However, a

Antenna and tissue matched - - - - -
Antenna and tissue mismatched _____

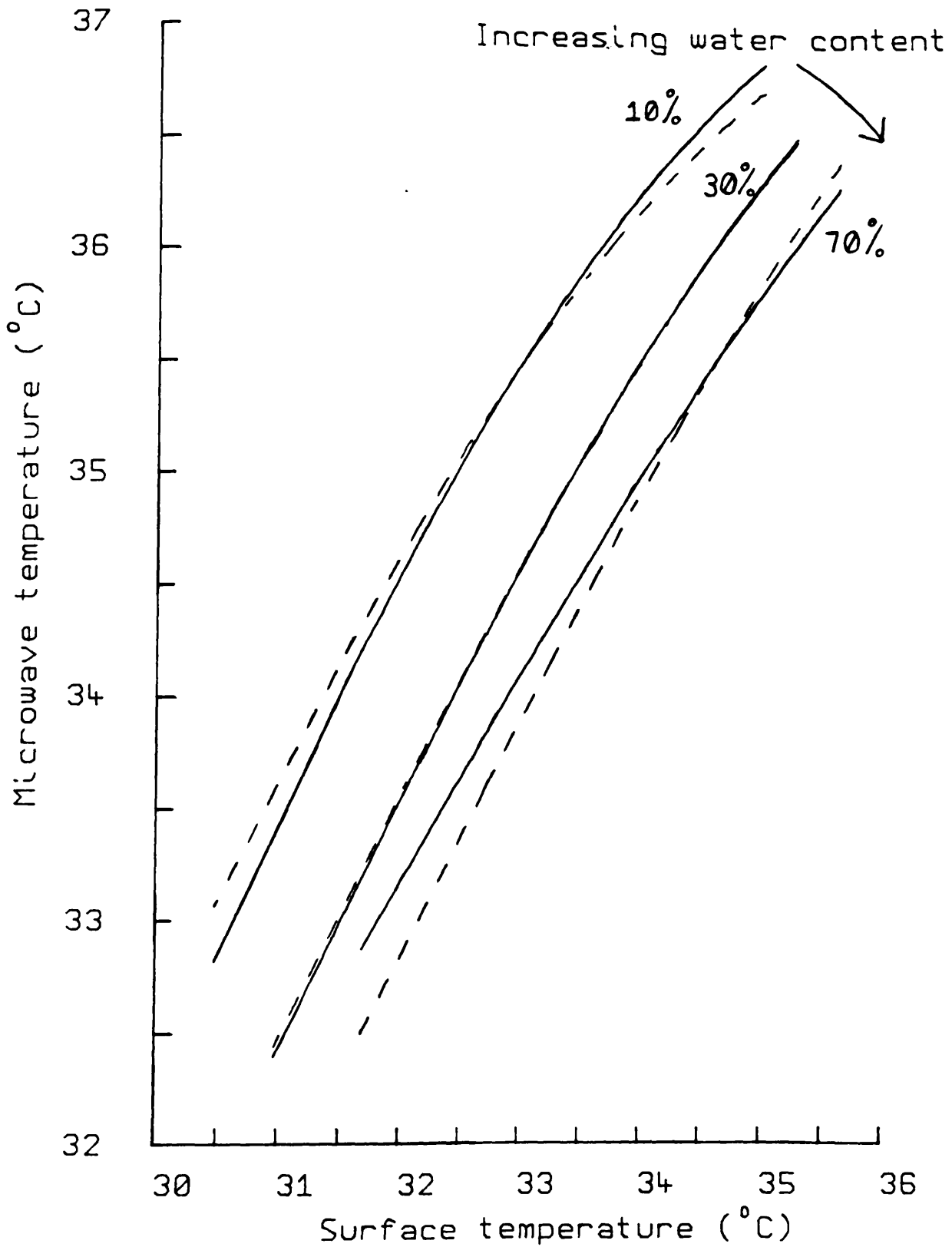


Figure 6.3 Microwave and surface temperatures for tissues with 10, 30 and 70% water content [see table 6.1] and varying blood perfusion rate.

significant difference exists among the 10, 30 and 70% water content tissues. This indicates that, for a single region of tissue, it is possible to determine from measurements of the microwave and surface temperatures the approximate water content and perfusion of the tissue. In practice, however, a single region of tissue is not an appropriate model for the human body since there always exists a thin layer of skin covering the tissue and in some cases it may also be necessary to consider other tissue layers, such as a layer of subcutaneous fat.

6.4.2 Effects of thin skin layer

The case of a thin layer of skin covering a planar volume of uniform tissue has been studied to determine the effects of the skin layer on the observed microwave and surface temperatures. As before the heat transfer equation has been solved to determine the temperature distribution in the tissue, with the appropriate boundary conditions of continuity of temperature and heat flux applied at the interface between the skin and the deeper tissue layer. The microwave temperature has been calculated by numerical integration of equation (2.3.18) to determine T_A , and using (6.4.5) to calculate the measured microwave temperature.

The thickness of the dermal skin layer, which is a high water content tissue, has been determined by ultrasound to be between 0.66 and 1.07 mm on the forearm (Miller, 1979). The upper limit of skin thickness may be taken to be 2 mm. The properties of the skin used in the calculations here are given in Table 6.1.

The skin temperature is given approximately, as a function of skin thickness d , for small thicknesses, by the expression

$$T_S(d) = T_S(0) + \frac{\partial T_S}{\partial d} d \quad (6.4.9)$$

where

$$\frac{\partial T_S}{\partial d} = \frac{4 K_1 \beta_1^2 (K_2 \beta_2^2 - K_1 \beta_1^2) h (T_e - T_a')}{[(h + K_1 \beta_1) (K_2 \beta_2 + K_1 \beta_1) e^{\beta_1 d} - (h - K_1 \beta_1) (K_2 \beta_2 - K_1 \beta_1) e^{-\beta_1 d}]^2} \quad (6.4.10)$$

The subscripts 1 and 2 refer to the properties of the skin and the inner tissue

respectively. This is a useful formulation since it can be used to illustrate the effect of the skin on the surface temperature.

If the thermal resistance of the skin is equal to that of the inner tissue then the temperature distribution will be unaltered from that of the single region case. This is an equivalent situation to that of impedance matched media in wave propagation. If the thermal resistance of the skin is less than that of the inner tissue the skin will cause a temperature rise above the single region surface temperature $T_S(0)$, while a larger resistance will cause a temperature drop. The variation of surface temperature with skin thickness decreases as the thickness increases and the limiting value of surface temperature is the surface temperature for a single region of skin.

For a fixed thickness of skin an increase in the skin blood flow will reduce the thermal resistance of the skin and cause an increase in surface temperature. Figure 6.4 shows the surface temperature as a function of blood perfusion in the inner region for different values of skin blood flow. The effect of the skin blood flow is greatest when the difference between the thermal resistance of the skin tissue and the inner tissue is largest.

The skin therefore affects the surface temperature in a manner which is determined by the thickness and thermal resistance of the skin. The most important effect to consider is the highly variable level of perfusion which may be found in the skin. In a study of forearm skin and muscle blood flow Cooper, Edholm and Mottram (1955) found that skin blood flows in 30 subjects, at room temperatures between 22 and 27°C, varied between 0 and 12.5 $\text{kgm}^{-3}\text{s}^{-1}$, with two thirds of these being below 2.3 $\text{kgm}^{-3}\text{s}^{-1}$. The range of values found for muscle was between 0.3 and 1.7 $\text{kgm}^{-3}\text{s}^{-1}$. This muscle blood flow is comparable to that expected in normal breast tissue and so it is reasonable to assume that the skin blood flow will also be in the same range.

The skin layer also affects the microwave temperature due to the changes which occur in the temperature distribution and in the antenna pattern. The thermal effects of

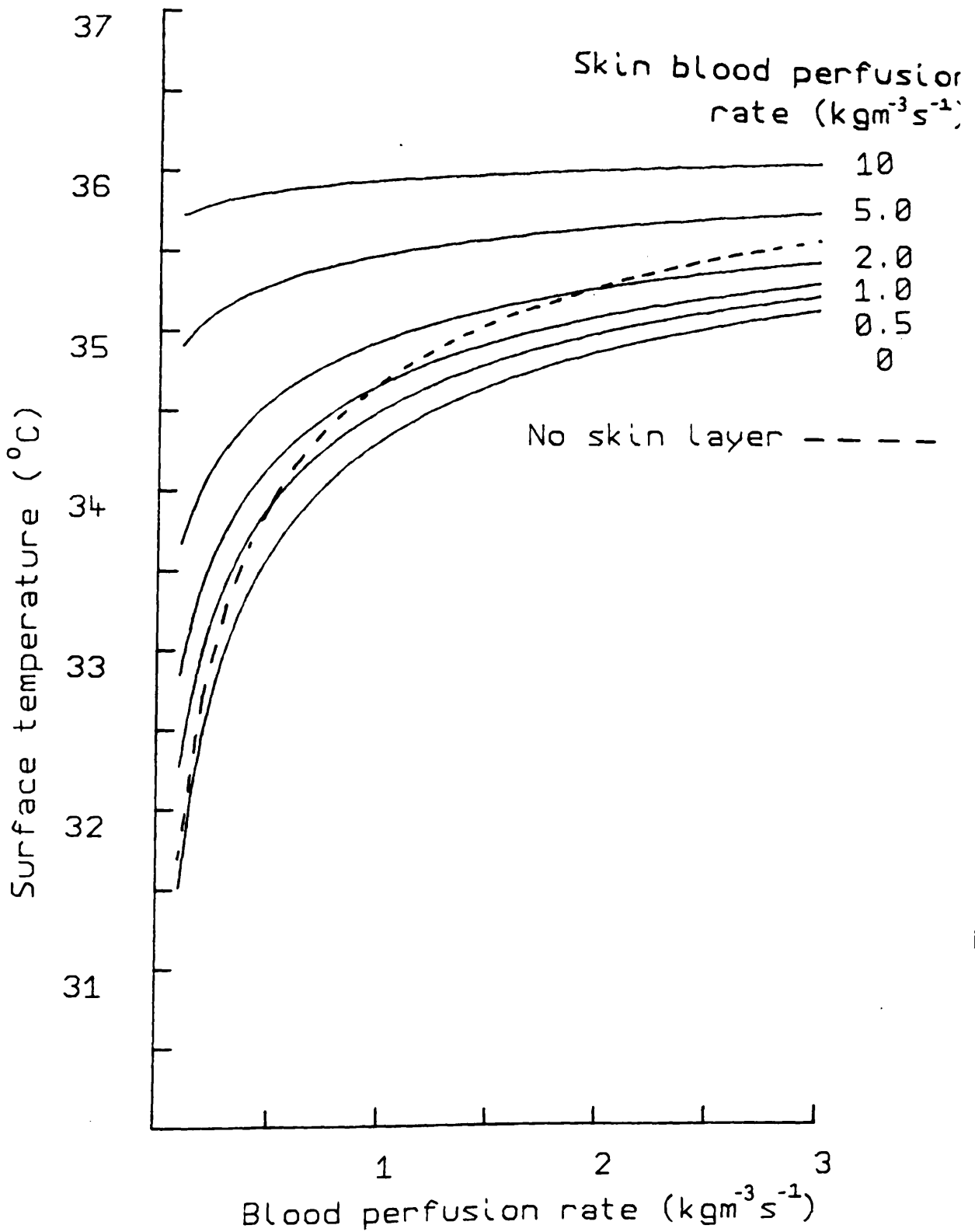
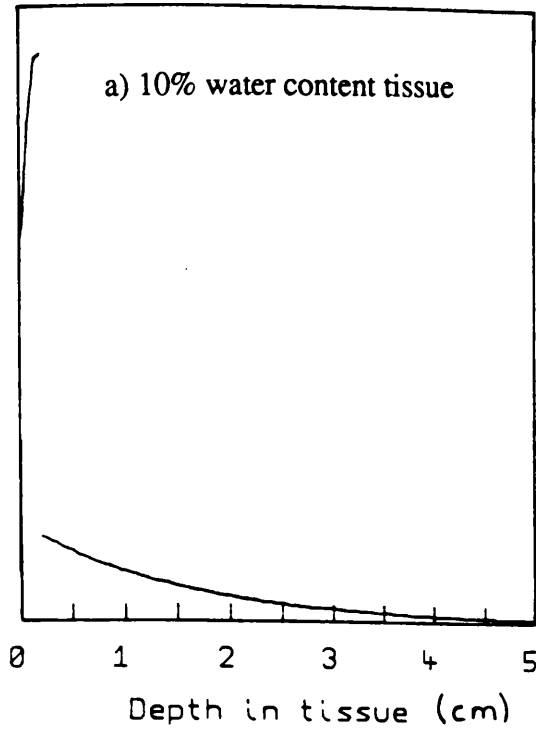


Figure 6.4 Surface temperature variation with blood perfusion rate for a 70% water content tissue with a 2mm layer of skin with different perfusion rates in the skin layer.

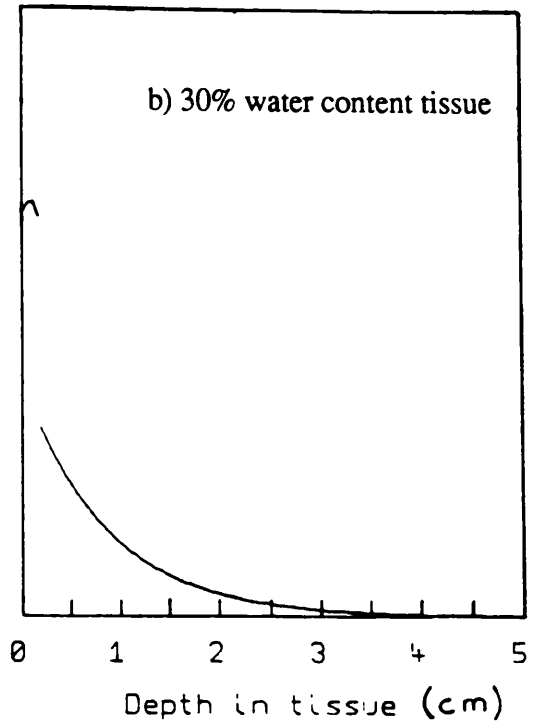
the skin on the microwave temperature will follow the same trends as those experienced by the surface temperature.

The pattern of power absorption, and by reciprocity, power emission also, dS_{av}/dz , in the presence of a 2mm layer of skin is shown in Figure 6.5 for different types of inner tissues, with properties as listed in Table 6.1. For low and medium water content tissues there is a significant impedance mismatch at the boundary between the skin and the inner region which results in a standing wave pattern in the skin layer and a larger contribution from this layer than in the higher water content tissues. The variation of the reflection coefficient at the antenna tissue interface for this 2mm skin layer can be seen in figure 6.6, along with the reflection coefficient for a 1mm skin layer. It can be seen that the 1mm skin layer results in a reflection coefficient which is close to that of a single region when the permittivity in the inner region is greater than about 33. In this region the impedance mismatch between the skin and inner region is small and the tissue behaves electrically in a manner similar to that of a single region. The thicker 2 mm layer of skin greatly increases the reflection coefficient at low values of relative permittivity, while at the higher values, above 33, it remains constant and the difference from the single region case is not so large.

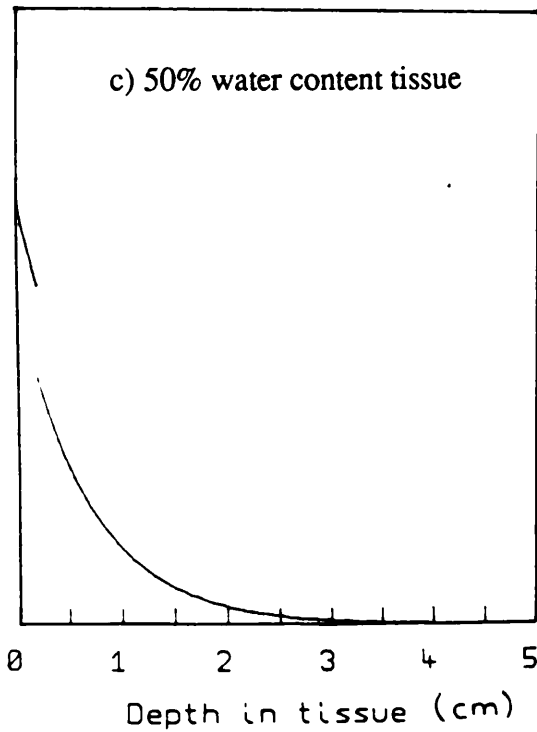
Figures 6.7 and 6.8 show the microwave temperature plotted against the corresponding surface temperature for a 2mm layer of skin and an inner tissue region of water content 70% and 10% respectively. The inner region perfusion rate, which causes the variation in surface temperature, is between 0.1 and 3 $\text{kgm}^{-3}\text{s}^{-1}$, while skin perfusion rates of 0.5, 2 and 10 $\text{kgm}^{-3}\text{s}^{-1}$ are shown. By comparison of these graphs with the single region case, it can be seen that the skin layer reduces the differences observed between the different water content tissues. The microwave temperature of the low 10% water content tissue is significantly reduced due to the increased attenuation of the signal from the inner region caused by the skin, while the 70% water content tissue has similar microwave temperatures to that of the single region. In the case of the skin blood flow of 2 $\text{kgm}^{-3}\text{s}^{-1}$, the increased skin temperature is accompanied by an



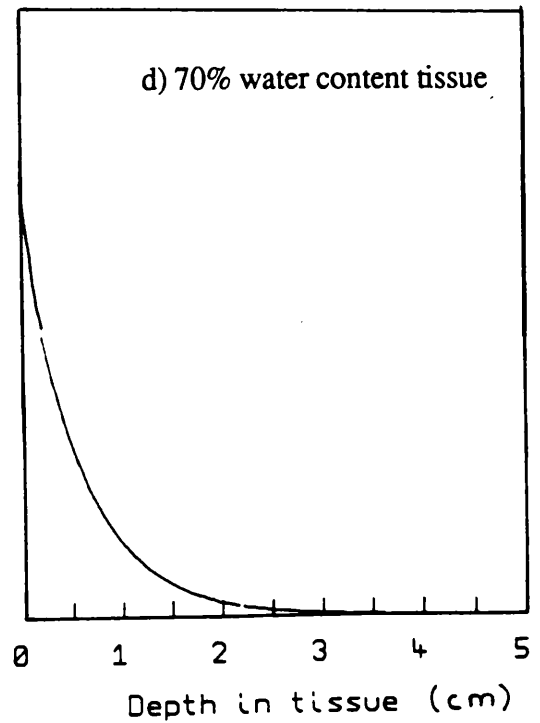
% of total signal reflected : 27.2
 % of total signal received from skin : 32.8
 % of total signal received from tissue
 beneath skin : 40.0



reflected : 21.0%
 received from skin : 27.1%
 received from
 beneath skin : 51.9%



reflected : 20.0%
 received from skin : 25.0%
 received from
 beneath skin : 55.0%



reflected : 20.2%
 received from skin : 23.6%
 received from
 beneath skin : 56.2%

Figure 6.5 Contribution to microwave signal as a function of depth in tissue from tissues of 10, 30, 50 and 70% water content with a 2mm layer of skin.

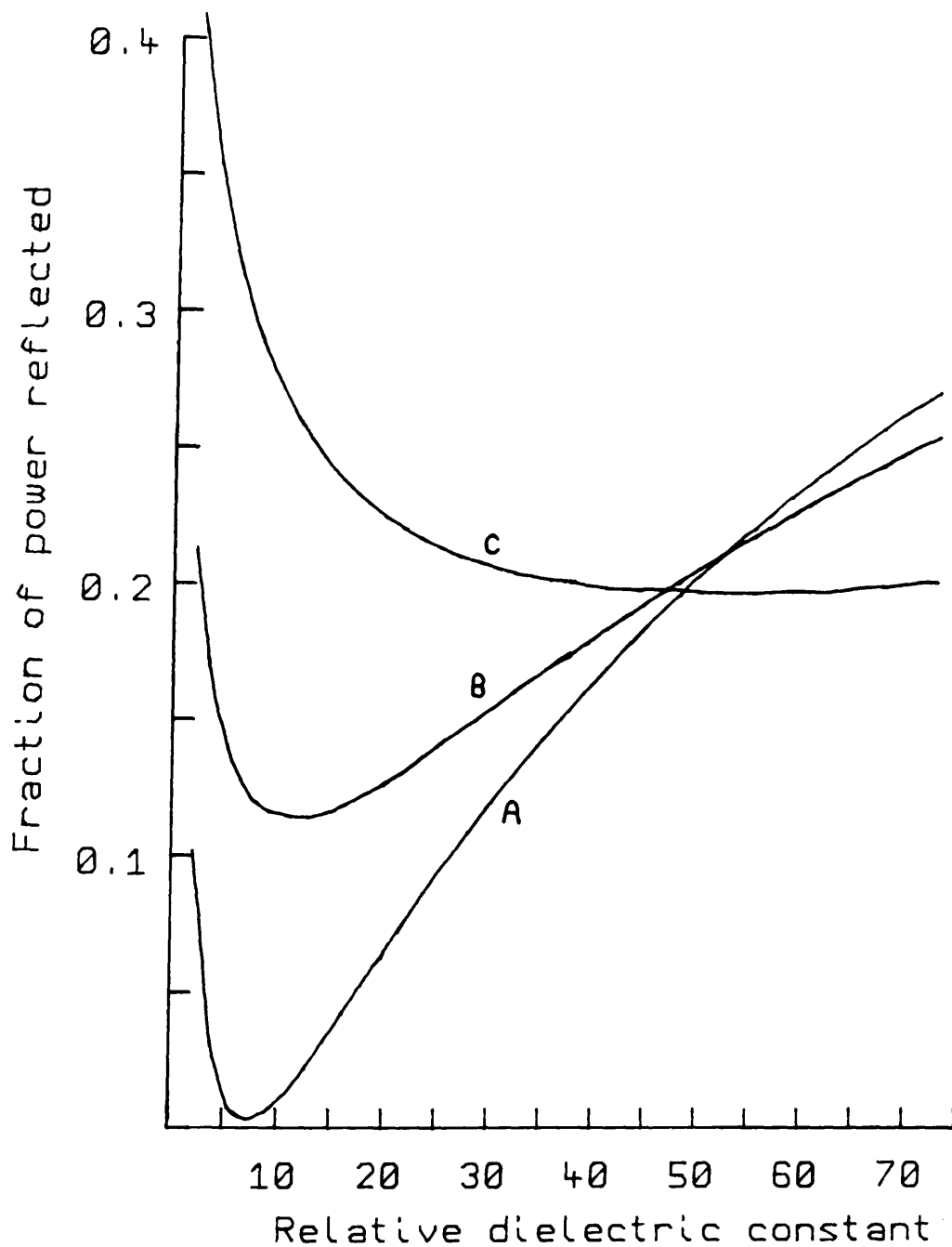


Figure 6.6 Power reflected at antenna-tissue boundary with varying dielectric constant of tissue and with

- A. no skin layer
- B. 1mm skin layer
- C. 2mm skin layer

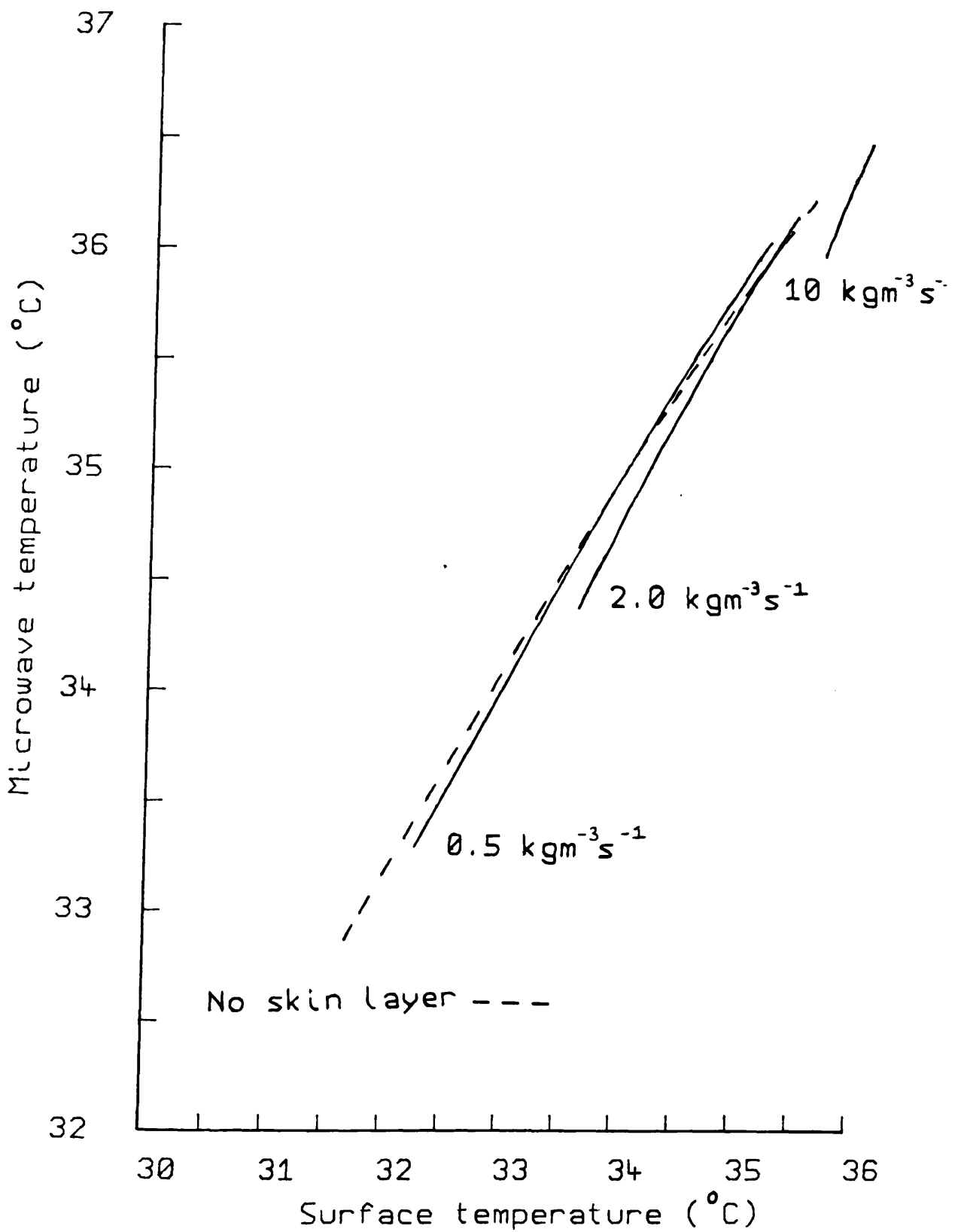


Figure 6.7 Microwave and surface temperatures for a 70% water content tissue with blood perfusion varying between 0.1 and 3 kgm⁻³s⁻¹, and a 2mm skin layer with blood perfusion rates of 0.5, 2 and 10 kgm⁻³s⁻¹

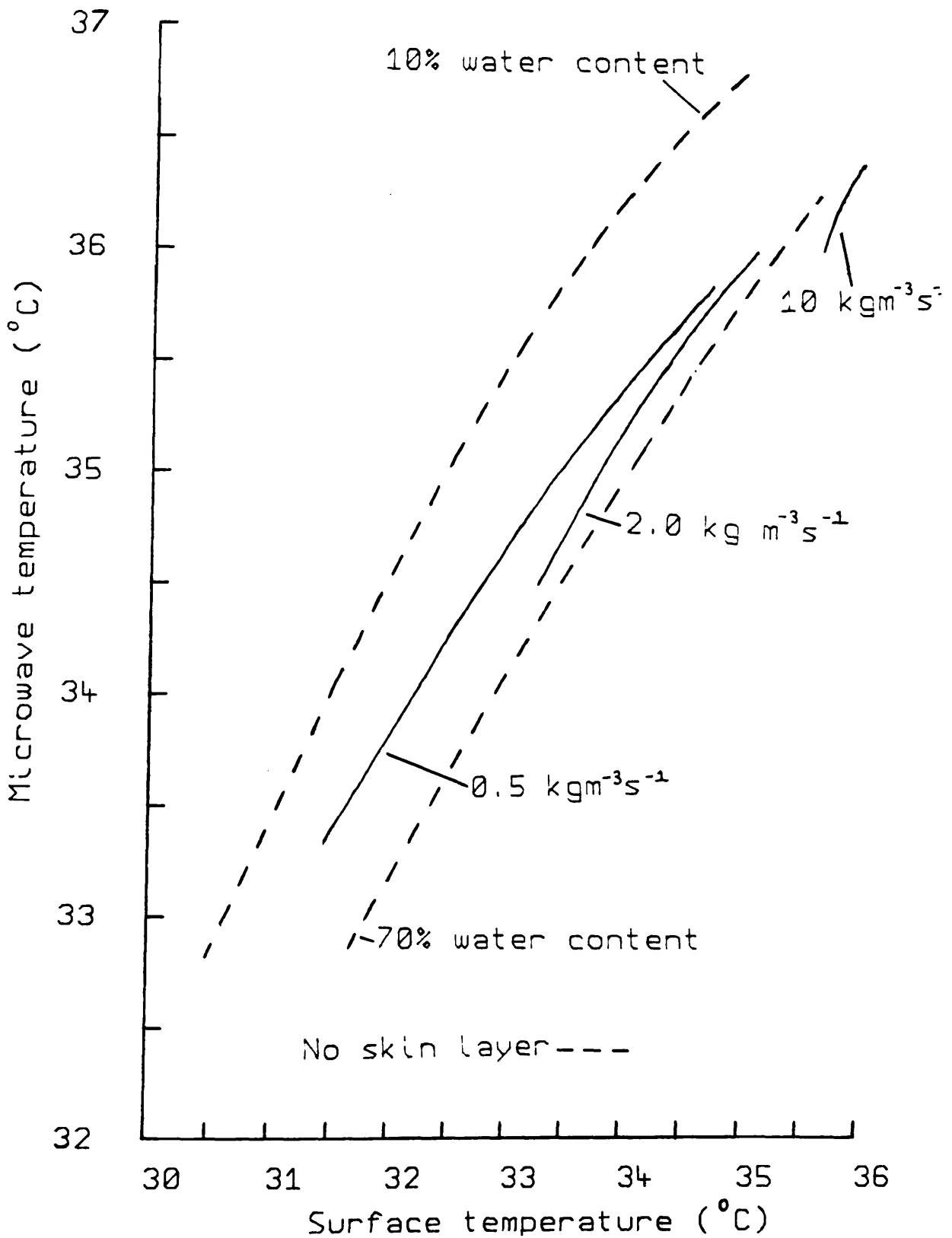


Figure 6.8 Microwave and surface temperatures for a 10% water content tissue with blood perfusion varying between 0.1 and 3 kgm⁻³s⁻¹, and a 2mm skin layer with blood perfusion rates of 0.5, 2 and 10 kgm⁻³s⁻¹ [70 % water content tissue with no skin layer shown for comparison]

increased microwave temperature and the range of temperatures observed for the same range of inner tissue perfusion rates is reduced. In this case the microwave and surface temperature pair correspond approximately to the single region case with an equivalent blood flow which is between that of the skin and the inner region. At high values of blood perfusion in the inner region, above about $2 \text{ kgm}^{-3}\text{s}^{-1}$, it becomes more difficult to identify differences among the microwave and surface temperature pairs of different water content tissues. At the very high skin perfusion rate of $10\text{kgm}^{-3}\text{s}^{-1}$ it is difficult to determine either water content or perfusion in the inner region. At values of perfusion in the inner region less than $2 \text{ kgm}^{-3}\text{s}^{-1}$, except in the case of very high skin perfusion, measurement of the microwave and surface temperature, including the effects of skin, should be able to differentiate between low and high water content tissues and provide an estimate of the blood flow.

6.5 Numerical modelling of normal breast

In order to determine the effects of the geometry of the breast the heat transfer equation was solved for a transverse cross-section of the breast using a finite-difference method. Figure 6.9 illustrates the model of the breast used. The breast is assumed to consist of a homogeneous layer of breast tissue backed by a high water content, well-perfused inner tissue. The temperature distribution was calculated for different types of breast tissue, to represent the varying relative compositions of fatty and glandular tissue found in the breast, and various perfusions. From this model the expected microwave and surface temperatures across the breast were determined. Three different types of breast tissue were considered, representing 30%, 50% and 70% water contents with properties as listed in Table 6.1. Perfusion rates in the breast tissue of 0.2, 0.5 and $2.0 \text{ kgm}^{-3}\text{s}^{-1}$ were used and, as previously, the environmental temperature was assumed to be $25 \text{ }^\circ\text{C}$.

The calculated microwave and surface temperatures for the 30% and the 70% water content tissue are shown in figures 6.10 and 6.11 respectively, as a function of

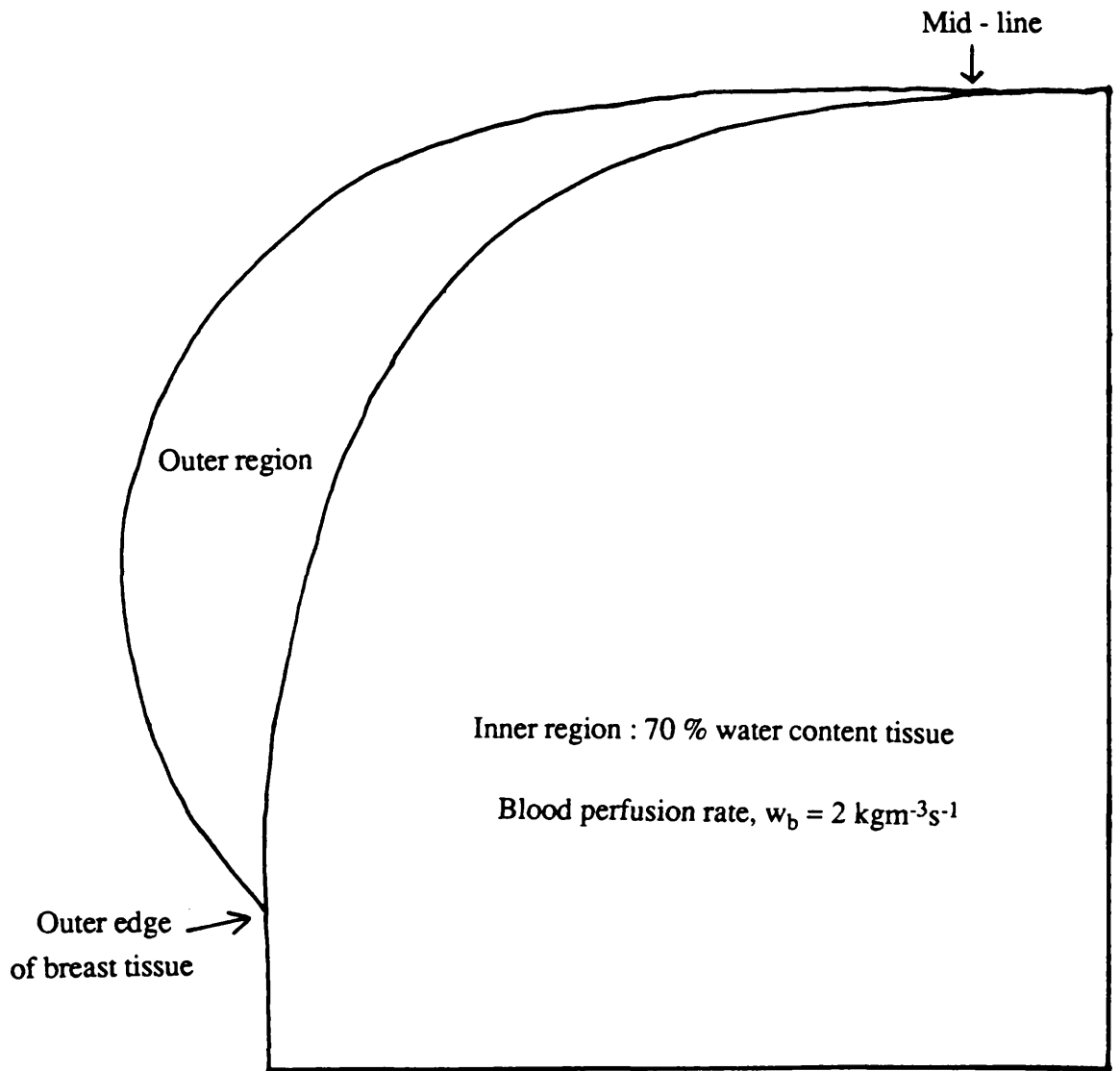


Figure 6.9 Model of breast

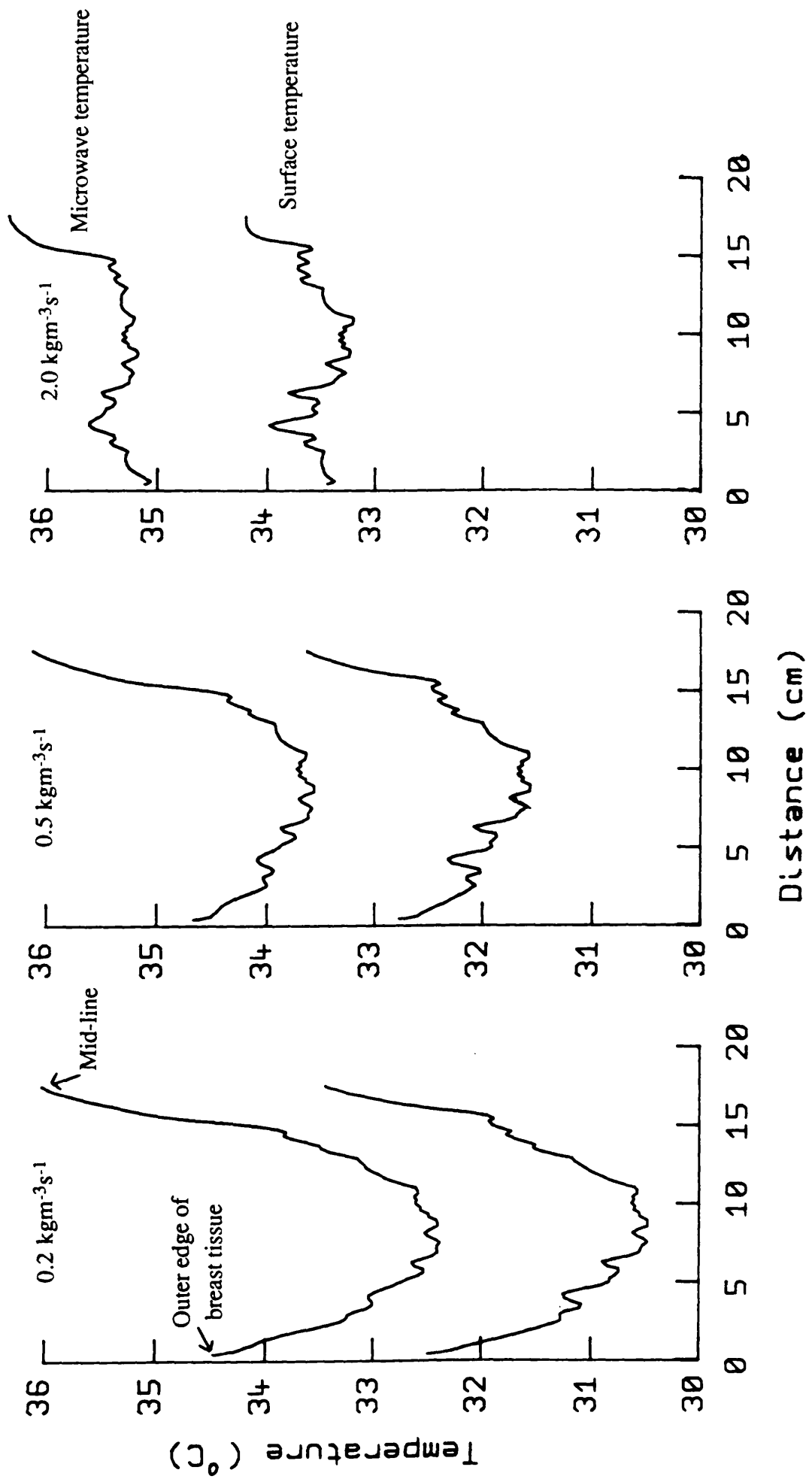


Figure 6.10 Modelled microwave and surface temperatures for 30% water content breast tissue and blood perfusion rates of 0.2, 0.5 and 2 kgm⁻³s⁻¹.

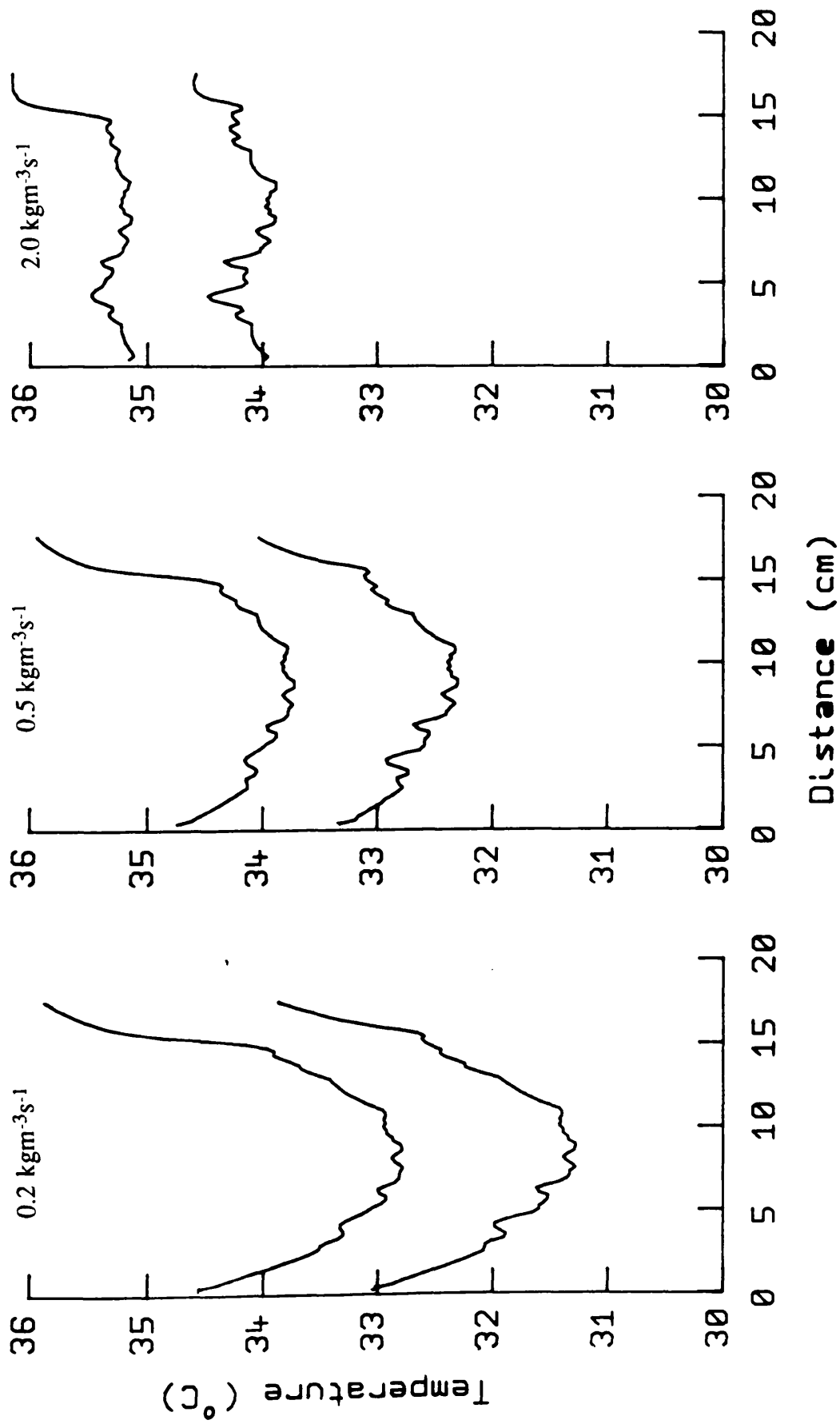


Figure 6.11 Modelled microwave and surface temperatures for 70% water content breast tissue and blood perfusion rates of 0.2, 0.5 and 2 kgm⁻³s⁻¹.

position on the breast. These graphs illustrate the expected form of the microwave and surface temperature variation across the breast. The effect of the varying thickness of the breast tissue is that of an effective perfusion whose value is between that of the inner and outer regions. The larger the difference in perfusion between these two regions the greater is the range of temperatures measured and, as in the case of the single region, the lower the water content of the tissue the greater is the microwave temperature at the same value of surface temperature.

For the dielectric properties of the different water content tissues used in the numerical model the penetration depths into the tissue do not vary greatly. The 70% water content tissue has, including the effects of the antenna, a penetration depth of 6 mm, while the 30% water content tissue has a penetration depth of 8.4 mm. This suggests that the microwave temperature will not vary greatly with the breast tissue water content but will predominantly reflect the level of perfusion in the breast.

Figure 6.12 shows the microwave and surface temperatures of the numerical model for the 30% water content tissue and a perfusion of $0.2 \text{ kgm}^{-3}\text{s}^{-1}$ as a function of breast tissue thickness. In this case the range of surface temperatures observed is larger than in the other cases because of the largest difference between the thermal resistance of the inner and outer tissues. The temperatures determined from a planar model of two regions, in which the thickness of the outer region is equivalent to the breast tissue thickness, is also shown. For the planar model the heat transfer coefficient at the skin surface has been increased to $20 \text{ Wm}^{-2}\text{C}^{-1}$ to account for the increased surface to volume ratio of the breast geometry. It can be seen that as the tissue thickness increases the change in microwave and surface temperature becomes more gradual and so the tissue thickness is not crucial.

6.6 Experimental determination of normal breast temperatures

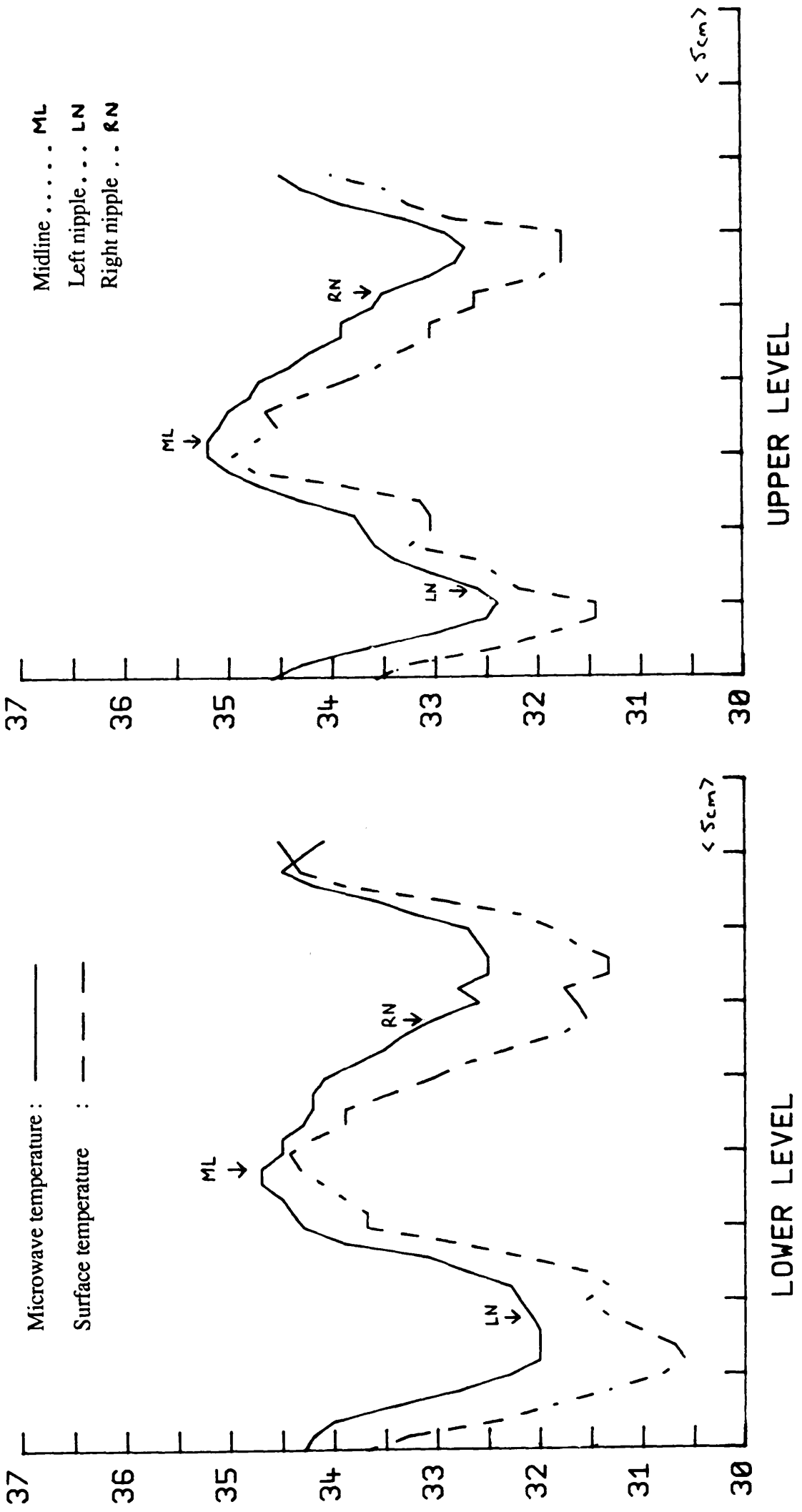
The microwave temperatures of 10 normal subjects, aged between 19 and 23, were measured with the Glasgow microwave thermography system. Measurements

were made at two levels, scanning continuously from the outer edge of the left breast to to the outer edge of the right breast, at approximately 2 cm above and below the nipple level, at intervals of 1 cm. ^{*}The measurements were made with the subjects lying comfortably in a room temperature of around 25 °C. The surface temperatures were recorded at the same positions as the microwave temperatures, using an infra-red thermometer. Surface temperature measurements were made immediately after completion of the microwave temperature measurements. The results of the measurements are shown in figures 6.13 to 6.22. The positions directly above and below the nipple are marked on these figures, as is the mid-line position.

It can be seen that in the 10 subjects there is a wide range of patterns observed, but these may be divided into three categories. Subjects 1-3 (figures 6.13 - 6.15) have a "dipping" pattern across the breast similar to that of the lower perfusion patterns of the numerical model (Pattern A), while subjects 4-6 (figures 6.16 - 6.18) show no trace of this pattern at all and exhibit a flat trace similar to the high perfusion case in the numerical model (Pattern C). Subjects 7-10 (figures 6.19 -6.22) are between these two cases with patterns which show a lesser decrease in temperature across the breast than that seen in subjects 1-3 (Pattern B). These patterns are the same as those observed by Draper and Jones (1969) using infra-red thermography alone, who classified the thermal patterns of 442 clinically normal women into 4 categories; those with cold breasts (Pattern A), those with some vascularity (Pattern B), those with warm breasts (Pattern C) and those with a "patchy pattern". The "patch pattern" of Draper and Jones will not be observed in the line scans of this study, since recognition of this pattern requires a thermographic image of the whole breast.

The minimum measured microwave and surface temperatures at both levels of each breast of subjects 1 to 3, with thermographic Pattern A, and subjects 7 to 10 with thermographic Pattern B, are shown in figure 6.23. If a minimum of microwave and surface temperature, corresponding to the form of the minimum seen in the numerical model was not present, for example at the lower level of the left breast of subject 8

* Scanning was carried out by holding the antenna in contact with the skin surface and moving it from one position to the next at intervals of 2.5 seconds. The antenna is therefore only held in contact with a particular area of the skin for a short period of time in order to attempt to minimise the thermal disturbance.



Midline ML
 Left nipple LN
 Right nipple . . . RN

Microwave temperature : ———
 Surface temperature : - - -

Figure 6.13 Measured microwave and surface temperatures for Subject 1

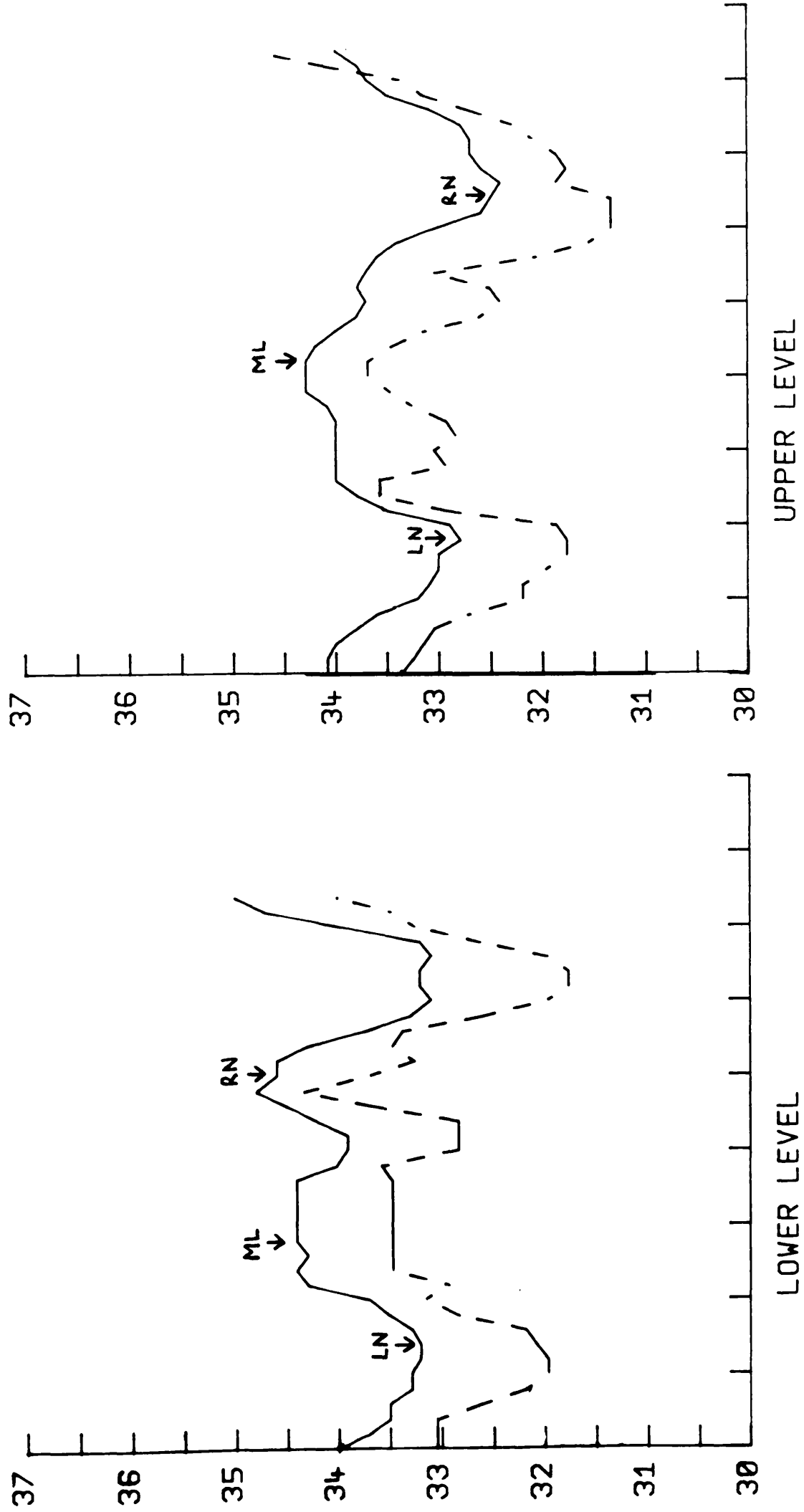


Figure 6.14 Measured microwave and surface temperatures for Subject 2

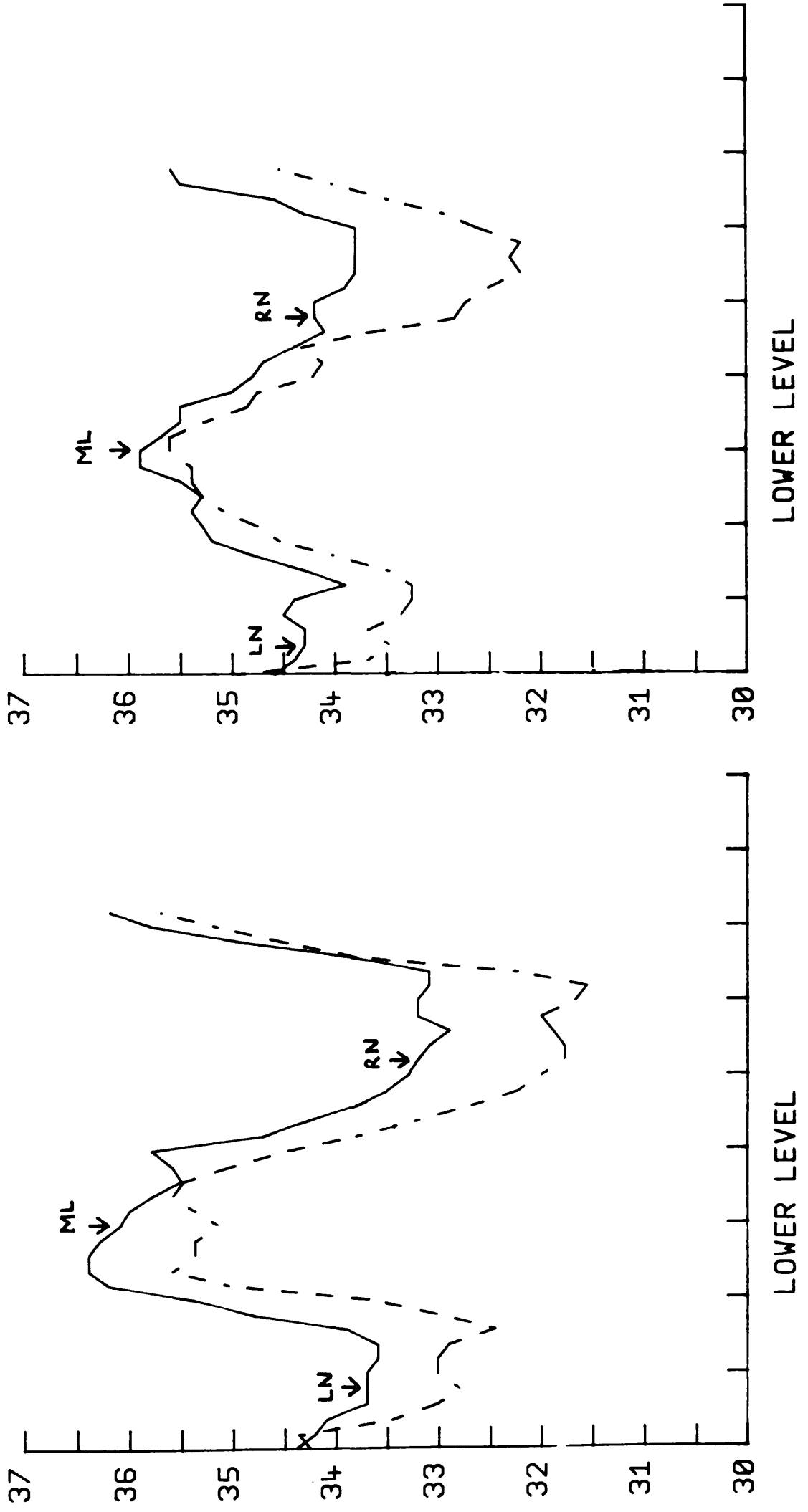


Figure 6.15 Measured microwave and surface temperatures for Subject 3

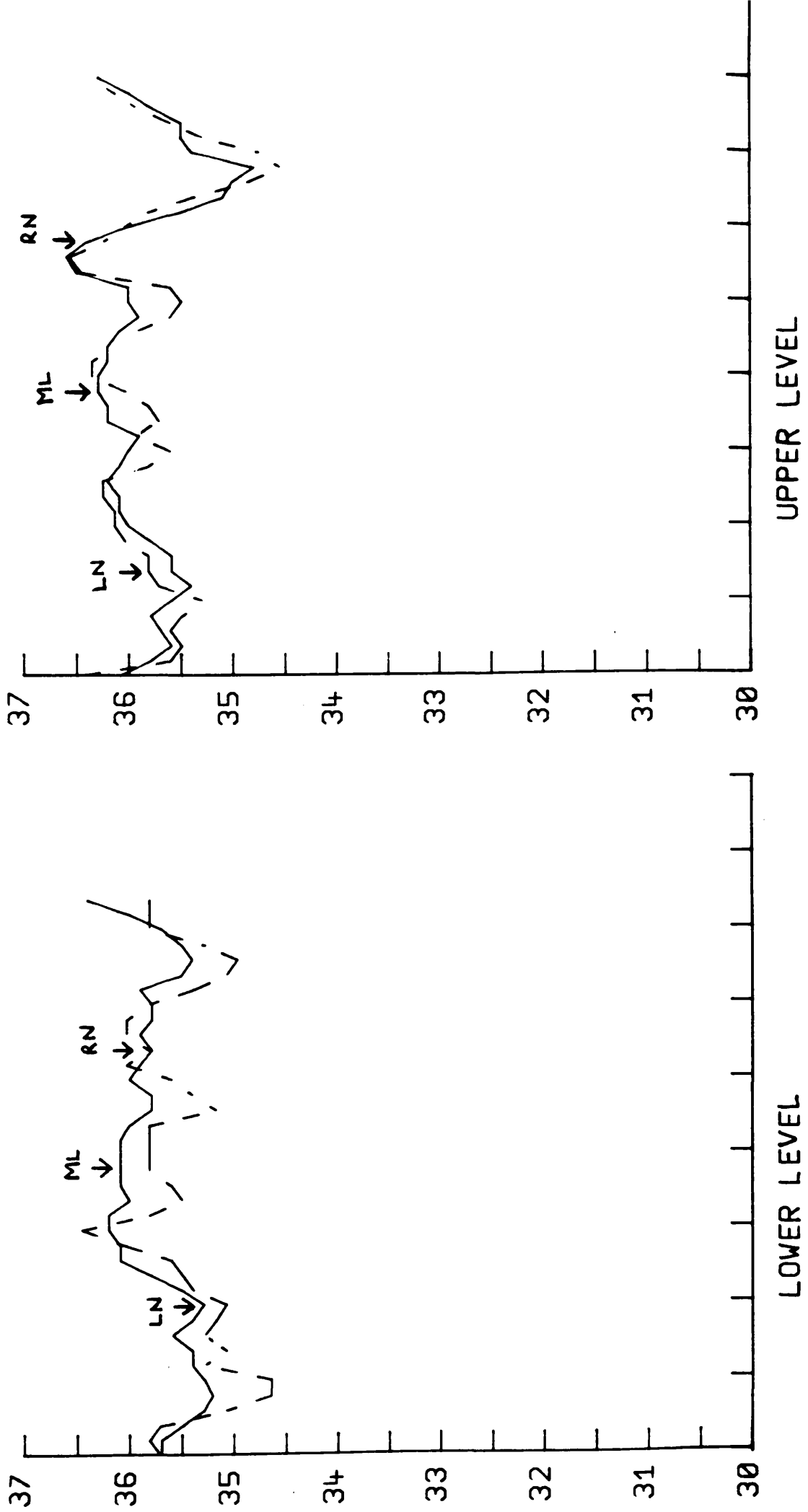


Figure 6.16 Measured microwave and surface temperatures for Subject 4

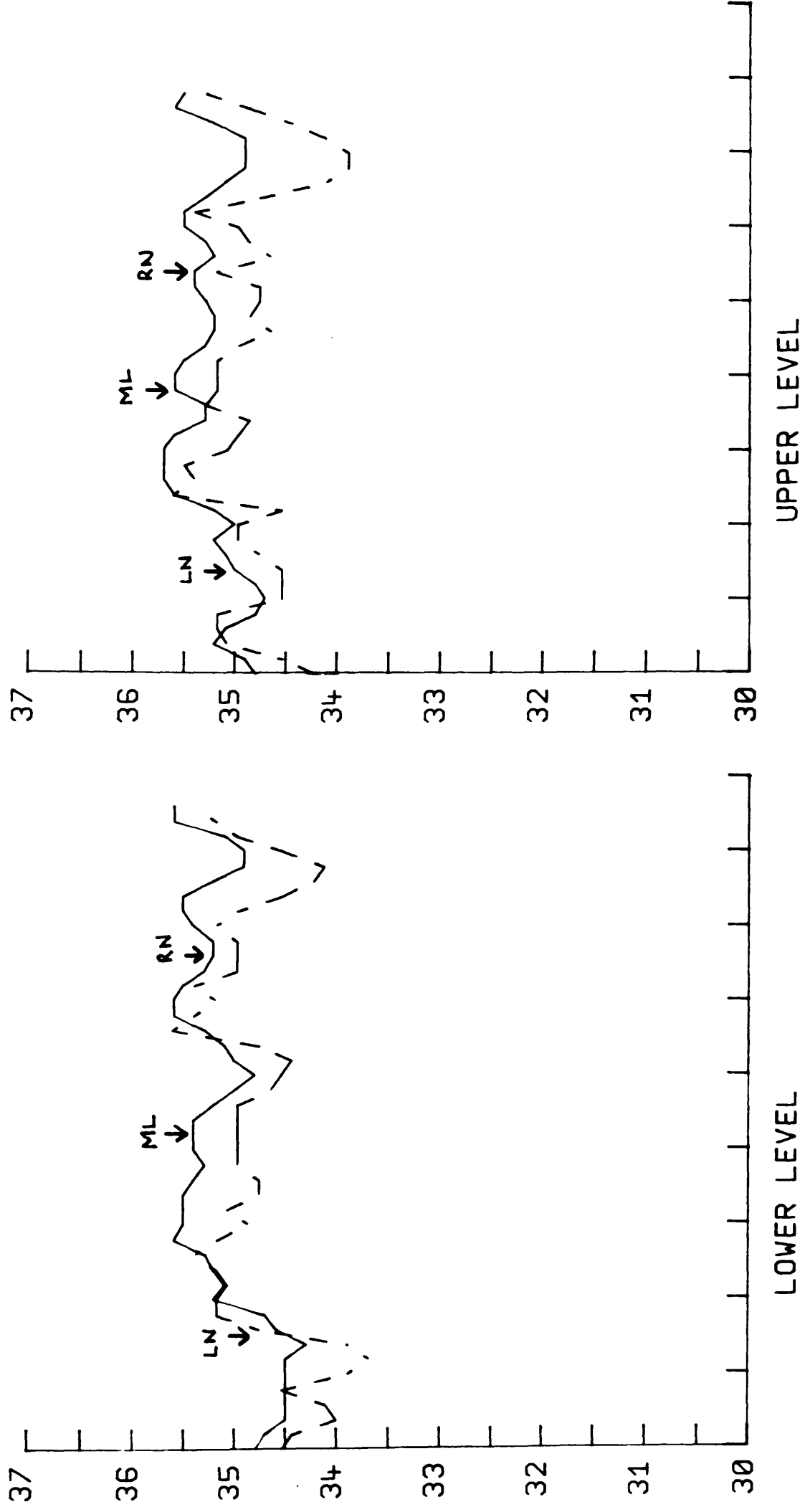


Figure 6.17 Measured microwave and surface temperatures for Subject 5

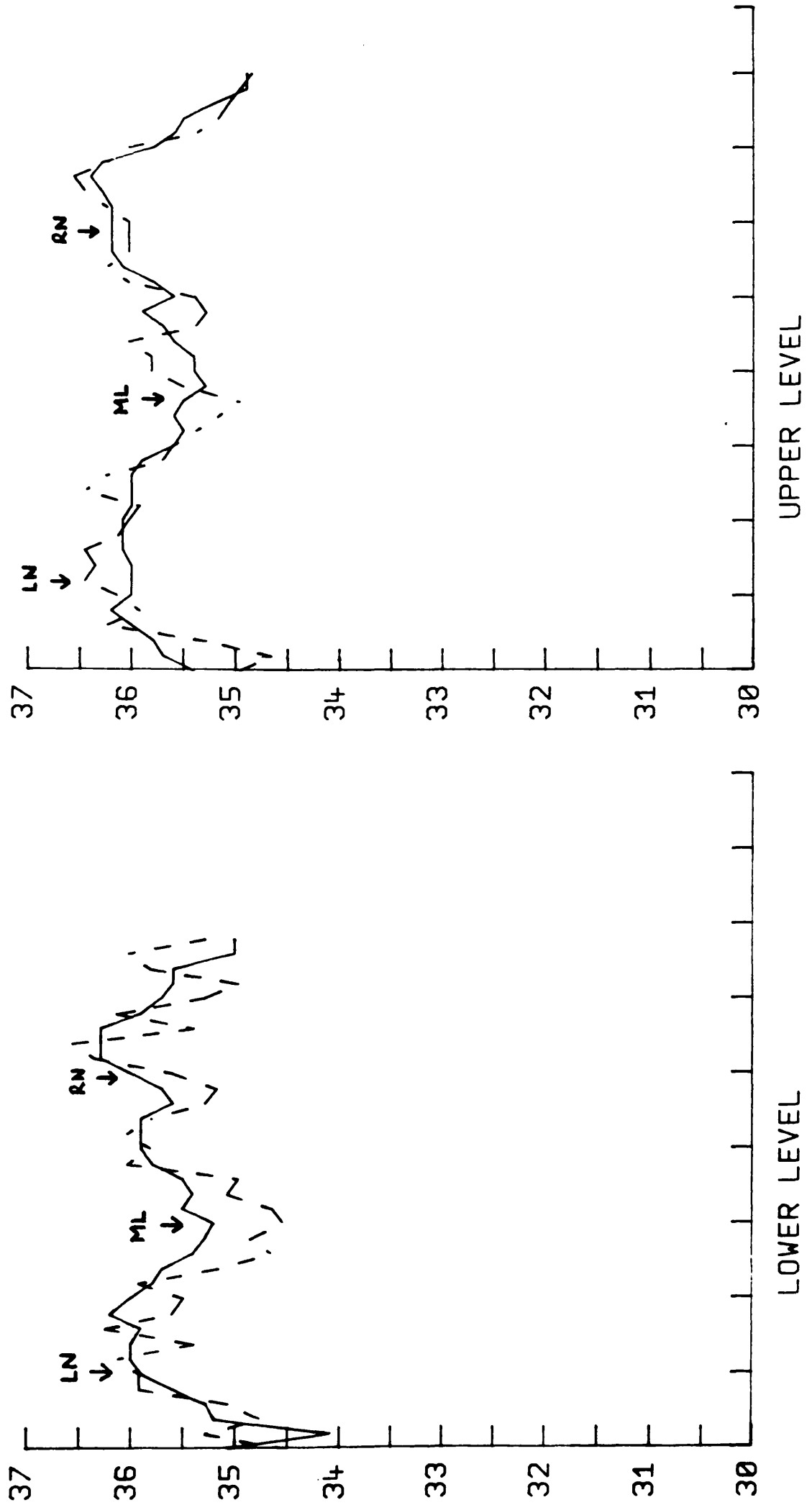


Figure 6.18 Measured microwave and surface temperatures for Subject 6

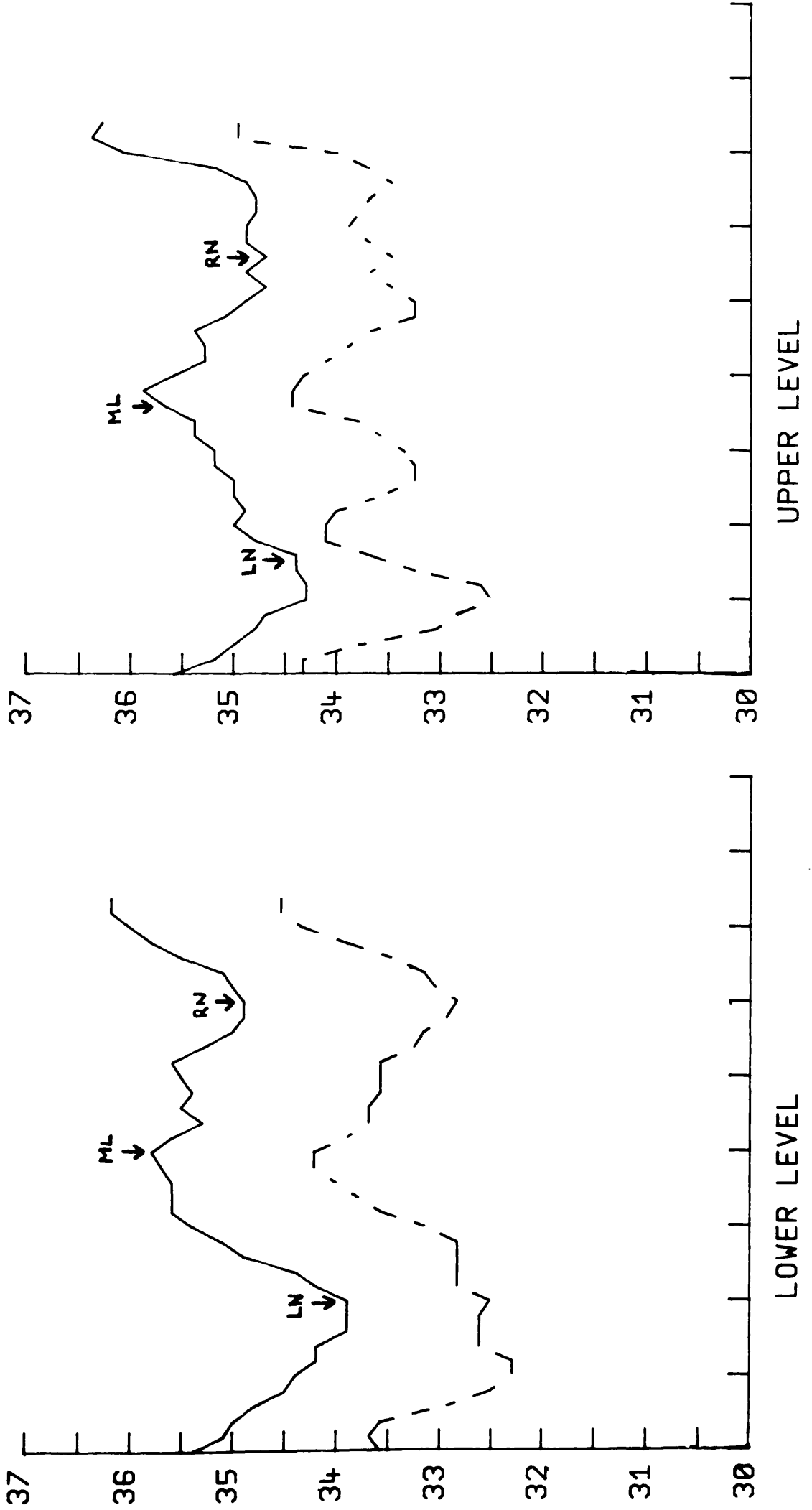


Figure 6.19 Measured microwave and surface temperatures for Subject 7

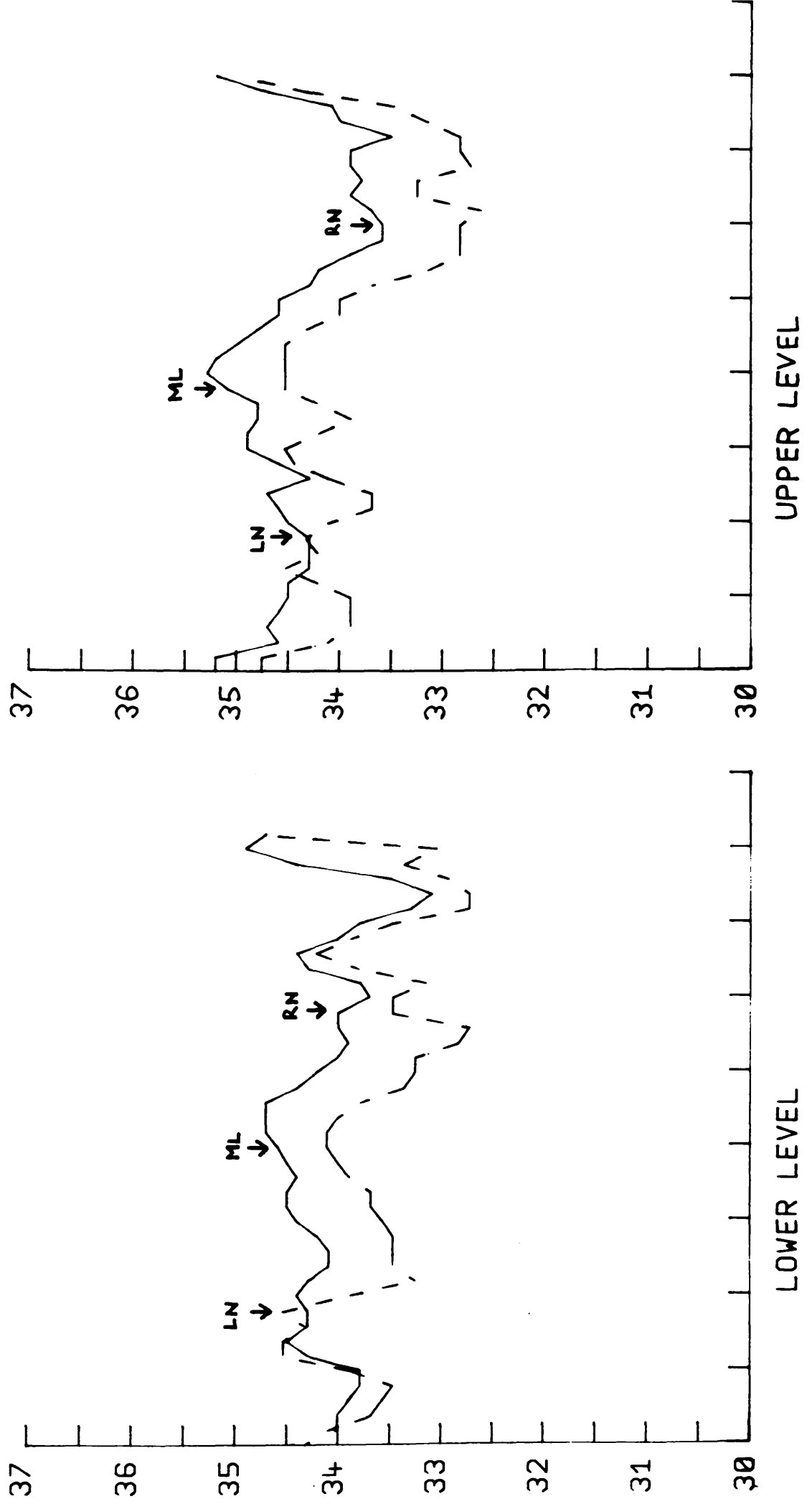


Figure 6.20 Measured microwave and surface temperatures for Subject 8

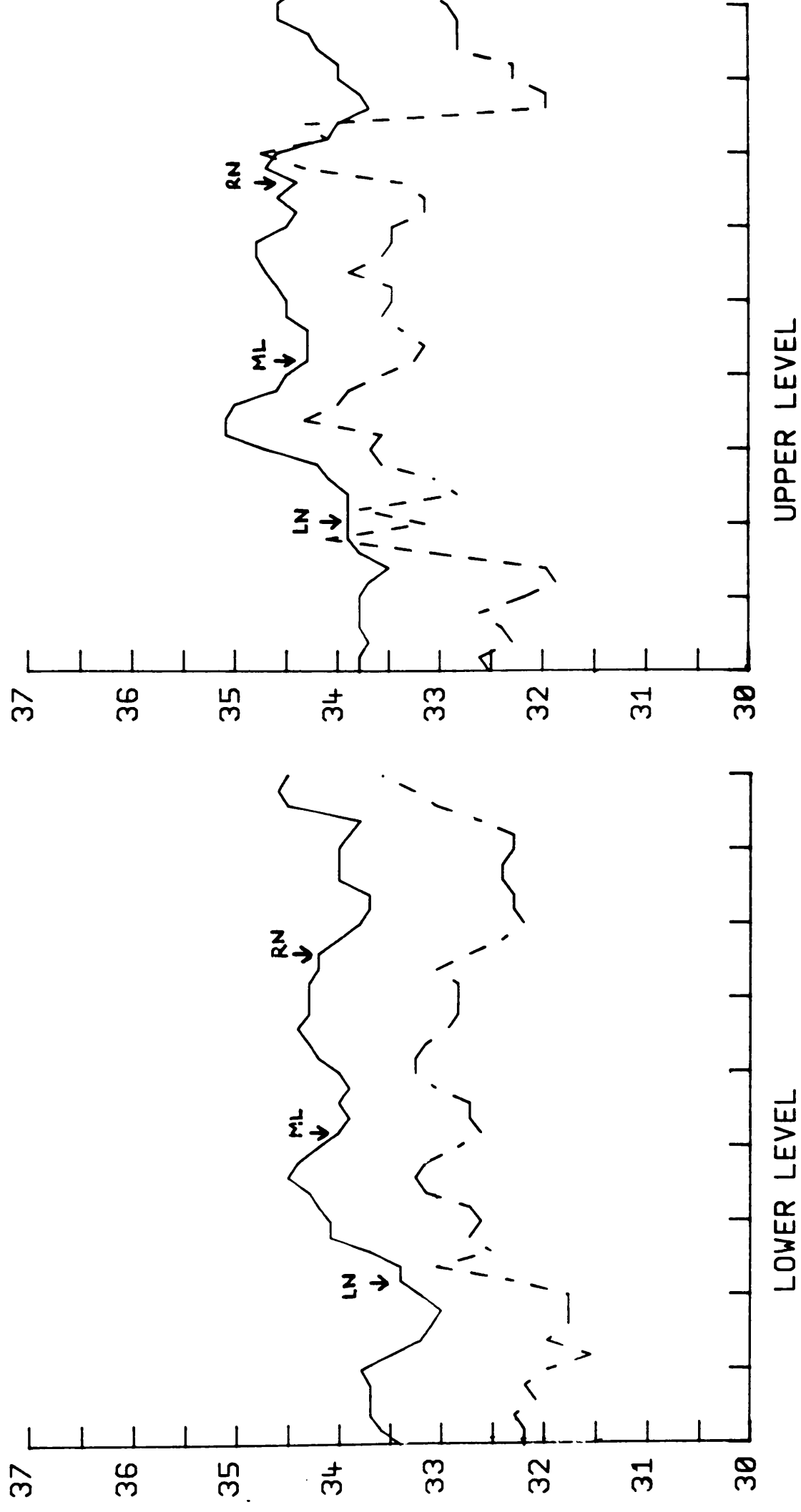


Figure 6.21 Measured microwave and surface temperatures for Subject 9

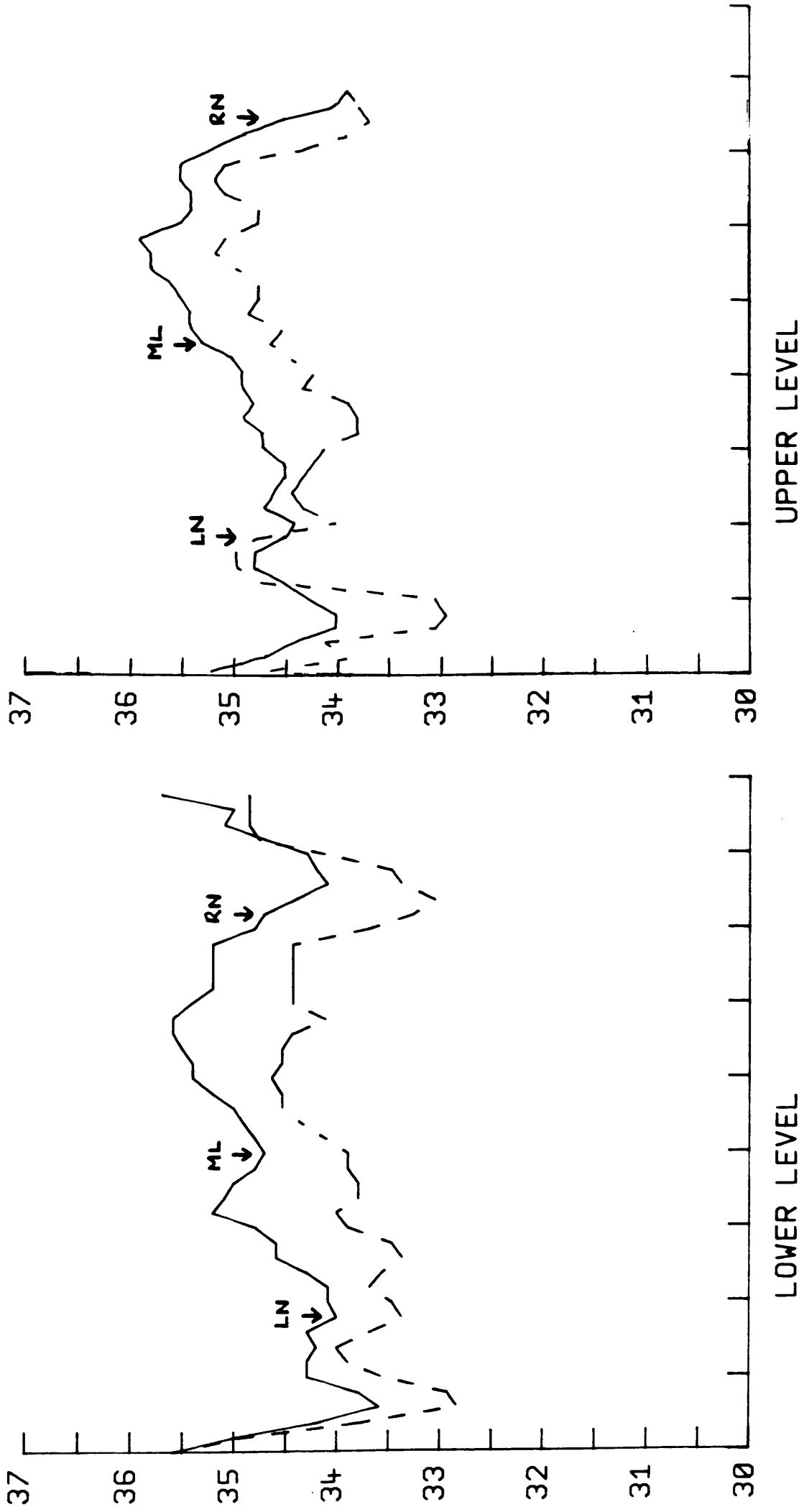
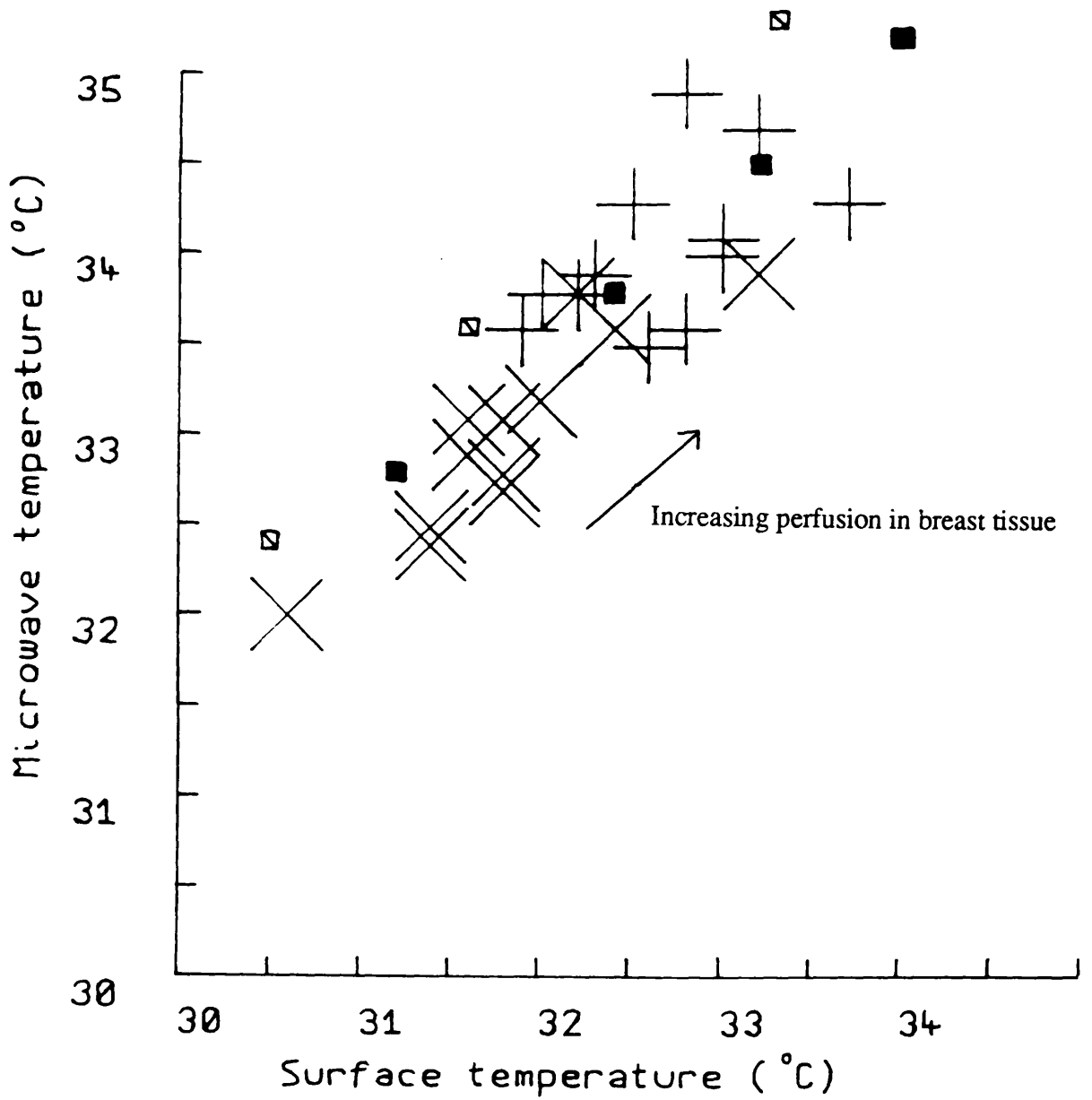


Figure 6.22 Measured microwave and surface temperatures for Subject 10



- Measured temperatures (Pattern A)
- Measured temperatures (Pattern B)
- 70% water content breast tissue (with perfusions of 0.2, 0.5, 1.0 and 2.0 $\text{kgm}^{-3}\text{s}^{-1}$)
- 30% water content breast tissue (with perfusions of 0.2, 0.5 and 2.0 $\text{kgm}^{-3}\text{s}^{-1}$)

Figure 6.23 Minimum measured microwave and surface temperatures for normal subjects with Pattern A or Pattern B compared with modelled temperatures.

(figure 6.20), no point was plotted. The calculated minimum temperatures from the numerical model are also shown. As discussed earlier, variations in breast tissue thickness have a small effect and these minimum temperatures should be close to the microwave and surface temperatures of a single region of breast tissue and hence may be used to estimate the properties of the breast tissue. It can be seen that the measured temperatures, except in one case, lie below the calculated temperatures for the 30% water content tissue, indicating that the effective microwave penetration depth in breast tissue is less than 8.4 mm. For the subjects with Pattern A the measured temperatures indicate, in general, perfusion rates of $0.5 \text{ kgm}^{-3}\text{s}^{-1}$ and less. For subjects 7-10, with Pattern B, comparison of the measured temperatures with those of the model indicate that the blood perfusion rate is around $0.5 \text{ kgm}^{-3}\text{s}^{-1}$ or greater but is clearly less than $2 \text{ kgm}^{-3}\text{s}^{-1}$.

In subject 9 (figure 6.21) the surface temperature measured at the upper level shows a sharp peak of increased surface temperature close to the nipple position in both breasts. A similar sharp peak is also observed at the upper level in the left breast of subject 10 (figure 6.22) at the same position.

Draper and Boag (1971a,b) have calculated the thermal pattern at the skin surface due to veins lying parallel to the surface at various depths. In their model heat was transported from the vein to the surface by conduction and a thermal gradient of $3 \text{ }^{\circ}\text{Ccm}^{-1}$ existed in the tissue. This is approximately the thermal gradient existing near the surface in the 70% water content model with a perfusion of $0.5 \text{ kgm}^{-3}\text{s}^{-1}$. The results of their calculations showed that subcutaneous veins carrying warm blood near the skin surface produce a linear thermal pattern with a high peak and small half-width, while deeper veins cause wide, shallow linear patterns. This indicates that the sharp peaks observed are due to subcutaneous veins carrying warmer venous blood from the deeper tissues close to the skin surface, and that the smaller, wider peaks observed, for example, in the left breast of subject 8 (figure 6.22) are due to deeper veins.

For subjects 4 to 6, with flat temperature profiles, the surface temperatures are

much higher than those of the other subjects, consistent with a high blood perfusion. The irregular surface temperature profile, shown particularly in the lower level surface temperatures of subject 6 (figure 6.18), suggests that a number of veins are carrying hot blood near the skin surface. Love (1980) points out that "collateral venous networks provide for blood returning to the vena cavae to flow in either the deep veins, the superficial system or both".

The results here indicate that in subjects 1 to 3, with low perfusion and an absence of temperature peaks, the venous blood is either returning through the deeper veins, or that the lower tissue temperatures cause the venous blood from the deeper tissues to lose its heat before it passes close to the skin surface. In subjects 7 to 10 some veins passing close to the surface and some deeper veins can be seen, while in subjects 4 to 6 the venous blood can be seen to be returning mainly through the superficial system and because of the higher tissue temperatures does not lose its heat as it travels from the deeper tissue to close to the surface. The use of the superficial system to drain the venous blood is consistent with a high blood flow in the breast tissue supplying a greater amount of heat to the tissue and therefore requiring greater heat loss at the skin surface to maintain thermal equilibrium. In subject 5 (figure 6.17) who exhibits the lowest surface temperature over breast tissue of those with Pattern C, the surface and microwave temperatures in the right breast, at the region of low surface temperature and therefore not close to a vein, are consistent with a blood perfusion rate of $2 \text{ kgm}^{-3}\text{s}^{-1}$.

In the case of Subjects 1 and 7, who have had repeated microwave temperature breast scans at intervals over a period of 4 years, the microwave temperature profile has been found to remain constant with time. It is likely therefore that it possible to determine a characteristic breast microwave temperature pattern for each woman. It is possible for this normal temperature pattern to be asymmetric, as in subject 7, where, at the nipple position at the lower level, the microwave temperature in the right breast is 1°C higher than that in the left. The false-positive detection rate in screening women for

breast cancer could therefore be improved by recording a normal temperature profile for each woman and comparing subsequent measurements with this.

The temperature profiles across the breast may be used to indicate qualitatively the blood perfusion in the breast, while the measured values of microwave and surface temperatures and the use of numerical modelling may be used to provide quantitative estimates of the breast perfusion. Love (1980) has suggested that infra-red thermographic measurements may be used to estimate blood perfusion. His suggested technique depends on the measurement of the avascular skin temperature and the estimation of the temperature of the blood in the superficial veins by measurement of the skin temperature over a vein. The vein temperature is considered to represent the average tissue temperature and these two temperatures may be used to eliminate the thermal conductivity effect and so estimate blood flow. The skin temperature superficial to the veins, however, is difficult to determine accurately with commercially available scanning infra-red cameras (Love 1985). The measurement of breast microwave temperatures may be used to determine a volume average of tissue temperature to be used in place of the vein temperature. The estimation of blood perfusion and water content from measurement of microwave and surface temperatures depends primarily on the difference between these two temperatures over an avascular skin region indicating the tissue water content. This estimation of water content would require improved knowledge of the variation in the microwave dielectric and thermal properties of breast tissue with water content from those available here. The skin temperature gives an estimate the thermal resistance of the tissue. If the estimated water content were used to determine the thermal conductivity then the blood perfusion rate could be found from the tissue thermal resistance.

The information gained from the modelling of the breast carried out here may be used to provide estimates of breast perfusion to be used in more accurate modelling of the breast. Osman and Afify (1984) have developed a three-dimensional mathematical model of the temperature distribution in a normal woman's breast using a finite element

method. More accurate modelling of this nature will be appropriate when more detailed information about the vascularity in the breast is available.

6.7 Microwave thermography in patients with breast disease

An initial clinical trial of the use of microwave thermography in breast disease, involving around 300 patients, is currently being carried out with the Glasgow microwave thermography system at the Glasgow Western infirmary (Land, Fraser and Shaw, 1986). The microwave temperature increases over the breast lesions of 104 patients relative to the contra-lateral area of the unaffected breast are shown in figure 6.24. It can be seen that a wide range of temperature increases, with some as large as 2.5 °C, have been measured. The temperature increase may be localised to the region over the lump or may be more widespread.

The infra-red thermographic findings in breasts with tumours include local or generalised increases in heat emission and increased vascularity. A number of possible causes for the temperature increase associated with malignant tumours have been proposed. Lawson and Gaston (1964) measured the temperature of blood flowing in the arteries supplying the breast, the temperature of the tumour and the temperature of the venous drainage from the tumour. They found that breast cancers were hotter than both the arterial supply and the venous drainage and that the blood flowing in the veins was hotter than that in the arteries. Similar results were found by Gautherie (1980) during surgical operations on breast cancer patients. This situation, similar to that found in the kidneys where the renal vein is normally hotter than the renal artery, implies that tumours have a very high metabolic rate and produce a large amount of heat. This increased heat production above that of the surrounding tissue has often been explained as the cause of the temperature rise measured by infra-red and microwave thermography. The arterial temperatures measured by both Lawson and Gautherie were around 34 °C for the lateral thoracic artery and 32 °C for the internal mammary artery. These temperatures are extremely low for arterial blood, especially considering that the

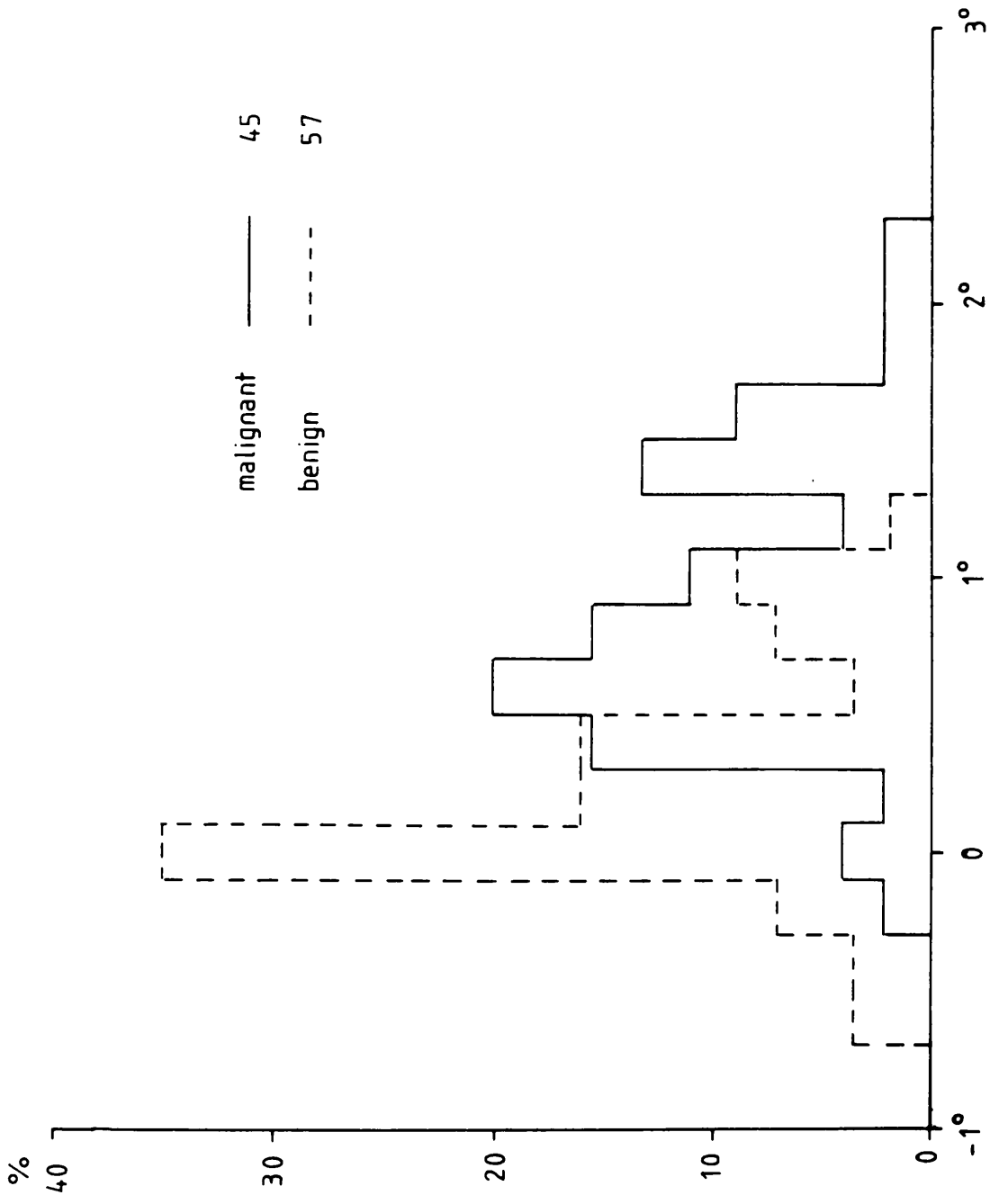


Figure 6.24 Measured microwave temperature increase over lump for malignant and benign lesions

arterial supply to the breast is deep and the measurements have been questioned by Love (1980), who stated that "the arterial blood temperatures that I am aware of in our surgery department and elsewhere generally runs at around 37-37.5 °C." The arterial temperatures measured by Lawson and Gaston, and Gautherie, would suggest that the arterial blood supply is at the same temperature as the surrounding tissue and does not therefore act as a source of heat. This seems unlikely and the calculations of Chen (1985) showed that blood flowing in the arteries does not reach equilibrium temperature with the surrounding tissue.

In order to show the expected temperature rise at the skin surface due to a tumour which is more metabolically active than its surroundings Draper and Boag (1971 a,b) have calculated the effects at the skin surface due to conduction of heat from a heat source in the tissue. Their results show that the thermal changes observed at the skin surface by infra-red thermography are often too large to be due only to increased metabolism of the tumour. Torell and Nilsson (1980) have studied theoretically the increase in skin temperature due to veins at 37 °C approaching the surface from deeper tissue, and found skin temperature increases comparable with those found associated with malignancies in clinical situations using infra-red thermography. These theoretical studies show that the "hot spots" seen by infra-red thermography in breasts with cancer are not due to an increased metabolic heat production in the tumour but to an effect of the tumour on the blood flow in the breast tissue. This is in agreement with the measurements of Beaney et al (1984) who found that the blood flow in tumour tissue is significantly greater than that in normal tissue. Beaney also did not find a significant increase in the oxygen metabolic rate of tumour tissue. Furthermore, if it is assumed that the blood flow does act as a supply of heat to the breast tissue then equation (6.4.3) can be used to approximately describe the temperature distribution with depth in the breast tissue and it can be seen that the maximum temperature increase, ΔT , due to an increase in metabolic heat production, ΔQ , is

$$\Delta T = \frac{\Delta Q}{W_b c_b} \quad (6.7.1)$$

It has already been shown in (5.7.1) that the rate of metabolic heat production is related to the blood perfusion rate by the equation

$$Q = 189 W_b d \quad (5.7.1)$$

and so the maximum possible increase in temperature assuming that all of the oxygen in the arterial blood supply (20 ml/ 100 ml) is extracted is 1 °C (Love 1985). Figure 6.24 shows that temperature rises greater than this have been measured by microwave thermography and so an increased metabolic rate in tissue cannot alone be the cause of the observed temperature increases.

The calculations of Draper and Boag (1971 a,b) and Torell and Nilsson (1980) indicate that hot blood flowing in veins near the skin surface will cause an infra-red temperature increase which becomes more diffuse as the depth of the vein increases. The microwave temperature, however, being an average temperature of a volume of tissue, will not indicate the skin vasculature and local temperature increases due to hot blood flowing in veins will not cause a significant change in the microwave thermographic pattern. This can be seen by referring to the infra-red and microwave measurements on the normal subjects. In subject 9 there are large temperature peaks in the infra-red pattern, most probably due to veins, but these are not reflected in the microwave pattern. The temperature increase observed by microwave thermography must therefore be due to increased blood flow in and around the region of the tumour increasing the supply of heat to the tissue. A contribution to this increase may be due to an increase in heat production due to the tumour metabolism.

6.8 Experimental determination of breast temperatures in patients with breast disease

Microwave and infra-red temperatures were measured on 16 patients with breast disease between the ages of 54 and 71. The measurements were carried out as on the group of normal volunteers and the room temperature was again around 25 °C. It was

found that within the accuracy of the measurements it was not possible to determine, by comparison of microwave and surface temperatures, a consistent difference between the breast water content of this older group and that of the younger group. This can be seen from figure 6.25 where the minimum microwave and surface temperatures are plotted for the younger group of women and for the normal breast of the older group.

The temperature patterns observed in this group were, except in one case, either pattern A or pattern B in the normal breast. This is consistent with the results of Draper and Jones who found less than 10% of normal women over 50 had "warm" breasts.

In breasts containing malignant tumours flat temperature profiles were observed, suggesting a high perfusion, while the normal breast often had the "dipping" profile of group A. An example of this is shown in figure 6.26. The left breast contains a large tumour of maximum diameter 5.5cm in the upper outer quadrant of the breast, which is intruding into the skin surface. The breast temperatures in the right breast are consistent with a low blood perfusion of around $0.2 \text{ kgm}^{-3}\text{s}^{-1}$, while the left breast lower level temperatures indicate a perfusion of about $2 \text{ kgm}^{-3}\text{s}^{-1}$ and the perfusion in this breast at the upper level, over the malignancy, is greater than this.

Figure 6.27 shows the temperature profiles, at 2cm above nipple level, of a woman with a malignant tumour of maximum diameter 2cm in the left breast. The temperature profile of the normal right breast is that of pattern B and by comparison with the model the blood perfusion is around $1 \text{ kgm}^{-3}\text{s}^{-1}$. The numerical model, with 70% water content breast tissue and a blood perfusion rate of $1 \text{ kgm}^{-3}\text{s}^{-1}$, was modified to include a 2 cm square region of increased perfusion representing the malignancy. The blood flow in the tumour was assumed to be $5 \text{ kgm}^{-3}\text{s}^{-1}$ and the thermal conductivity and microwave penetration depth were taken to be the same as that of the surrounding tissue. The calculated microwave and surface temperatures from this model are shown in figure 6.28, together with the temperature profiles for this breast without a tumour region. It can be seen that the localised increase in perfusion gives rise to a local temperature increase, unlike that observed. The temperature increase

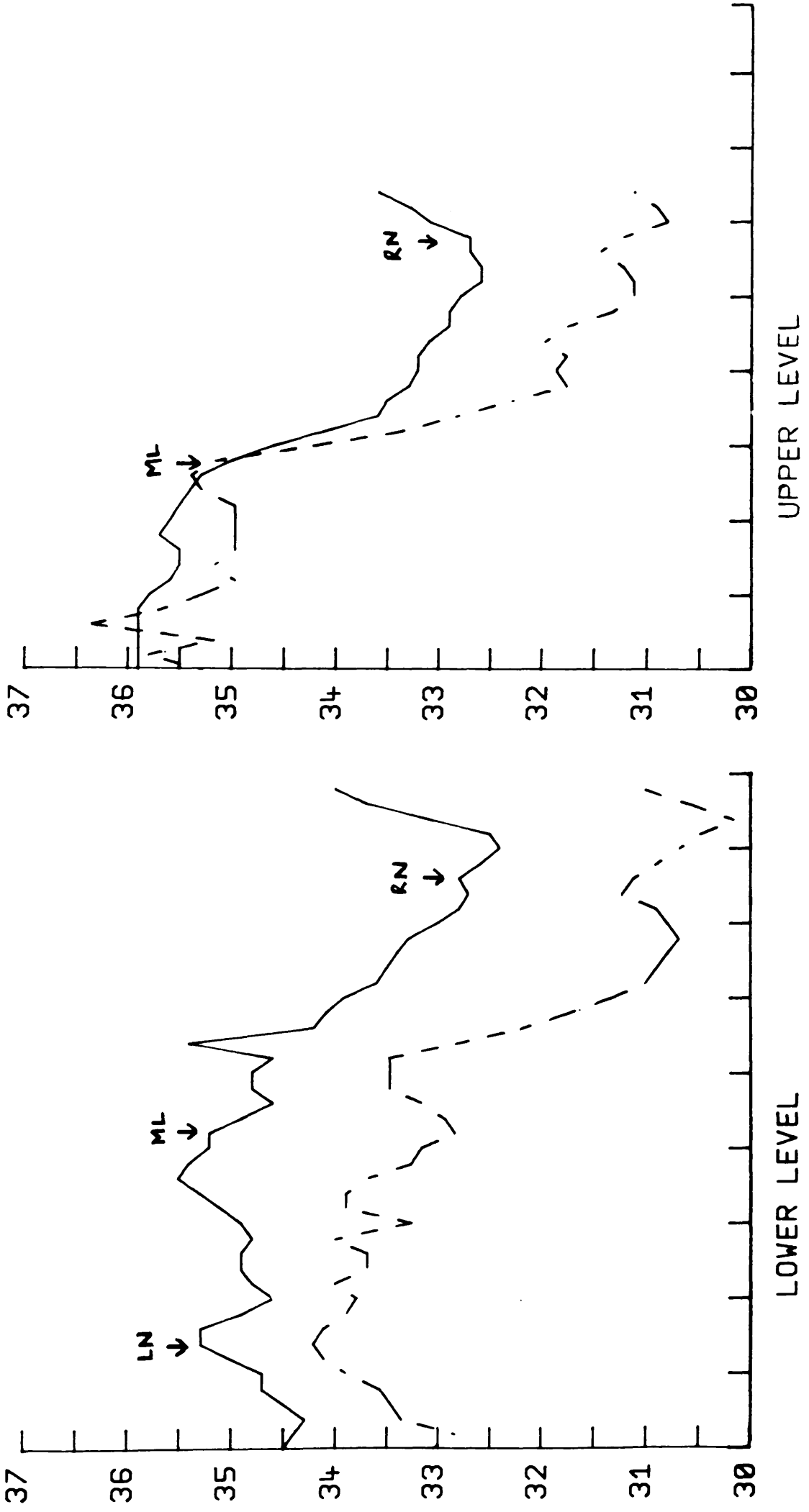


Figure 6.26 Measured microwave and surface temperatures of patient with 5.5 cm malignant tumour in left breast

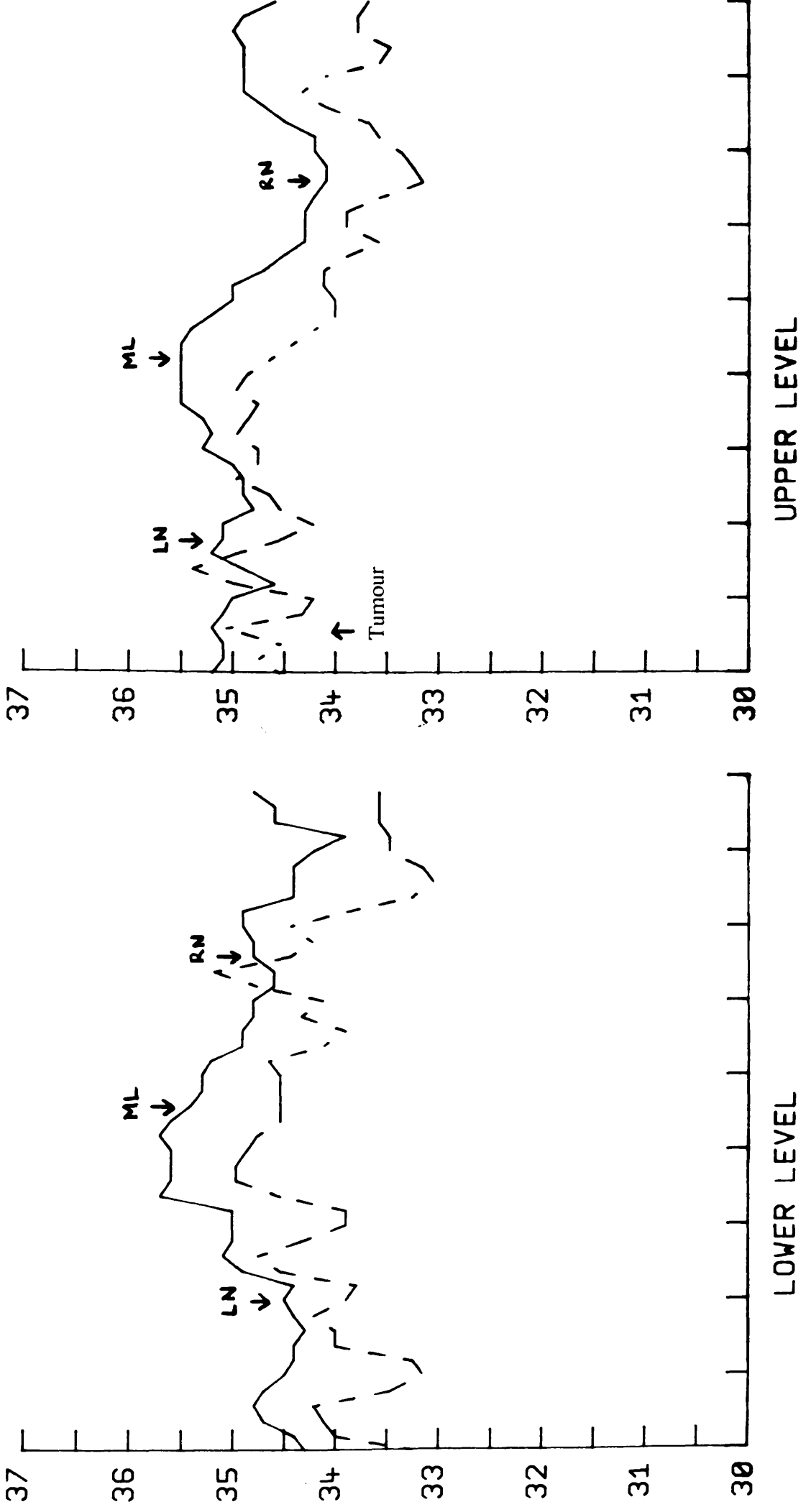


Figure 6.27 Measured microwave and surface temperatures of patient with 2cm malignant tumour in left breast.

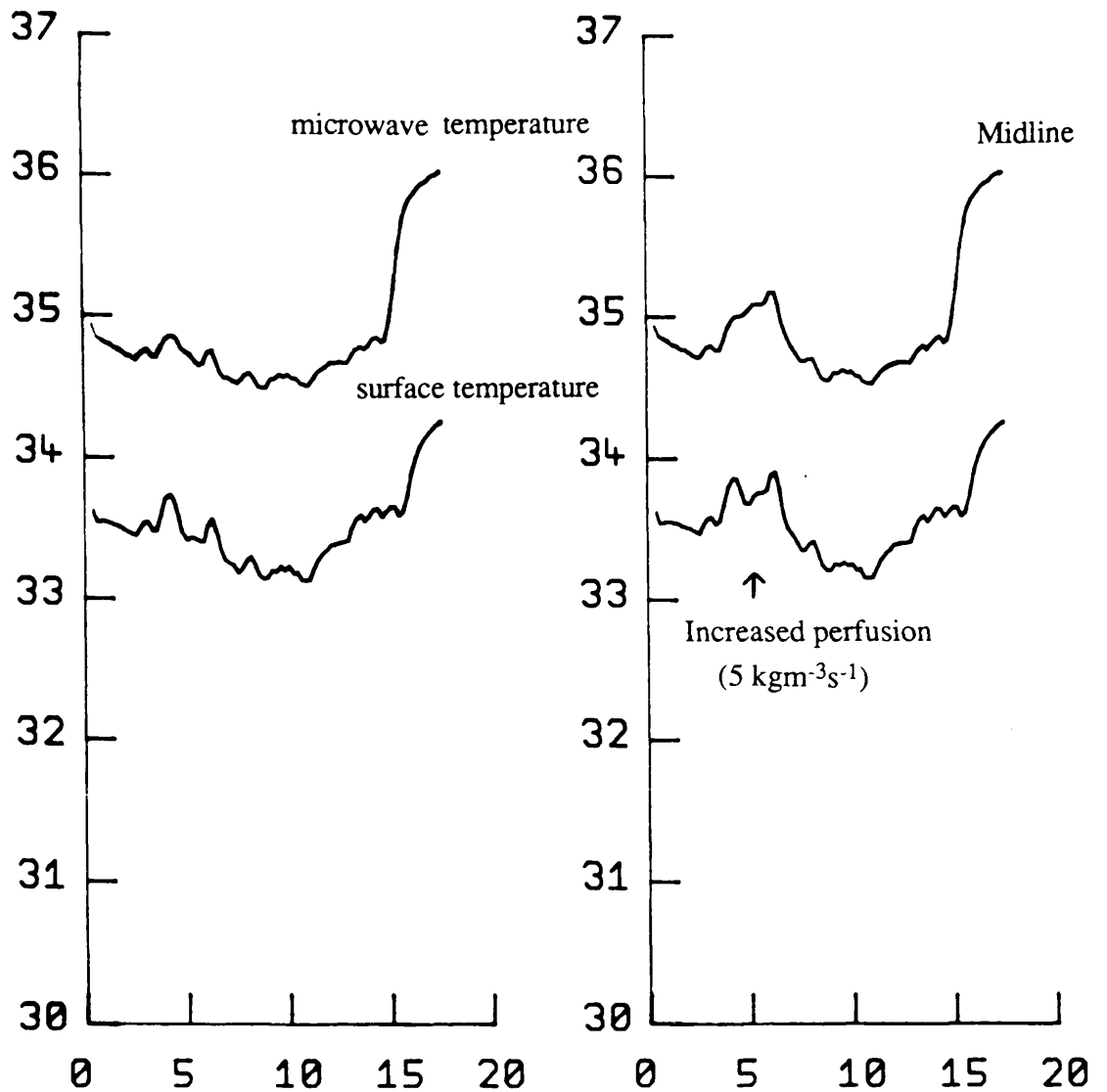


Figure 6.28 Modelled microwave and surface temperatures for 70% water content breast tissue with blood perfusion rate of $1 \text{ kgm}^{-3}\text{s}^{-1}$, with and without area of increased perfusion.

observed indicates that the increase in perfusion is over a larger region than that of the tumour. The temperature profiles measured in the lower part of the breast do not show a large difference between the left and right breast and the change in perfusion does not, therefore, extend over the entire breast.

An important factor to consider in assessing the temperature increase over a malignancy is the level of perfusion in the normal breast. A woman with a low perfusion rate in the normal breast may have a much larger temperature rise between the the normal breast and that containing the malignancy than a woman with the same type of malignancy and the same perfusion rate in the affected breast but with a higher perfusion rate in the normal breast.

The microwave and infra-red temperatures of a woman of 30 with a fibroadenoma in her right breast are shown in figure 6.29. It can be seen that the temperatures here are those of pattern C and no abnormality is observed.

Microwave thermographic measurements may be used to estimate quantitatively the changes in blood perfusion which occur in breasts with malignant tumours. By comparison of the temperatures in the affected and the normal breast the extent of this perfusion change may be determined. This information may be of use in prognosis of cancer patients and in treatment monitoring as well as in diagnosis.

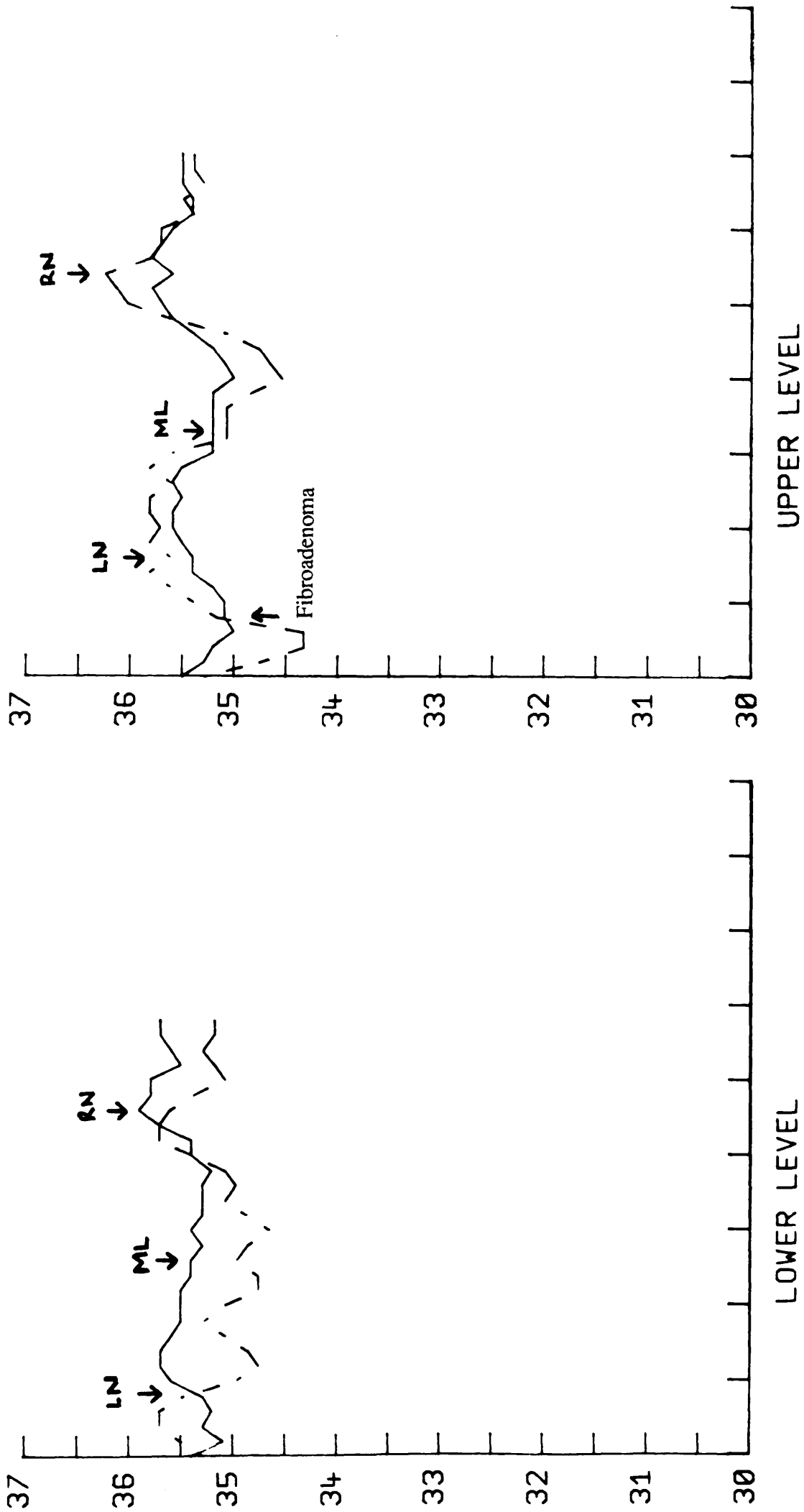


Figure 6.29 Measured microwave and surface temperatures of 30 year old patient with fibroadenoma in left breast.

Chapter 7 - Microwave Thermography in Rheumatology

7.1 Introduction

This chapter discusses the potential role of microwave thermography in the assessment of disease activity in rheumatology. Present methods of assessment are described and compared. Measurements of microwave and infra-red temperatures of normal and arthritic knee joints are compared with modelled temperatures and used to estimate the physiological changes in diseased knee joints which can be determined by thermographic methods.

7.2 Disease assessment in rheumatology

In patients suffering from rheumatic diseases there is a need to quantitatively assess the activity of the disease, most particularly in order to monitor objectively the patient's response to treatment. A large number of rheumatic diseases, including rheumatoid arthritis and ankylosing spondylitis, are inflammatory diseases and the measurement of inflammatory activity is therefore extremely important in assessment of these diseases. Inflammation, however, involving multiple factors such as temperature rise, pain, redness, swelling and stiffness, is known to be extremely difficult to measure, both in clinical practice and in laboratory tests. Consequently, the lack of any measurement which can accurately reflect disease activity has led to the development of a large number of methods of assessment. At present these include clinical assessments, laboratory tests, radionuclide measurements and infra-red thermography. The use of microwave thermography in this field is currently being investigated.

Clinical assessment involves measurement of joint tenderness, grip strength, joint circumference, morning stiffness and range of movement. The patient's own assessment of pain is quantified, most commonly using a visual analogue scale. Certain laboratory tests reflect to some extent the severity of joint inflammation but these play a relatively small part in assessment because of the very indirect relationship between these tests and the discomfort of the patient.

Radionuclides can be used to quantify factors related to joint inflammation either by measurement of the rate of clearance after intra-articular injection or by measurement of the rate of accumulation over a joint following intravenous administration. The most frequently used radioisotopic technique is ^{99m}Tc pertechnetate uptake, described by Dick et al (1970). A correlation between pertechnetate uptake and clinical assessment has been confirmed by a number of workers (Dick and Grennan 1976; Haataja et al 1975; Paterson et al 1978); De Silva et al (1986), although Huskisson (1973) did not find such a correlation.

Since inflammatory activity causes an increase in the tissue temperature thermographic methods can also be used and infra-red techniques have been developed with the aim of providing a reliable quantitative assessment of disease activity. The use of infra-red thermography in the assessment of disease activity has been compared with radioisotopic and clinical methods in a number of studies. This form of comparison is necessary since, without invasive investigation of the inflamed tissue, it is not possible to directly determine the absolute merit of any one assessment technique.

The relationships found between thermographic measurements and clinical assessment have been variable. This is probably due to differences in examination technique and difficulties in the quantitative interpretation of the results of infra-red thermography. A number of forms of interpretation have been employed. Collins et al (1974) have proposed a Thermographic Index (TI) which is the mean skin temperature over the region of the joint of interest. A good correlation between this value and clinical assessment has been found by Bacon et al (1976). Paterson et al (1978) calculated the mean temperature of a 10 cm square drawn on the knee, which is closely related to the Thermographic Index of Collins et al, but found considerable variations in this value between patients and with time in a single patient. As a result the difference in mean temperature between each subject's knees was used. No significant correlation was found in this study between the thermographic assessment and the subjective pain assessment or the physician's assessment of joint inflammation. Huskisson (1973)

used the maximum temperature over the joint as a measure of inflammation and did not find a significant correlation between this value and clinical assessment. In this investigation, however, although the ambient temperature was kept constant for a single set of measurements on an individual patient, it varied by as much as 3.5 °C between each set and this probably accounts for the lack of correlation. Salisbury et al (1983) have proposed the use of a heat distribution index (HDI) which is related to the pattern and spread of temperature over a joint. This form of quantification overcomes the difficulties in standardization of absolute infra-red temperatures. Salisbury et al found that this index correlated better with clinical assessment than the Thermographic Index. In a further study (De Silva et al, 1986) this heat distribution index was shown to correlate significantly with both pertechnetate uptake and all components of clinical assessment except pain. The correlations between pertechnetate uptake and clinical assessments were, however, generally better than those between the heat distribution index and clinical assessments.

It appears that for routine assessment the estimates of inflammation by patient and clinician give satisfactory results which are as accurate as those of the current objective tests. The value of the objective tests provided by thermography and radionuclides is in drug assessment where stability, operator independence and sensitivity to change are required. In this area pertechnetate uptake appears to be more successful than infra-red thermography. Infra-red thermography has the advantage, however, of being easier to perform and avoiding the use of a radioisotope.

The major difficulty with infra-red thermography, however, is the stability of the skin temperature. The skin temperature is very sensitive to changes in the environmental conditions and in order to achieve accurate, reproducible results it is extremely important to have a standardised examination procedure. The most important factor of which is a constant ambient temperature with a uniform, constant airflow. This requirement of a strictly controlled environment is most probably the reason for the success of infra-red thermography at Bath, where a number of drug studies have

been carried out using this technique (Bird, Ring and Bacon, 1978; Ring, 1980), and the difficulties encountered by other researchers in using absolute infra-red temperature measurements in disease assessment.

Microwave thermography, however, can be used to determine a volume average of joint temperature. This is less sensitive to changes in environmental conditions since it measures the temperature of the subcutaneous tissues as well as the skin temperature. This method also has the advantage of providing a more direct indication of the temperature deeper in the joint than that given by infra-red thermography.

An invasive method of direct intra-articular temperature measurement, involving insertion of a thermocouple into the joint, has been developed by Haimovici (1982) and carried out on 316 normal and 575 diseased joints. Skin temperature was measured around the joint before determination of the intra-articular temperature and patients with a highly increased local skin temperature were excluded from the trial. The comparison of intra-articular temperature with skin temperature showed that the skin temperature often bore no relation to the temperature in the joint itself. A single measurement of intra-articular temperature was able to differentiate a healthy joint from a pathologically altered or injured one through a temperature increase. In the knee joint, for example, the mean normal temperature was 32.8 ± 1.1 °C, while in joints with active osteoarthritis the mean temperature was 36.1 ± 1.2 °C, in rheumatoid arthritis 35.8 ± 1.5 °C, and in posttraumatic arthritis 35.2 ± 1.4 °C. In patients with latent osteoarthritis the temperature in the joint was not significantly different from that in the normal joints. These internal measurements verify that the internal temperature in a diseased joint is increased above that in a healthy joint. This initial study did not include investigation of the correlation between joint temperature and other assessments of disease activity and so did not indicate the sensitivity of this determination of joint temperature as a measurement of disease activity.

7.3 Microwave thermography in rheumatology

In a current evaluation of disease assessment using microwave thermography longitudinal scans of the knee, from 16 cm above the centre of the patella to 8cm below, have been taken on 44 knees of patients with rheumatoid arthritis and 8 normal knees (Fraser et al, 1987). Typical microwave thermographic profiles for a normal and an inflamed knee are shown in figure 7.1. In the normal knee a cool region is seen over the patella. This is also observed with infra-red thermography (Salisbury et al, 1983). In patients with inflammatory arthritis an increase in temperature over the patella is observed giving a flat temperature profile. The microwave temperature measurements were classified by using twice the amplitude of the first oscillatory term obtained by Fourier analysis of the curve. This "microwave thermographic index" was found to correlate significantly with a clinical assessment of pain and of synovitis.

The possible causes of this increased joint temperature are, as in the case of breast cancer, an increase in metabolic heat production and an increase in perfusion.

The maximum temperature increase which can be caused by increased metabolic heat production alone is approximately 1 °C (see section 6.7), and so the observed temperature increases, which may be much greater than this, must be due to increased perfusion. The increased perfusion will have a much larger effect on the temperature distribution than any increase in metabolic heat production.

In an inflamed knee joint the most likely site of an increase in perfusion is the synovial membrane (Salisbury et al, 1983), but the problem of measurement of synovial blood flow has not yet been solved (Simkin, 1989). The synovial membrane, also known as the synovium, is the tissue lining the narrow cavity (joint space) containing the lubricating synovial fluid (see figure 7.2). The use of xenon clearance as a technique for the study of blood flow in this synovial tissue has been abandoned following recognition of the fact that the recorded clearance of the isotope was from perisynovial fat rather than from the joint space (Phelps et al, 1977). However, in rheumatoid arthritis and degenerative joint disease, the clearance of ionic sodium and

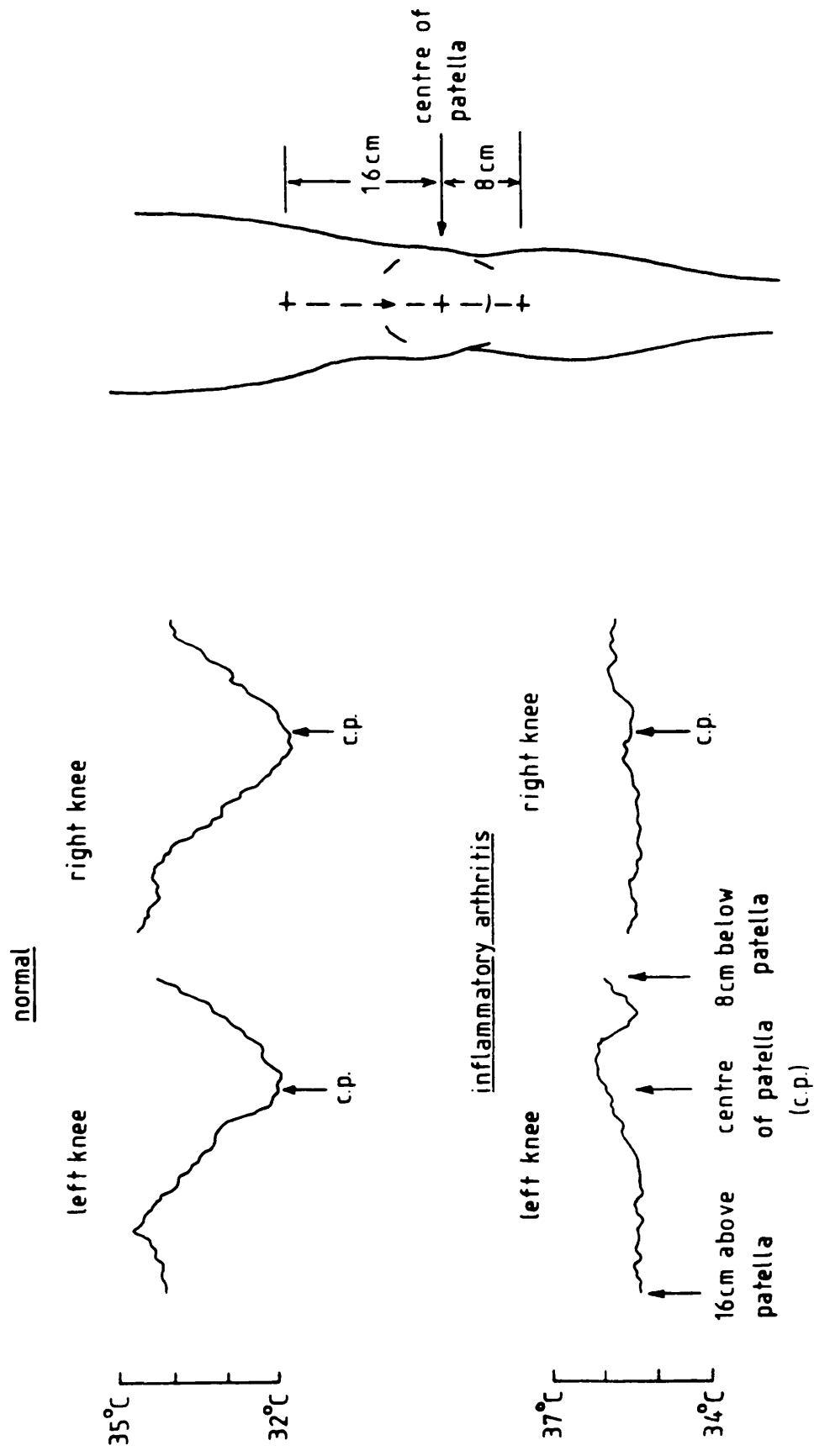


Figure 7.1 Typical microwave temperature profiles over a normal and an inflated knee joint

iodine is consistently increased above the rates of clearance in normal knees and has been found to correlate well with clinical signs of synovial inflammation. This effect has been attributed to an enhanced synovial blood flow in active synovitis (Simkin and Nilson, 1981).

The increased temperature observed in inflamed joints is, therefore, most probably due primarily to an increase in blood perfusion in the synovium.

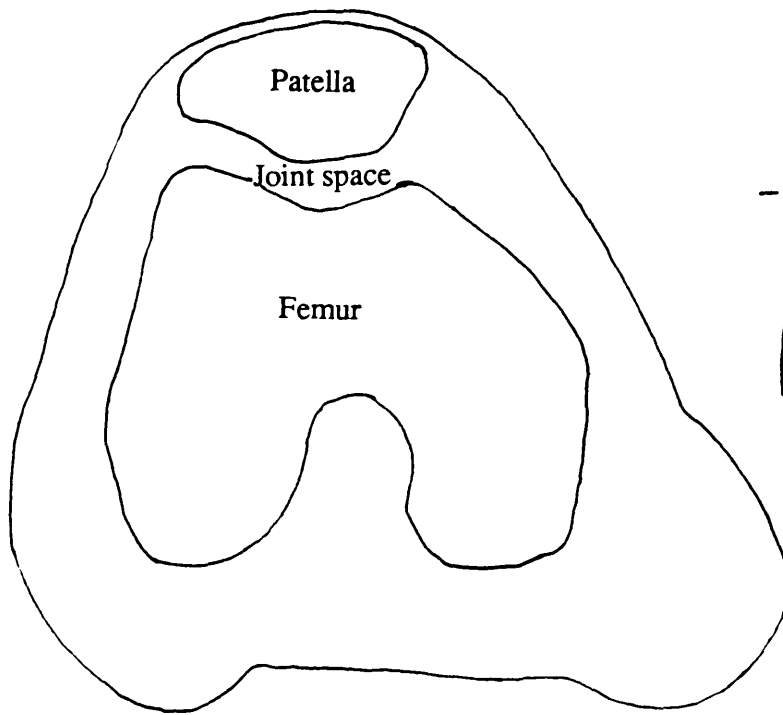
7.4 Modelling of temperature distributions in the knee joint

The method of evaluation of the microwave temperature profile measured over the knee joint, which has been applied in the study of disease assessment in patients with rheumatoid arthritis (Fraser et al, 1987) depends primarily on the microwave temperatures measured over the quadriceps muscle at the beginning of the scan and over the centre of the patella. The expected temperature distributions in both these regions have been modelled by solution of the heat transfer equation (4.2.1). The expected microwave and surface temperatures have been determined and compared with measurements of microwave and infra-red temperature measurements on normal patients and patients with rheumatoid arthritis.*

The temperature distribution over the quadriceps muscle, for a range of blood perfusion values in the muscle tissue, was determined analytically by considering this region of the limb to be a homogeneous cylinder of muscle, of radius 8 cm, surrounded by a 2 mm layer of fat. This is a reasonable approximation since in this region only a small percentage of the leg is composed of the femoral bone. The expected temperatures have also been calculated without inclusion of the fat layer.

At the knee joint the temperature distribution was calculated numerically, using a finite difference method, from the model shown in figure 7.2; a two-dimensional representation of the cross-section of the knee joint. The accuracy of the numerical solution was determined by comparison of the analytical and numerical solutions for a circle of equivalent dimensions to the knee joint model.

* The infra-red temperature measurements, used to determine surface temperature, were made with a hand-held infra-red thermometer.



Properties of tissue used in model

	ϵ_r'	ϵ_r''	δ' (cm)	K ($Wm^{-1}C^{-1}$)	W_b ($kgm^{-3}s^{-1}$)
Bone (patella, femur)	7	1.7	1.45	0.8	0.1
Muscle	51	14	0.60	0.46	0.5
Synovium (knee joint cavity)	51	14	0.60	0.46	0.2 - 5

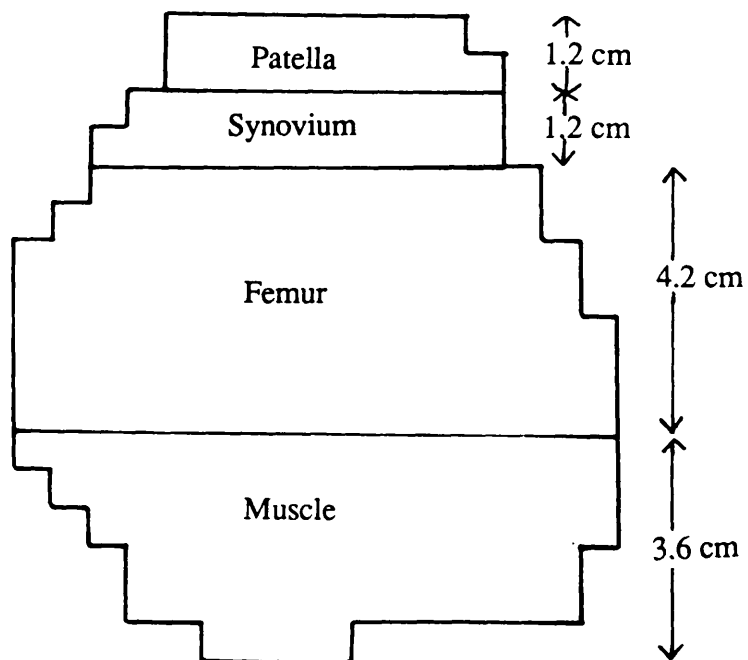


Figure 7.2 Cross-sectional model of knee joint

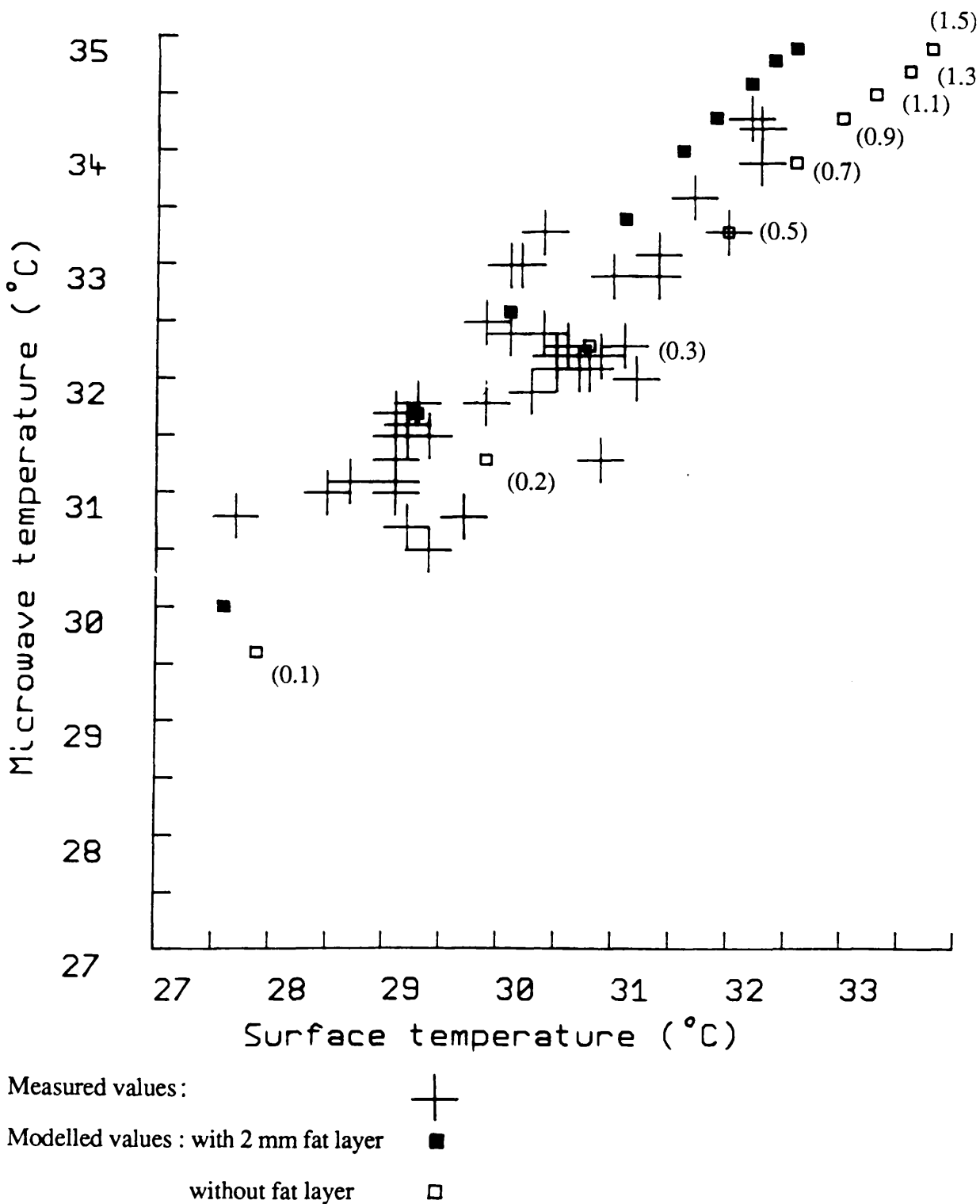
Forty-six pairs of microwave and infra-red temperature measurements over the left and right quadriceps of 12 normal subjects are shown in figure 7.3. The ambient temperature at which these measurements and subsequent knee joint temperature measurements were made was between 18 and 23 °C and calculated temperatures were determined with an environmental temperature of 20 °C. The calculated microwave and surface temperatures over the quadriceps muscle, both with and without a fat layer, are also shown in figure 7.3. The agreement between the measured and calculated microwave and surface temperatures indicate that the appropriate value for the effective attenuation in muscle tissue has been chosen. The muscle blood flow indicated by the modelled temperatures is in the range 0.1 to 0.9 kgm⁻³s⁻¹. This is in reasonable agreement with the results of Lassen (1964) who found blood perfusion rates in the human calf muscle of 0.6±0.3 kgm⁻³s⁻¹ using radioisotopic clearance methods. The lower blood flow values indicated by the modelled temperatures are perhaps due to the effects of skin blood flow, which, if lower than muscle blood flow reduce the effective blood flow of the tissue.

Figure 7.4 shows the results of 52 measurements of microwave and surface temperatures over the centre of the patella of the same 12 normal subjects under the same conditions. The microwave and surface temperatures calculated from the numerical model for different values of blood flow in the synovium are also shown in this figure.

The measured temperatures are generally consistent with a blood flow in the synovium of between 0.2 and 2.0 kgm⁻³s⁻¹. The calculated temperature distribution through the knee joint for this range of perfusion values in the synovium is shown in figure 7.5. The range of intra-articular knee joint temperatures, measured by Haimovici in normal joints was 32.8±1.1 °C. This temperature should be equal to the modelled temperature in, or close to, the synovium. Figure 7.5 indicates that modelled blood perfusion rates in the synovium of between 1 and 2 kgm⁻³s⁻¹ are consistent with this temperature. A number of measurements, however, indicated blood flows in the

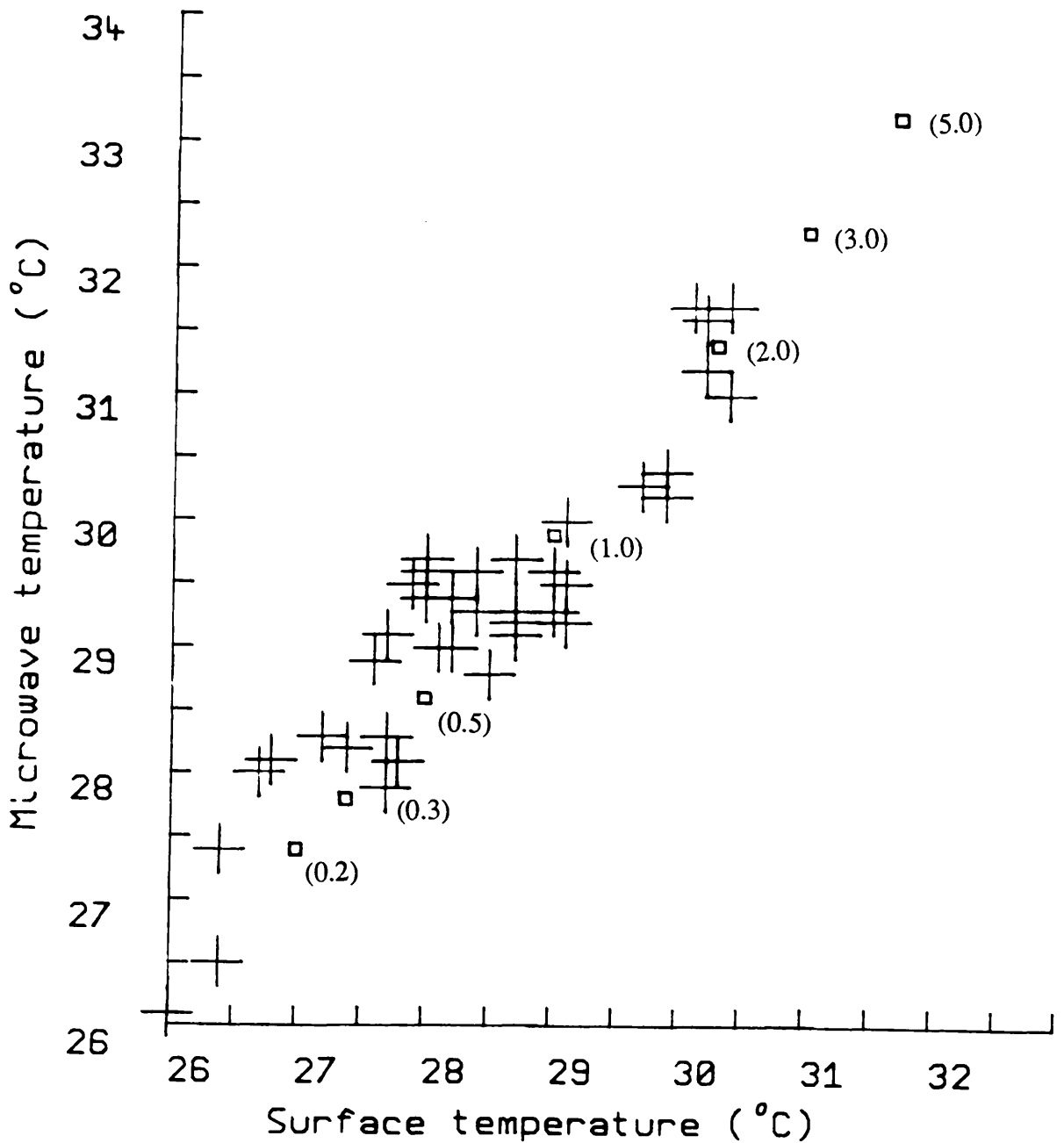
Properties of tissue used in model

	ϵ_r'	ϵ_r''	δ' (cm)	K ($Wm^{-1}C^{-1}$)	W_b ($kgm^{-3}s^{-1}$)
Muscle	51	14	0.60	0.46	0.1 - 1.5
Fat	7	1.7	1.45	0.21	0.06



Figures in brackets: perfusion in muscle tissue ($kgm^{-3}s^{-1}$)

Figure 7.3 Measured values of microwave and surface temperatures over the quadriceps muscle of normal subjects compared with modelled values.



Measured values : +

Modelled values : \square

Figures in brackets : perfusion in synovium ($\text{kgm}^{-3}\text{s}^{-1}$)

Figure 7.4 Measured values of microwave and surface temperatures over the centre of the patella of normal subjects compared with modelled values.

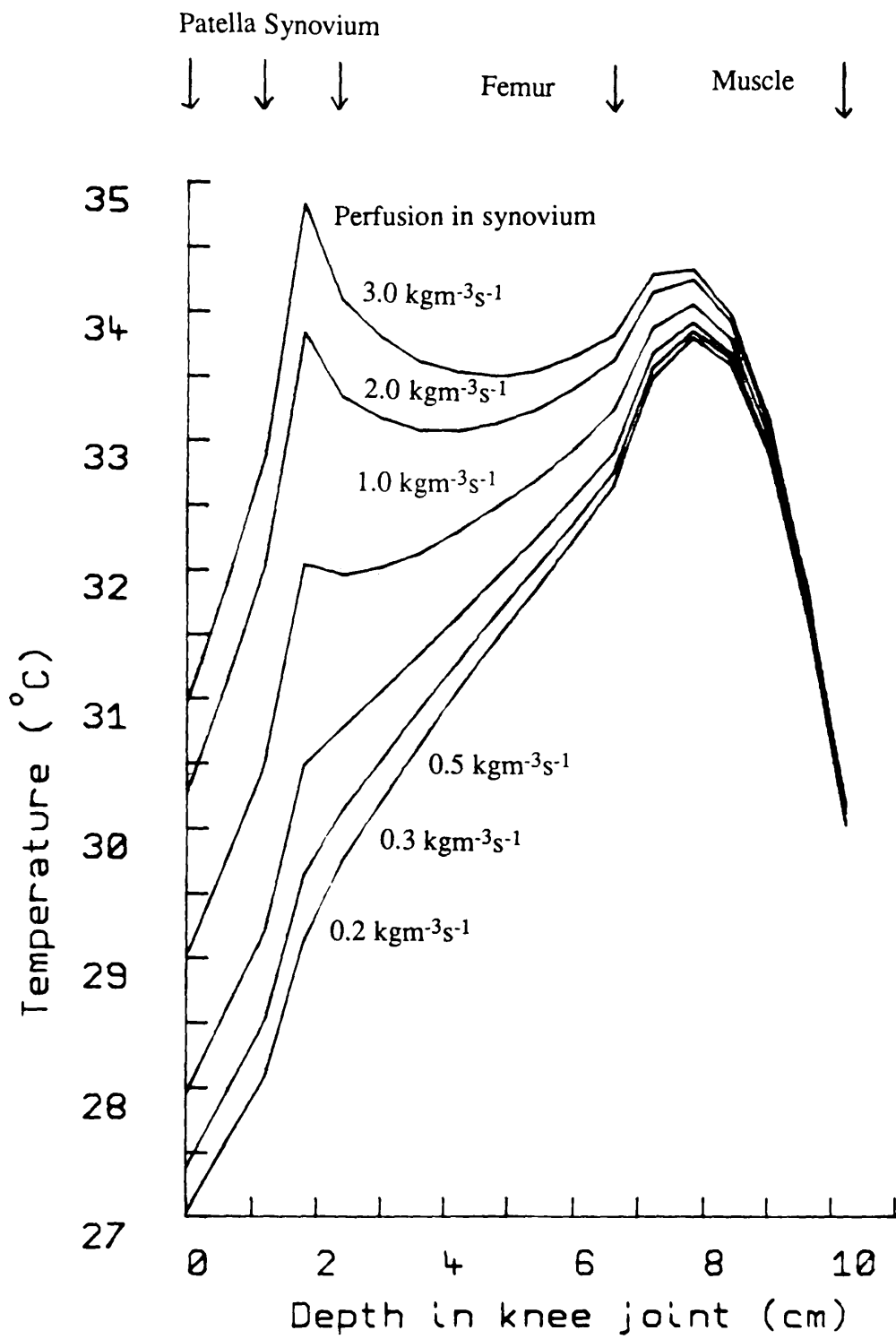
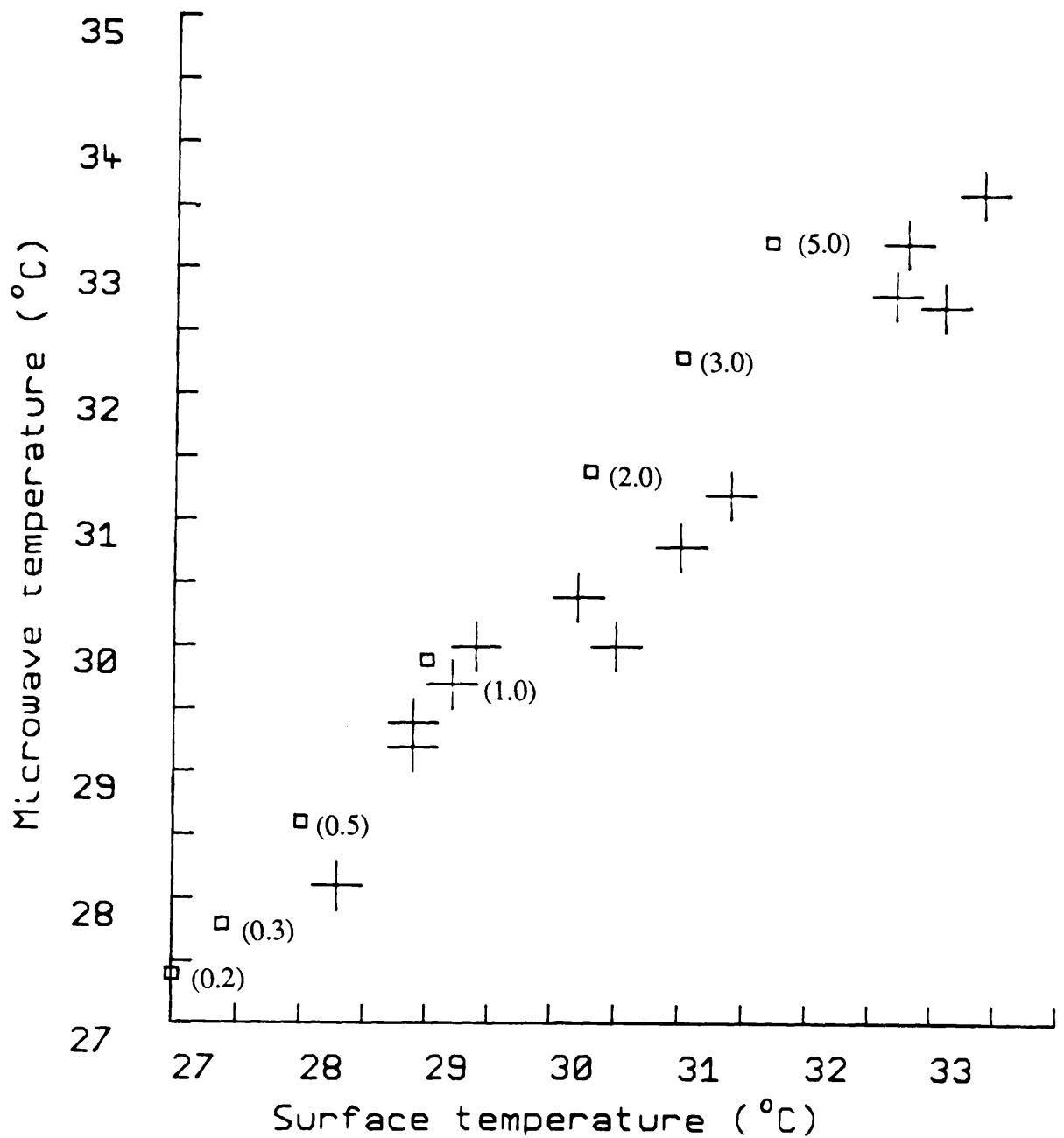


Figure 7.5 Temperature distribution through modelled knee joint

synovium which were lower than this, and hence indicated lower intra-articular knee joint temperatures. Simultaneous measurement of microwave, infra-red and invasive intra-articular temperatures are required to verify the relationship between microwave and infra-red temperatures and synovial blood flow indicated by the numerical model.

The calculated temperature distribution through the knee joint is dependent on the thickness of the synovium. In normal joints more accurate knowledge of the anatomical structure of the knee joint will lead to improved modelling. In diseased joints the volume of synovium is often increased (Simkin, 1989) and this increased volume alone can result in an increased temperature to to the increase in the overall blood supply to the tissue. If the increased volume is accompanied by an increase in perfusion rate this will lead to a further increase in the knee joint temperature.

Figure 7.6 shows the measured microwave and infra-red temperatures over the centre of the patella of 13 knee joints of patients suffering from rheumatoid arthritis of varying degrees of activity from inactive to very active. Figure 7.7 shows the corresponding temperatures over the quadriceps muscles of the same rheumatoid patients. The muscle temperatures are similar to those of the normal group with indicated muscle blood flows of between 0.1 and $0.5 \text{ kgm}^{-3}\text{s}^{-1}$. The microwave and infra-red temperatures over the patella are similar to those of the normal joints for patients with inactive disease, while for patients with active disease the temperatures are much higher. The surface temperatures for these patients are higher than expected from the model and this is most probably due to an increased blood flow through the skin removing the excess heat from the joint. The microwave temperatures of these patients were between 32.7 and $33.6 \text{ }^\circ\text{C}$. These temperatures would require a synovial perfusion of greater than $3 \text{ kgm}^{-3}\text{s}^{-1}$ (corresponding to a microwave temperature of $32.2 \text{ }^\circ\text{C}$) if the volume of synovium is assumed the same as that in the normal group. A blood perfusion rate of $5 \text{ kgm}^{-3}\text{s}^{-1}$ in the synovium would produce a microwave temperature of $33.2 \text{ }^\circ\text{C}$. For twice the volume of synovium the microwave temperature at $3 \text{ kgm}^{-3}\text{s}^{-1}$ blood perfusion is $33.8 \text{ }^\circ\text{C}$. The calculated maximum temperature in the

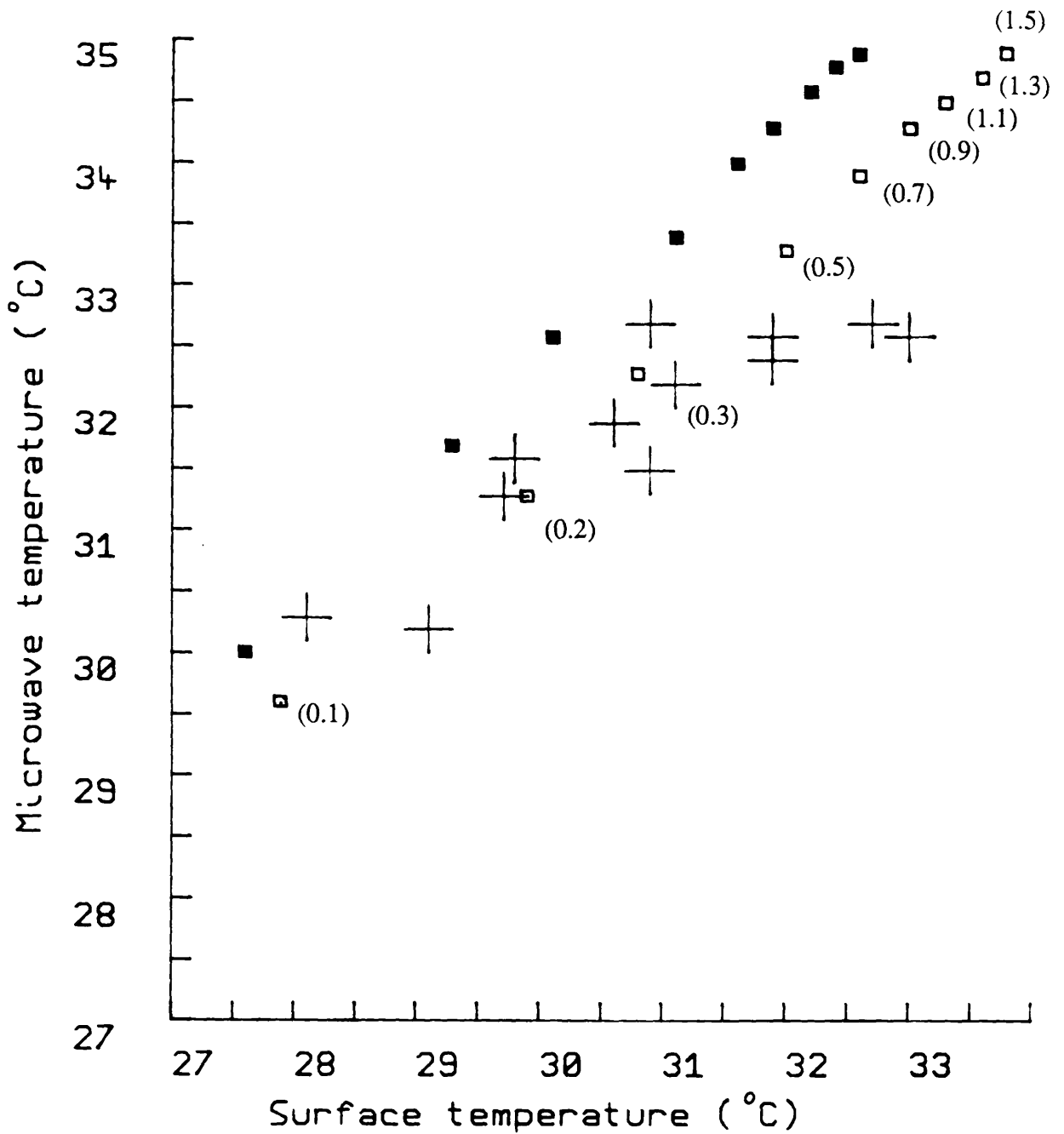


Measured values : +

Modelled values : □

Figures in brackets : perfusion in synovium (kgm⁻³s⁻¹)

Figure 7.6 Measured values of microwave and surface temperatures over the centre of the patella of patients suffering from rheumatoid arthritis compared with modelled values.



Measured values : +

Modelled values : with 2 mm fat layer ■

without fat layer □

Figures in brackets: perfusion in muscle tissue (kgm⁻³s⁻¹)

Figure 7.7 Measured values of microwave and surface temperatures over the quadriceps muscle of patients suffering from rheumatoid arthritis compared with modelled values.

synovium for the normal thickness of synovium at $3 \text{ kgm}^{-3}\text{s}^{-1}$ is $34.8 \text{ }^\circ\text{C}$ and at $5 \text{ kgm}^{-3}\text{s}^{-1}$ this temperature is $35.9 \text{ }^\circ\text{C}$, while for twice this thickness of synovium the maximum temperatures in this tissue at perfusion rates of 1.0 and $3.0 \text{ kgm}^{-3}\text{s}^{-1}$ are 35.1° and $37 \text{ }^\circ\text{C}$ respectively. These temperatures are in agreement with the value of $35.8 \pm 1.5 \text{ }^\circ\text{C}$ intra-articular temperature measured by Haimovici on patients with active arthritis. The synovium blood perfusion rate in patients with active rheumatoid arthritis is therefore consistent with modelled values of greater than $1 \text{ kgm}^{-3}\text{s}^{-1}$.

In patients with rheumatoid arthritis the microwave temperature increase above the level found in normal joints may be explained in terms of a perfusion increase in the synovium accompanied by an increase in the volume of this tissue. In order to determine more accurate quantitative estimates of the perfusion in this tissue it would be necessary to extend the numerical modelling of the temperature distribution to three dimensions and to have accurate anatomical knowledge of the of patient's knee joint.

Chapter 8 - Conclusions

is a technique which can be used to Microwave thermography obtain information about the temperature of internal body tissues by measuring the effective source temperature of the microwave radiation emitted in a certain frequency range by the tissues of the body. The measured microwave temperature is a weighted volume average of the tissue temperature and is influenced by a large number of factors which include the measurement frequency, the dielectric properties and anatomical structure of the body tissues and the characteristics of the radiometer antenna as well as the temperature distribution in the tissue. For medical applications it is the tissue temperature distribution which is the quantity of interest since abnormal distributions indicate sites of disease. Alterations in the temperature distribution from that found in normal, healthy tissue are due to changes in the tissue vascularity and metabolic activity.

The temperature distribution in tissue may be estimated by modelling the heat transfer processes which occur in the tissue. The expected microwave temperature may be calculated from the modelled temperature distribution, provided that the weighting function is known, and compared to clinically obtained temperatures. The most important parameters in this modelling are the water contents of the tissues present and the blood perfusion rate through these tissues. This is because, with the exception of bone, the water content determines both the tissue microwave penetration depth and the thermal conductivity, while the blood perfusion, with the exception of the major organs, determines the heat carried to the tissue and overwhelms the effect of metabolic heat production. The modelling of the temperature distribution is limited by the accuracy of the model of biological heat transfer, which itself is limited by knowledge of the microcirculation. Since the microwave temperature is measured over a volume of centimetric dimensions it is reasonable to use the heat transfer equation of Pennes (1948) and to assume that each tissue has homogeneous properties which are equal to the average properties.

For the antenna used in the Glasgow microwave thermography system the

weighting function in a single region of tissue may be described by an exponential with an effective penetration depth which is less than the plane wave penetration depth (Mimi, to be published). This allows the weighting function to be determined from plane wave analysis using appropriate effective penetration depths for each tissue. More accurate determination of the weighting function is possible by suitable electromagnetic modelling using numerical methods, but the practical benefits to be gained from this improved accuracy, considering the uncertainty in the dielectric properties of tissue and the heterogeneity of the tissue, are likely to be small.

This approach to determining temperature distributions in tissue by solution of the direct problem is particularly suited to the study of breast disease using microwave thermography. This is due to the relatively simple anatomical structure. The breast may be considered to be a region of homogeneous tissue supported by an inner region of well-perfused tissue which represents the core of the body. A set of modelled microwave temperature profiles may be produced which represent different values of blood perfusion in the breast and different breast tissue water contents. The shape and size of the breast is relatively unimportant since the temperature distribution tends to the limit of the single region temperature distribution as the thickness of breast tissue increases. The largest variation in microwave temperature occurs over thin regions of breast tissue.

Additional information may be provided by measurement of the skin temperature using infra-red or contact thermography. The surface temperature is calculated by the modelling of the tissue temperature distribution and the theoretical and experimental values of this may also be compared. The microwave and surface temperatures allow estimation of the two unknown properties of the breast tissue; water content and blood perfusion.

The modelled temperature profiles across the breast agree well with those observed clinically. In addition to the quantitative values of these temperatures, the temperature pattern also indicates the level of perfusion in the breast. Three forms of

pattern have been identified for the microwave temperature profiles. These patterns represent a continuous progression from low to high blood perfusion in the breast. This is confirmed by the corresponding infra-red temperature profiles and the observations of Draper and Jones (1969) who carried out full infra-red thermographic examinations on a large number of women. It appears that as the perfusion in the breast increases the vascularity observable by infra-red thermography increases. This is consistent with venous blood making increasing use of the more superficial channels of drainage, in order to transfer more heat to the surface, as the increasing perfusion in the breast tissue supplies more heat to the breast.

In normal young women the perfusion was found to be in the range $0.2 - >2 \text{ kgm}^{-3}\text{s}^{-1}$. At high values of perfusion, greater than $2 \text{ kgm}^{-3}\text{s}^{-1}$, the microwave and surface temperatures both change gradually as perfusion is increased, making estimation of perfusion in this region difficult. At lower values of perfusion, however, both the microwave and surface temperatures are considerably more sensitive to changes in perfusion. This means that the accuracy in estimation of perfusion is relatively greater in tissues with lower blood perfusion rates.

In post-menopausal women the water content of the normal breast tissue, indicated by the microwave and surface temperatures, showed no difference from that of the younger pre-menopausal women. Any increase in the amount of fat present in the post-menopausal breast is not therefore large enough to cause an observable increase in the microwave penetration depth. A similar range of perfusion values to that in the younger women was found in the normal breast tissue of the post-menopausal women indicating that the level of perfusion in the breast is not determined solely by the menstrual cycle.

In breasts with malignant tumours the temperature rise observed is almost certainly due to an increase in perfusion. The area of increased perfusion may be either localised to the site of the tumour or may be more widespread. In the case of a widespread perfusion increase the temperature profile of the affected breast may be

widely different from that of the normal breast. The difference in dielectric properties of the very high water content tumour tissue from the surrounding normal tissue has an insignificant effect compared to blood perfusion since the effective microwave power penetration depths are not greatly different.

Using comparisons with modelled temperatures microwave thermographic measurements on the breast may therefore be used to estimate perfusion both in normal and diseased breasts. This technique may have applications in the study of perfusion changes associated with the menstrual cycle or with malignant disease.

In clinical detection of breast cancer the most effective use of this technique is comparison of the temperatures of the left and right breast. The difference in temperature between breasts, which is due to perfusion changes, should be considered as well as differences in the temperature patterns. Infra-red thermography will give complementary information to microwave thermography since it reflects the perfusion in the skin. This skin perfusion is dependent, however, on the environmental conditions as well as the physiological conditions in the underlying tissue.

In rheumatoid disease measurement of microwave temperatures over the knee joint reflects disease activity. The increased temperature observed is most probably due to increased perfusion in the synovium and the increased volume of this tissue. Comparison of modelled microwave and surface temperatures with those obtained on both normal and arthritic knee joints indicated that these effects could account for the temperatures observed.

Infra-red thermography has already shown that a significant relationship exists between joint temperature and disease activity. Microwave thermography, since it indicates more directly the internal temperature in the joint, should provide an improved measure of disease activity. Furthermore, microwave thermography is an easier technique to apply since it does not require such rigorous control of the environment.

The aim of this study was to develop computer modelling techniques for microwave thermography. It has been found that the microwave thermographic

measurements on both the breast and the knee joint primarily reflect the level of perfusion in the breast tissue and the synovium respectively. Continued clinical studies are required to determine the significance of these changes. Further studies on the microwave dielectric and thermal properties of tissue, and on antenna patterns, will improve the accuracy with which perfusion estimates can be made.

Microwave thermography techniques may be improved by correlation radiometry, using more than one antenna, and multi-frequency radiometry, where measurements are made at more than one frequency. The stability of single frequency microwave thermographic measurements could be improved by use of a thermostatically temperature controlled antenna, which could be heated to close to skin temperature to further reduce the the thermal disturbance caused by the contact of the antenna with the skin surface.

- Abdul-Razzak M M et al (1987). Microwave thermography for medical applications. IEE Proc., 134, 171 - 174
- Altman P L and Dittmer D S (1964). *The Biology Data Book*. Fed. of Amer. Socs. for Experimental Biology, Washington D C.
- Audet J, Bolomey J C, Nguyen D D, Robillard M, Chive M and Leroy Y (1980). Electrical characteristics of waveguide applicators for medical applications. J. Microwave Power, 15, 177 - 186
- Bacon P, Collins A J, Ring E F J and Cosh J (1976). Thermography in the assessment of inflammatory arthritis. Clin. Rheum. Dis., 2, 51 - 65
- Bardati F and Solimini D (1984). On the emissivity of layered materials. IEEE Trans. Geosci. and Remote Sensing, GE-22, 374 - 376
- Bardati F, Bertero M, Mongiardo M and Solimini D (1987). Singular system analysis of the inversion of microwave radiometric data : applications to biological temperature retrieval. Inverse Problems, 3, 347 - 370
- Bardati F, Calamai G, Mongiardo M, Paolone B, Solimini D and Tognolatti P (1987). Multispectral microwave radiometric system for biological temperature retrieval: experimental tests. Proceedings of the 17th European Microwave Conference, 5 - 9 September, Rome
- Bardati F, Mongiardo M and Solimini D (1986). Synthetic array for radiometric retrieval of thermal fields in tissues. IEEE Trans Microwave Theory and Techniques, MTT-34, 579 - 583
- Barrett A H and Myers P C (1986). "Basic principles and applications of microwave thermography" in *Medical Applications of Microwave Imaging*, L E Larsen and J H Jacobi (eds), IEEE Press, 41 - 46
- Barrett A H, Myers P C and Sadowsky N L (1980). Microwave thermography in the detection of breast cancer. Amer. J. Roent., 134, 365 - 368
- Beaney R P et al (1984). Positron emission tomography for in - vivo measurement of regional blood flow, oxygen utilization and blood volume in patients with breast cancer. The Lancet, 1, 131 - 134
- Best C H and Taylor N B (1950). *The Physiological Basis of Medical Practice*. 5th Edition. Bulliere, Tindall and Cox, London.

- Bird H A, Ring E F J and Bacon P A (1978). A thermographic and clinical comparison of three intra-articular steroid preparations in rheumatoid arthritis. *Ann. of the Rheum. Dis.*, 38, 36 - 39
- Bocquet B, Leroy Y, Mamouni A, Van de Velde J C, Delannoy J, Delvaley D and Giaux G (1988). Microwave imaging process by multi-probe radiometry: present state of exploration of the breast. IEE Colloquium "Medical Applications of Microwaves", Digest no. 1988/60, April
- Bocquet B, Mamouni A, Hochedez M, Van de Velde J C and Leroy Y (1986). Visibility of local thermal structures and temperature retrieval by microwave radiometry. *Elect. Lett.*, 22, 120 - 122
- Brady M M, Symons S A and Stuchly S S (1981). Dielectric behaviour of selected animal tissues in vitro at frequencies from 2 - 4 GHz. *IEEE Trans. Biomed. Eng.*, BME-28, 305 - 307
- Brebner D F, Kerslake D McK and Waddell J L (1956). The diffusion of water vapour through human skin. *J. Physiol.*, 132, 225 - 231
- Brown A C (1973). "Energy metabolism" in *Physiology and Biophysics III*. T C Ruch and H D Patton (eds.), W B Saunders Co., Philadelphia
- Bruggeman D A G (1935). Berechnung verschiedener physikalischer Konstanten von heterogenen Substanzen. *Ann. Physik. (Leipzig)*, 24, 636 - 679
- Buettner K J K (1934). Die Wärmeübertragung durch Leitung und Konvektion, Verdunstung und Strahlung in Bioklimatologie und Meteorologie. Berlin: Veröffentlichungen des Preussischen meteorologischen Instituts Abwandlungen, vol. X, no. 5
- Buettner K J K (1953). Diffusion of water and water vapor through human skin. *J. Appl. Physiol.*, 6, 299 - 241
- Burdette E C, Cain F L and Seals J (1980). In vivo probe measurement technique for determining dielectric properties at UHF through microwave frequencies. *IEEE Trans. Microwave Theory and Techniques*, MTT-28, 414 - 427
- Carr K L, El-Mahdi A M and Shaeffer J (1982). Passive microwave thermography coupled with microwave heating to enhance early detection of breast cancer. *Microwave J.*, 25, 125 - 136

- Cetas T C, (1985), "Temperature measurement" in *Heat Transfer in Medicine and Biology* . Vol. 2, A Shitzer and R C Eberhart (eds), Plenum Press, 373 - 391
- Chandrasekhar S (1939). *An Introduction to the Study of Stellar Structure*. Dover Publications, Inc., 198 - 203
- Chato J C (1969). "Heat transfer in bioengineering" in *Lectures on Advanced Heat Transfer*. B T Chao (ed.), University of Illinois Press, Urbana.
- Cheever E, Leonard J B and Foster K R (1987). Depth of penetration of fields from rectangular apertures into lossy media. *IEEE Trans Microwave Theory and Techniques*, MTT-35, 865 - 867
- Chen M M (1985). "The tissue energy balance equation" in *Heat Transfer in Medicine and Biology Vol. I*. A Schitzer and R C Eberhart (eds.), Plenum Press, New York.
- Chen M M and Holmes K R (1980). Microvascular contributions in tissue heat transfer. *Ann. New York Acad. Sci.*, 335, 137 -150
- Cheung A Y, Golding W M and Samaras G M (1981). Direct contact applicators for microwave hyperthermia. *J. Microwave Power*, 16, 151 - 159
- Christensen D A and Durney C H (1981). Hyperthermia production for cancer therapy : A review of fundamentals and methods. *J. Microwave Power*, 16, 151 - 159
- Colin J and Houdas Y (1967). Experimental determination of coefficient of heat exchanges by convection of human body. *J. Appl. Physiol.*, 22, 31 - 38
- Collins A J, Ring E F J, Cosh J A and Bacon P A (1974). Quantitation of thermography in arthritis using multi-isothermal analysis I. The thermographic index. *Ann. Rheum. Dis.*, 33, 113 - 115
- Cook H F (1951). Dielectric behaviour of human blood at microwave frequencies. *Nature*, 168, 247 - 248
- Cook H F (1951). The dielectric behaviour of some types of human tissues at microwave frequencies. *Brit. J. Appl. Phys.*, 2, 295 - 300
- Cook H F (1952). A comparison of the dielectric behaviour of pure water and human blood at microwave frequencies. *Brit. J. Appl. Phys.*, 3, 249 - 255

- Cooke R and Kuntz I D (1974). The properties of water in biological systems. *Ann. Rev. Biophys. Bioeng.*, 3, 95 - 126
- Cooper K E, Edholm O G and Mottram R F (1955). The blood flow in the skin and muscle of the human forearm. *J. Physiol.*, 128, 258 - 267
- CRC Handbook of Chemistry and Physics* (1977). 58th edition, R C Weast (ed.), CRC Press, Inc., Cleveland, Ohio.
- De Silva M, Kyle V, Hazleman B, Salisbury R, Page Thomas P and Wraight P (1986). Assessment of inflammation in the rheumatoid knee joint: correlation between clinical, radioisotopic and thermographic methods. *Ann. Rheum. Dis.*, 45, 277 - 280
- Dick W C, Grennan D M (1976). Radioisotopes in the study of normal and inflamed joints. *Clin. Rheum. Dis.*, 2, 67 - 75
- Dick W C, Neufeld R R, Prentice A G, Woodburn A, Whaley K, Nuki G and Buchanan W N (1970). Measurement of joint inflammation: a radioisotopic method. *Ann. Rheum. Dis.*, 29, 135 - 137
- Dicke R H (1946). The measurement of thermal radiation at microwave frequencies. *Rev. Sci. Instr.*, 17, 268 - 275
- Draper J W and Boag J W (1971a). The calculation of skin temperature distributions in thermography. *Phys. Med. Biol.*, 16, 201 - 211
- Draper J W and Boag J W (1971b). Skin temperature distributions over veins and tumours. *Phys. Med. Biol.*, 16, 645 - 654
- Draper J W and Jones C H (1969). Thermal patterns of the female breast. *Brit. J. Radiol.*, 42, 401 - 410
- Eckert E R G and Drake R M (1959). *Heat and mass transfer*. McGraw-Hill Book Co.
- Edenhofer P, Grunner K, Steiner M and Suss H (1982). "Near field characteristics of antenna sensors for microwave thermography: preliminary results of multi-spectral radiometric experiments" in *Biomedical Thermology*, M Gautherie and E Albert (eds), Alan R. Liss, Inc., 523 - 537
- Edrich J (1979). Centimeter and millimeter wave thermography : A survey of tumour detection. *J. Microwave Power*, 14, 95 - 103

- Edrich J et al (1980). Imaging thermograms at centimeter and millimeter wavelengths .
Ann. N Y Acad. Sci., 335, 456 - 471
- Enander B and Larson G (1974). Microwave radiometric measurements of the
temperature inside a body. Elect. Lett., 10, 317
- Enel L, Leroy Y, Van de Velde J C and Mamouni A (1984). Improved recognition of
thermal structures by microwave radiometry. Elect. Lett., 20, 293 - 294
- England T S (1950). Dielectric properties of the human body for wavelengths in the 1 -
10 cm range. Nature, 166, 480
- Evans K T and Gravelle I H (1973). *Mammography, thermography and
ultrasonography in breast disease*. Butterworth and Co., Ltd.
- Fallone B G, Moran P R and Podgorsak E B (1982) "Non-invasive thermometry with
a clinical X-ray CT scanner. Med. Phys., 9, 715 - 721
- Foster K R and Schwan H P (1986). "Dielectric properties of tissue" in *CRC
Handbook of biological effects in electromagnetic fields*. C Polk and E
Postow (eds), CRC Press, Florida.
- Foster K R, Schepps J L and Schwan H P (1980). Microwave dielectric relaxation in
muscle: a second look. Biophys. J, 29, 271 - 282
- Foster K R, Schepps J L, Stoy R D and Schwan H P (1979). Dielectric properties of
brain tissue between 0.01 and 10 GHz. Phys. Med. Biol., 24, 1177 - 1187
- Franks F (1972). *Water - A comprehensive Treatise, Vol. 1*. Plenum Press, London
- Fraser S, Land D V and Sturrock R D (1987). Microwave thermography - an index of
inflammatory joint disease. Brit. J. Radiol., 26, 37 - 39
- Fricke H (1924). A mathematical treatment of the electrical conductivity and capacity of
disperse systems. Phys. Rev., 24, 575 - 587
- Gabriel C, Sheppard R J and Grant E H (1983). Dielectric properties of ocular tissue at
37 °C. Phys. Med. Biol., 28, 43 - 49
- Gagge A P, Stolwijk J A J and Hardy J D (1965). A novel approach to measurement of
man's heat exchanges with a complex radiant environment. J. Aerospace
Med., 36, 431 - 435

- Gautherie M (1980). Thermopathology of breast cancer: measurement and analysis of in vivo temperature and blood flow. *Ann. New York Acad. Sci.*, 335, 383 - 415
- Goodman A B and Wolf A V (1969). Insensible water loss from human skin as a function of ambient vapour concentration. *J. Appl. Physiol.*, 26, 203 - 207
- Grant E H, Keefe S E and Takashima S (1968). The dielectric behaviour of aqueous solutions of bovine serum albumin from radiowave to microwave frequencies. *J. Physical. Chem.*, 72, 4343 - 4380
- Guy A W (1971). Electromagnetic fields and relative heating patterns due to a rectangular aperture source in direct contact with bilayered biological tissue. *IEEE Trans. Microwave Theory and Techniques*, MTT-19, 214 - 223
- Haagensen C D (1971). *Disease of the breast*. 2nd edition, Saunders, Philadelphia.
- Haataja M (1975). Evaluation of the activity of rheumatoid arthritis. *Scand. J. Rheumatol.*, 4 (supp), 1 - 54
- Haimovici N (1982). "Three years experience in direct intra-articular temperature measurement" in *Biomedical Thermology*. M Gautherie and E Albert (eds.), Alan R Liss, Inc.
- Hardy J D and Dubois E F (1938). Basal metabolism, radiation, convection and vaporization at temperatures of 22 ° to 35 °C. *J. Nutr.*, 15, 477 - 492
- Harrington R F (1961). *Time Harmonic Electromagnetic Fields*. McGraw-Hill Book Co., New York.
- Hatfield H S (1953). Measurement of the thermal conductivity of animal tissue. *J. Physiol.*, 120, 35P - 36P
- Herrick J F, D G Jelatis and M Lee (1950). Dielectric properties of tissues important in microwave diathermy. *Fed. Proc.*, 9, 60
- Homburger F and Fishman W H (eds) (1953). *The Physiopathology of cancer*. Hoeber-Harper, New York.
- Huskisson E C, Berry H, Browett J P, Balme H W (1973). Measurements of inflammation. II Comparison of technetium clearance and thermography with standard methods in a clinical trial. *Ann. Rheum. Dis.*, 32, 99 -102

- Iskander M F and Durney C H (1983). Microwave methods for measuring changes in lung water. *J. Microwave Power*, 18, 265 - 275
- Johnk C T A (1975). *Engineering Electromagnetic Fields and Waves*. John Wiley & Sons, Inc.
- Johnson S A et al (1977). Non-intrusive measurement of microwave and ultra-sound induced hyperthermia by acoustic temperature tomography. *Ultrasonics Symp. Proc.*, IEEE Cat. No. 77 Ch 1264- 1SU, 977 - 982
- Jones C (1987). Medical thermography. *IEE Proc.*, 134, 225 - 236
- Jones C H (1982). Methods of breast imaging. *Phys. Med. Biol.*, 27, 463 - 499
- Kirkland R W (1967). In vivo thermal conductivity values for bovine and caprine osseus tissue. *Proceedings of the Annual Conference on Engineering in Medicine and Biology*, Boston, Massachusetts, 9, 204
- Klinger H G (1974). Heat transfer in perfused biological tissue - I : General theory. *Bull. Math. Biol.*, 36, 403 - 415
- Klinger H G (1980). The description of heat transfer in biological tissue. *Ann. New York Acad. Sci.*, 335, 133 - 136
- Kraszewski A, Stuchly M A, Stuchly S S and Smith A M (1982). In vivo and in vitro dielectric properties of animal tissues at radiofrequencies. *Bioelectromagnetics*, 3, 421 - 432
- Kraus J D (1966). *Radio Astronomy*. McGraw-Hill Book Co.
- Land D V (1983). Radiometer receivers for microwave thermography. *Microwave J.*, 26, 196 - 201
- Land D V (1987). A clinical microwave thermography system. *IEE Proc.*, 134A, 193 - 200
- Land D V (1988). Application of non-resonant perturbation technique to the measurement of high frequency fields in biological phantom materials. *Elect. Lett*, 24, 70 - 72
- Land D V, Fraser S and Shaw R (1986). A review of the clinical experience of microwave thermography. *J. Med. Eng. and Tech. (Supp: Recent developments in medical and physiological imaging)*, 109 - 113

- Lassen N A (1964). Muscle blood flow in normal man and in patients with intermittent claudication evaluated by simultaneous xenon - 133 and sodium - 24 clearances. *J. Clin. Invest.*, 43, 1805 - 1812
- Lawson R (1956). Implications of surface temperature measurements in the diagnosis of breast cancer. *Canad. Med. Assoc. J.*, 75, 309 - 310
- Lawson R N and Gaston J P (1964). Temperature measurements of localised pathological processes. *Ann. New York. Acad. Sci.*, 121, 90 - 98
- Lewin R (1947). The electrical constants of a material loaded with spherical particles. *J Instn. Elect. Eng.*, 94, 65 - 67
- Leyton L (1975). *Fluid behaviour in biological systems*. Clarendon Press, Oxford.
- Lin J C (1975). Microwave properties of fresh mammalian brain tissue at body temperature. *IEEE Trans. Biomed. Eng.*, BME-22, 74 - 76
- Lipkin M and Hardy J D (1954). Measurement of some thermal properties of human tissues. *J. Appl. Physiol.*, 7, 212 - 217
- Lorrain P and Corson D (1970). *Electromagnetic Fields and Waves*. W H Freeman & Co., San Francisco, 471 - 472
- Love T J (1980). Thermography as an indicator of blood perfusion. *Ann New York Acad. Sci.*, 335, 429 - 437
- Love T J (1985). "Analysis and application of thermography in medical diagnosis" in *Heat Transfer in Medicine and Biology Vol. II*. A Schitzer and R C Eberhart (eds.), Plenum Press, New York.
- Ludecke K M, Schiek B and Ohler J K (1978). Radiation balance thermograph for industrial and medical applications. *Elect. Lett.*, 14, 194 - 196
- Malmberg C G and Maryott A A (1956). Dielectric constant of water from 0 ° to 100 °C. *J. Res. Nat. Bur. Standards*, 56, 1 - 8
- Mamouni A, Bliot F, Leroy Y and Moschetto Y (1977). A modified radiometer for temperature and microwave property measurements of biological substances. *Proceedings of the 7th European Microwave Conference, Copenhagen, September*, 703 - 707
- Mamouni A, Leroy Y, Van de Velde J C and Bellarbi L (1983). Introduction to correlation microwave thermography. *J. Microwave Power*, 18, 285 - 293

- Mantyla M J (1979). Regional blood flow in human tumours. *Can. Res.*, 39, 2304 - 2306
- Maxwell J C (1881). *A treatise on electricity and magnetism Vol. 1*. Clarendon Press, Oxford.
- McLean J A (1974). "Loss of heat by evaporation" in *Heat loss from animals and man*. J L Monteith and L E Mount (eds.). Butterworths, London.
- Meredith R, Warner F L, Davis Q V, Clarke J L (1964). Superheterodyne radiometers for short mm wavelengths. *Proc IEEE*, 111, 241 - 256
- Miller D L (1979). Determining skin thickness with pulsed Doppler Ultrasound. *J. Invest. Dermatol.*, 72, 17 - 19
- Mimi M (in preparation). PhD thesis, University of Glasgow.
- Missenard F A (1973). Coefficient d'échange de chaleur du corps humain par convection, en fonction de la position, de l'activité du sujet et de l'environnement. *Arch. Sci. Physiol.*, 27, A45 - A50
- Mitchell D, Wyndham C H, Hodgson T and Nabarro F R N (1967). Measurement of the total normal emissivity of skin without the need for measuring skin temperature. *Phys. Med. Biol.* 12, 359 - 366
- Mitchell H H, Hamilton T S, Steggerda F R and Bean H W (1945). The chemical composition of the adult human body and its bearing on the biochemistry of growth. *J. Biol. Chem.*, 158, 625 - 637
- Myers P C, Barrett A H and Sadowsky N L (1980). Microwave thermography of normal and cancerous breast tissue. *Ann. N Y Acad. Sci.*, 335, 443 - 455
- Myers P C, Sadowsky N L and Barrett A H (1979). Microwave thermography : Principles, methods and clinical applications. *J. Microwave Power*, 14, 105 - 113
- Newton R (1986). Non-invasive thermometry by correlation and multi-frequency microwave thermometry. PhD thesis, University of Aberdeen.
- Nguyen D D, Robillard M, Chive M, Leroy Y, Audet J, Pichot C and Bolomey J C (1980). Microwave thermography - the modelling of probes and approach towards thermal pattern recognition. *Proceedings of the 10th European Microwave Conference, Warsaw, September.*

- Nightingale N R V, Goodridge V D, Sheppard R J and Christie J L (1983). The dielectric properties of the cerebellum, cerebrum and brain stem of mouse brain at radiowave and microwave frequencies. *Phys. Med. Biol.* 28, 897 - 903
- Nishi Y (1973). Direct evaluation of the convective heat transfer coefficient for various activities and environment. *Arch. Sci. Physiol.*, 27, A59 - A 66
- Nishi Y and Gagge A P (1970). Direct evaluation of convective heat transfer coefficient by naphthalene sublimation. *J. Appl. Physiol.*, 29, 830 - 838
- Nyquist H (1928). Thermal agitation of electric charge in conductors. *Phys. Rev.*, 32, 110 - 113
- Osman M M and Afify E M (1984). Thermal modelling of the normal woman's breast. *J. Biomech. Eng.*, 106, 123 - 130
- Parker D C (1984). Applications of NMR imaging in hyperthermia : an evaluation of the potential for localized tissue heating and non-invasive temperature monitoring. *IEE Trans. Biomed. Eng.*, BME-31, 161 - 167
- Paterson J, Watson W S, Tensdale E et al (1978). Assessment of rheumatoid inflammation in the knee joint. *Ann. Rheum. Dis.*, 37, 48 - 52
- Pennes H H (1948). Analysis of tissue and arterial blood temperatures in the resting human forearm. *J. Appl. Physiol.*, 1, 93 - 122
- Perronet G et al (1983). A microwave diffraction tomography system for biomedical applications. *Proceedings of the 13th European Microwave Conference, Nurnberg, 5 - 8 September*
- Pethig R (1984). Dielectric properties of biological materials: Biological and medical applications. *IEEE Trans. Electrical Insulation.*, EI - 19, 453 - 474
- Phelps P, Steele A D and McCarty D J (1977). Significance of xenon-133 clearance rate from canine and human joints. *Arthritis Rheumatol.*, 15, 360 - 369
- Poppendiek H F, Randall R, Breeden J A, Chambers J E and Murphy J R (1966). Thermal conductivity measurements and predictions for biological fluids and tissues. *Cryobiology*, 3, 318 - 327
- Rao P S, Santosh K and Gregg E C (1980). Computed tomography with microwaves. *Radiology*, 135, 769 - 770

- Rehman I (1978). "Embryology and anatomy of the breast" in *The Breast*. H S Gallacher, H P Leis, R K Snyderman and J A Urban (eds.), The C V Mosby Company, Saint Louis.
- Richards S A (1973). *Temperature regulation*. Wykeham Publications.
- Ring E F J (1980). Quantitative thermography and Thermographic Index. *Verh. Dtsch. Ges. Rheumatol.*, 6, 287 - 288
- Robillard H, Chive M, Leroy Y, Audet J, Pichot C and Bolomey J C (1982). Microwave Thermography - Characteristics of waveguide applicators and signatures of thermal structures. *J. Microwave Power*, 17, 97 - 105
- Robillard M, Nguyen D D, Chive M, Leroy Y, Audet J, Bolomey J C and Pichot C (1980). Profondeur de penetration et resolution spatiale de sondes atraumatiques utilisées en microondes. Symposium URSI "Ondes Electromagnetiques et Biologie", Jouy-en Josas, July.
- Roebuck E J (1986). Mammography and screening for breast cancer. *Brit. Med. J.*, 292, 223 - 226
- Salisbury R S, Parr G, De Silva M, Hazleman B L and Page Thomas D P (1983). Heat distribution over normal and abnormal joints: Thermal pattern and quantification. *Ann. Rheum. Dis.*, 42, 494 - 499
- Schepps J L and Foster K R (1980). The UHF and microwave dielectric properties of normal and tumour tissues: variation in dielectric properties with tissue water content. *Phys. Med. Biol.*, 25, 1149 - 1159
- Schwan H P (1957). Electrical properties of tissue and cell suspensions. *Adv. Biol. Med. Phys.*, 5, 147 - 209
- Schwan H P and Foster K R (1977). Microwave dielectric properties of tissue - some comments on the rotational mobility of tissue water. *Biophysical J.*, 17, 193 - 197
- Seagrave R C (1971). *Biomedical applications of heat and mass transfer*. The Iowa State University Press, Ames, Iowa.
- Shaeffer J, El-Mahdi A M and Carr K L (1982). "Thermographic detection of human cancers by microwave radiometry" in *Biomedical Thermology*, M Gautherie and E Albert (eds), Alan R. Liss, Inc., 509 - 523

- Simkin P A (1989). "Synovial Physiology" in *Arthritis and allied conditions*. D J McCarty (ed.), 11th edition, Lea and Ferbiger, Philadelphia.
- Simkin P A and Nilson K L (1981). Trans-synovial fluid exchange of large and small molecules. *Clin. Rheum. Dis.*, 7, 99 - 129
- Slater J C (1942). *Microwave transmission*. McGraw-Hill Book Co., Inc., 245 - 256
- Smith J J and Kampine J P (1984). *Circulatory Physiology - the essentials*. Williams and Windle.
- Snellen J W, Mitchell D and Wyndham C H (1970). Heat of evaporation of sweat. *J. Appl. Physiol.*, 29, 40 -44
- Solsona F (1978). The history of thermography. *Acta Thermographica*, 3, 83 - 85
- Spells K E (1960). The thermal conductivities of some biological fluids. *Phys. Med. Biol.*, 5, 139 - 153
- Stogryn A (1971). Equations for calculating the dielectric constant of saline water. *IEEE Trans. Microwave Theory and Techniques*, MTT-19, 733 - 736
- Stuchly M A and Stuchly S S (1980). Dielectric properties of biological substances - Tabulated. *J. Microwave Power*, 15, 19 - 26
- Stuchly M A and Stuchly S S (1984). Permittivity of mammalian tissues in vivo and in vitro: Advances in experimental techniques and recent results. *Int. J. Electronics*, 56, 443 - 456
- Thouvenot P, Robert J, Mamouni A and Renard C (1982). "Microwave thermography in intracranial pathology" in *Biomedical Thermology*, M Gautherie and E Albert (eds), Alan R. Liss, Inc., 501 - 509
- Torell L M and Nilsson S K (1980). Calculation of skin temperature increase caused by subcutaneous veins perpendicular to the skin surface. *Phys. Med. Biol.*, 25, 85 - 91
- Valvano J W, Cochran J R and Diller K R (1985). Thermal conductivity and diffusivity of biomaterials measured with self-heated thermistors. *Int. J. Thermophys.*, 6, 301 - 311
- Webb P, Garlington L N and Schwarz M J (1957). Insensible weight loss at high skin temperatures. *J. Appl. Physiol.*, 11, 41 - 44

- Weinbaum S and Jiji L M (1985). A new simplified bioheat equation for the effect of blood flow on local average tissue temperature. *J. Biomech. Eng.*, 107, 131 - 139
- Weinbaum S, Jiji L M and Lemons D E (1984 a). Theory and experiment for the effect of vascular microstructure on surface tissue heat transfer - Part I: Anatomical foundation and model conceptualization. *J. Biomech. Eng.*, 106, 321 - 329
- Weinbaum S, Jiji L M and Lemons D E (1984 b). Theory and experiment for the effect of vascular microstructure on surface tissue heat transfer - Part II: Model formulation and solution. *J. Biomech. Eng.*, 106, 331 - 341
- Wells P NT, Halliwell M, Skidmore R, Webb A J and Woodcock J P (1977). Tumour detection by ultrasonic Doppler blood flow signals. *Ultrasonics*, 15, 231 - 232
- Wilheit T T (1978). Radiative transfer in a plane stratified dielectric. *IEEE Trans. Geosci. and Remote Sensing*, GE-16, 138 - 143
- Windle W F (1976). *Textbook of histology*. McGraw-Hill Book Co., 5th ed.
- Winslow C E A, Herrington L P and Gagge A P (1937). Physiological reaction of the human body to varying environmental temperature. *Am. J. Physiol.*, 120, 1 -22
- Wislow C E A and Herrington L P (1949). *Temperature and human life*. Princeton University Press, Princeton
- Wissler E H (1961). Steady - state temperature distribution in man. *J. Appl. Physiol.*, 16, 734 - 740
- Wissler E H (1987 a). Comments on the new bioheat equation proposed by Weinbaum and Jiji. *J. Biomech. Eng.*, 109, 226 - 233
- Wissler E H (1987 b). Comments on Weinbaum and Jiji's discussion of their proposed bioheat equation. *J. Biomech Eng.*, 109, 355 - 356
- Wulff W (1974). The energy equation for living tissue. *IEEE Trans. Biomed. Eng.*, BME-21, 494 - 495
- Zollner G, Thauer R and Kauffman W (1955). Der insensible Gewichtverlust als Funktion der Umweltbedingungen. *Plüger's Arch. Ges. Physiol.*, 260, 261 - 273

- 1) Cetas T C, Lehmann F (editor) (1982) Thermometry in therapeutic heat and cold 3rd edition. Baltimore, Williams and Wilkins, pp35-69.
- 2) Culliton B J (1976). Science 193, pp555.
- 3) Gosdues M, Thurman T G, Chance B and Reinhold M (1972). Regional variation in the oxygenation of mouse mammary tumours in vivo demonstrated by fluorescence of pyridine nucleotide. Brit. J. Rad. 45. 510-514.
- 4) Gullino P M, Gauthrie M and Albert E (editors) (1982). Considerations on blood supply and fluid exchange in tumours. Biomedical Thermology, Alan K. Liss Inc.
- 5) Moskowitz M, Milbrath J, Gartside P, Zermeno A and Mandel D (1976). Lack of efficiency of thermography as a screening tool for minimal and stage I breast cancer. New Eng. J. Med. 295, 249-252.
- 6) Ring E F J (1986). Skin temperature measurement. Bioeng. Skin 2, 15-30.
- 7) Tonegutte M, Acciairi L and Racanelli A (1981). Fundamentals of contact thermography in female breast diseases. Acta Thermographica 1981 Supplement 3, 11-52.
- 8) Tricoire J, Mariel L, and Amiel JP (1972). Thermographie en plaque et diagnostic des affections du sein (Plate thermography and diagnosis of breast diseases). J. Radiol. Electrol. Med. Nucl. 53, 13-16.

- 9) Warren B A and Shubik P (1966). The growth of the blood supply to melanoma transplants in the hamster cheek pouch. Lab. Invest. 15, 464-478.

- 10) Watmough D J and Oliver K (1969). The emission of IR radiation from human skin - implications for clinical thermography. Br. J. Radiol. 1969 42, 411-415.

- 11) Watmough D J and Ross W M (editors) (1986). Hyperthermia, Blackie, Glasgow.